universität wien

MASTERARBEIT / MASTER'S THESIS

Titel der Masterarbeit / Title of the Master's Thesis

„Functional Elucidation of Auxin Signalling Manipulating Effectors of *Ustilago maydis*"

verfasst von / submitted by

Julia Freund, BSc

angestrebter akademischer Grad / in partial fulfilment of the requirements for the degree of

Master of Science (MSc)

Wien, 2019 / Vienna 2019

Studienkennzahl lt. Studienblatt / degree programme code as it appears on the student record sheet:	A 066 834
Studienrichtung lt. Studienblatt / degree programme as it appears on the student record sheet:	Masterstudium Molekulare Biologie UG2002
Betreut von / Supervisor:	Dipl.-Biol. Dr. Armin Djamei

Confidentiality Clause

This master thesis contains confidential data of the Gregor Mendel Institute. This work may only be made available to the first and second reviewers and authorized members of the board of examiners. Any publication and duplication of this master thesis - even in part - is prohibited. An inspection of this work by third parties requires the expressed permission of the author and the Gregor Mendel Institute.

Acknowledgments

I want to point out that this project was possible thanks to a lot of people. First of all, I want to show my appreciation for Dipl.-Biol. Dr. Armin Djamei who gave me the opportunity to conduct my master thesis in his lab. I give thanks to you for always guiding, supporting and encouraging me throughout my time as a master student in your lab.

Furthermore, two very special people deserve to be mentioned here: my friends Joana Marques and Indira Saado who made this experience one of the best times in my life.

Next, I would like to mention the outstanding help of all the members of the group. Thank you Janos, Jason, Andre, Denise, Angelika, Fernando, Emiliya, David, Julia, Daniel, Gesa, Lukas, Nenad, Sam, Martin and Ruben.

Also, many thanks go to all the members of the Gregor Mendel Institut and the support facilities at the whole Vienna Biocenter Campus.

Finally, I want to express my very profound gratitude to my parents and to my sister for providing me with unfailing support and continuous encouragement throughout my years of study and through the process of researching and writing this thesis. This accomplishment would not have been possible without them. Thank you for all your love.

Abstract

The study of plant-pathogen interaction is a very crucial area of plant research and a fundamental understanding of its mechanisms and principles is of ecological and economical importance. In this thesis the focus is on the fungal model organism *U. maydis*, which is a biotrophic pathogen to the crop plant *Z. mays* and on how the fungus colonizes the host by manipulating hormonal regulated pathways such as indole 3-acetic acid (auxin) signalling, which triggers complex plant growth and developmental processes.

An effector candidate library-wide screen performed by Janos Bindics and Fernando Navarrete identified beforehand two effectors which interfere with the plant defence by inducing the auxin signalling pathway. The purpose of this study was to explore the underlying mechanisms and to characterize the molecular function of the effectors Inducer of Auxin Signalling (IAS1 & IAS2).

Therefore, the effectors were transiently expressed without signal peptide and with epitope tags in the heterologous system *N. benthamiana*. The DR5 reporter system was applied as an indicator for auxin signalling response and the experiments could confirm the inducing effect of both effectors. Additionally, a subcellular localization assays linked to a DR5 induction assay provided essential information about the place of action within the cell.

The experimental data revealed that C-terminal fused tags stabilized the proteins and that IAS1 induced the most with a small tag whereas IAS2 showed the highest results when expressed with large tags. The ectopically expressed effectors fused to various mislocalization tags were visualized via confocal microscopy. IAS1 showed a strong signal in the nucleolus, a very prominent localization, (but a weak in the cytosol) and IAS2 appeared in the cytosol and the nucleus. In both cases I hypothesize a dual function due to the dual localization and weaker induction whenever fused to a localization tag.

In order to separate primary and secondary effects in the plant signalling cascades, the identification of potential effector-interaction partners (PEIPs) via co-immunoprecipitation of the effector followed by mass spectrometry has been applied. Finally, by examining alterations in the outcome of the DR5 induction assay in planta where PEIPs were silenced first, conclusions about their molecular connection in auxin signalling could be drawn. However, due to contaminations in the reporter system no valid evaluation could be made.

Noteworthy are the observed phenotypes that the silenced plants displayed. Among the physical alterations were crippled and bleached leaves as well as dwarf-sized plants.

Zusammenfassung

Die Untersuchung der Wechselwirkung zwischen Pflanzen und Krankheitserregern ist ein sehr wichtiges Gebiet der Pflanzenforschung und ein grundlegendes Verständnis ihrer Mechanismen und Prinzipien ist von ökologischer und wirtschaftlicher Bedeutung. In dieser Arbeit liegt der Fokus auf dem Pilzmodellorganismus *U. maydis*, der ein biotropher Erreger der Kulturpflanze *Z. mays* ist, und darauf, wie der Pilz den Wirt durch Manipulation hormonell regulierter Stoffwechselwege wie Indol-3-essigsäure (Auxin) Signalisierung, die komplexe Pflanzenwachstums- und Entwicklungsprozesse auslöst, besiedelt.

Ein zuvor von Janos Bindics durchgeführtes Screening der Effektorproteinbibliothek identifizierte zwei Effektoren, die die Pflanzenabwehr durch Induzieren des Auxin-Signalwegs stören. Ziel dieser Studie war es, den Wirkungsmechanismus zu untersuchen und die molekulare Funktion der Effektoren Inducer of Auxin Signalling (IAS1 & IAS2) zu charakterisieren.

Daher wurden die Effektoren vorübergehend ohne Signalpeptid und mit Epitopmarkierungen im heterologen System *N. benthamiana* exprimiert. Das DR5-Reportersystem wurde als Indikator für die Auxin-Signalantwort verwendet, und die Experimente konnten die induzierende Wirkung beider Effektoren bestätigen. Zusätzlich lieferte ein mit einem DR5-Induktionstest verbundener subzellulärer Lokalisierungstest wesentliche Informationen über den Wirkort innerhalb der Zelle.

Die experimentellen Daten zeigten, dass C-terminal fusionierte Tags die Proteine stabilisierten und dass IAS1 am meisten mit einem kleinen Tag induzierte, während IAS2 die höchsten Ergebnisse zeigte, wenn es mit großen Tags exprimiert wurde. Die ektopisch exprimierten Effektoren, die mit verschiedenen Fehllokalisierungsmarkierungen fusioniert waren, wurden durch konfokale Mikroskopie sichtbar gemacht. IAS1 zeigte ein starkes Signal im Nucleolus, eine sehr ausgeprägte Lokalisation (aber eine schwache im Zytosol) und IAS2 erschien im Zytosol und im Nucleus. In beiden Fällen gehe ich aufgrund der doppelten Lokalisierung und der schwächeren Induktion, wenn diese mit einem Lokalisierungs-Tag fusioniert wurden, von einer Doppelfunktion aus.

Um primäre und sekundäre Effekte in den pflanzlichen Signalkaskaden zu trennen, wurde die Identifizierung potenzieller Effektor-Interaktionspartner (PEIPs) mittels Co-

Immunopräzipitation des Effektors und anschließender Massenspektrometrie durchgeführt. Schließlich konnten durch Untersuchung der Veränderungen der Ergebnisse des DR5-Induktionstests in Planta, in denen PEIPs zuerst gesilenct wurden, Schlussfolgerungen über ihre molekulare Verbindung bei der Auxinsignalübertragung gezogen werden. Aufgrund von Kontaminationen im Reportersystem konnte jedoch keine gültige Auswertung vorgenommen werden. Bemerkenswert sind die beobachteten Phänotypen, die die gesilencten Pflanzen zeigten. Zu den physischen Veränderungen gehörten verkrüppelte und gebleichte Blätter sowie zwerggroße Pflanzen.

Table of Content

Figures

Tables

Abbreviations

%	Percent	**ng**	nanogram
°C	degree celsius	**NLS**	nuclear localization signal
∞	Infinity	**N-terminal**	amino terminal
A. th.	Arabidopsis thaliana		
Aa	amino acids	**OD_{600}**	optical density at 600 nm
ANOVA	analysis of variance	**PAGE**	polyacrylamide gel electrophoresis
ARM	agrobacterium resuspension medium	**PAMP**	pathogen-associated molecular pattern
BIG	auxin transport protein BIG-like	**PCD**	programmed cell death
bp	base pair(s)	**PCR**	polymerase chain reaction
cDNA	complementary DNA	**PDS**	phytoene desaturase
Ch	chromosome	**PEIP**	Possible effector interacting protein
CITRX2	Thioredoxin-like protein CITRX2	**PR**	pathogenesis related
C-terminal	carboxy-terminal	**PRR**	pattern recognition receptor
ddH20	double distilled water	**PS**	ponceau staining
DMSO	dimethyl sulphoxide	**PTI**	PAMP-triggered immunity
DNA	deoxyribonucleic acid	**qPCR**	quantitative PCR
dNTP	deoxy nucleoside triphosphate	**RNA**	ribonucleic acid
dpi	days post infection	**rpm**	rounds per minute

ET	Ethylene	**RT**	room temperature
HR	hypersensitive cell death	**SA**	salicylic acid
	Response	**SD**	standard deviation
HRP	horse radish peroxidase	**SDS**	sodium dodecyl sulphate
IAA	indole 3-acetic acid	**SE**	standard error
JA	jasmonic acid	**sec**	second(s)
kb	kilobase pair(s)	**ß**	beta
kDa	kilodalton(s)	**Tris**	Tris(hydroxymethyl)-aminomethane
L	Liter	**TRV**	tobacco rattle virus
M	Molar	**TRXDC9**	Thioredoxin domain-containing protein 9-like protein
min	minute(s)	**Unchar-Prot**	Uncharacterized protein A4A49_29707
MYR	myristylation	**VAMP714**	Vesicle associated membrane protein 714-like protein
NaCl	natrium chloride	**VIGS**	virus induced gene silencing
N. b. (Nb)	nicotiana benthamiana	**α**	alpha
NB-LRR	nucleotide binding/leucin rich repeat	**Δ**	deletion
NES	nuclear export signal	**µ**	micro

1 Introduction

Plants are fundamental to all life on earth. They provide us with food, fuel, fibre, industrial feedstocks, and medicines and are therefore indispensable for medical care, clothes, shelter, energy and nutrition. Hence, they play an enormous role in the current most pressing issues like increasing energy demand, regulation of biogeochemical cycles, global warming, air pollution and a sustainable agriculture for the exponentially growing world population. All the more, it is of greatest importance, especially to human society, to study and understand the fundamental principles of plant organisms and invest in research (States, National Research Council Committee on Examination of Plant Science Research Programs in the United 1992; Usman et al. 2014).

The Food and Agriculture Organization of the United Nations (FAO) predicted with statistical analysis that global population would exceed 9 billion by the year 2050 leading to a rise of world hunger and making the supply of humanity with enough food a very pressing subject (FAO 2009). Most of the world's crops are lost due to abiotic stresses like temperature, radiation, water or nutrients. A considerably high amount is also lost due to biotic stresses like weeds, animal pests and microbial pathogens; Pathogenic fungi, bacteria and viruses cause a loss of up to 14% of the total yield amount (OERKE 2006). Given that fungal diseases in plants are rising (Brefort et al. 2009), research is therefore keen on studying these pathogens and their strategies to colonize plants. For example, some fungi are necrotrophs, meaning in order to feed and grow, they need to kill their host by secreting toxins. Others, called biotrophs, depend on living tissue to prosper, making them economically extremely harmful organisms (Doehlemann et al. 2017).

> *"Understanding how plants defend themselves from pathogens and herbivores is essential in order to protect our food supply and develop highly disease-resistant plant species." (Freeman 2008, p. 1)*

Lacking an immune system comparable to animals and the ability to flee from danger, plants have developed their own strategies to evade extensive harm caused by many organisms including pathogenic bacteria, fungi, protists, insects, and vertebrates (Freeman 2008). One branch of modern biology specializes on the elucidation of the mechanisms behind these plant-pathogen interactions. Maize (*Zea mays*) seems to be a suitable plant model for

such studies (Strable and Scanlon 2009), because, besides rice (*Oryza sativa*), it is one of the most popular cultivated cereals, especially in the USA (OERKE 2006) and a host to numerous pathogenic species, which affect its yield and quality (Pechanova and Pechan 2015). Being a prominent representative of maize pathogens makes the biotrophic fungus *Ustilago maydis* (*U. maydis*) (Brefort et al. 2009) a relevant candidate to study the plant-pathogen interactions as well.

1.1 Pathogen Model Systems

1.1.1 Ustilago maydis

U. maydis, commonly known as corn smut, belongs to the division *Basidiomycota*, in the order of *Ustilaginales* (Doehlemann et al. 2017) and is a well characterized model organism. *U. maydis* has a genome of 20.5 Mb, which is rather small compared to other pathogenic fungi. Its genome consists of 23 chromosomes containing approximately 6,900 protein-encoding genes with only a low number of introns incorporated. Possessing a lot of intronless genes and little redundancy in the genome might cause the amenability to efficient homologous recombination and reverse genetics, which was observed in previous research (Kämper et al. 2006; Doehlemann et al. 2017). 12 clusters of genes were identified to be genomic features responsible for the pathogenicity of this organism, because they are regulated together and induced during infection (Kämper et al. 2006). Important for using *U. maydis* as a model system is its feature to prosper in axenic culture and to enter a haploid life cycle. The real advantage of a strain like SG200 is solo-pathogenicity, because in its haploid stage gene functions can be studied unbiasedly during the infection process. The developed SG200, a haploid strain, no longer needs a mating partner to cause diseases. Furthermore, the prominent production of galls on all aerial parts of infected maize in less than a week makes scoring of pathogenic effects easy (Brefort et al. 2009). Ultimately all those traits make *U. maydis* a suitable model organism to study fungal genetics and cell biology as has been shown previously in the following topics: mating, morphogenesis, pathogenicity, signal transduction, mycoviruses, DNA recombination, and genomics (Martínez-Espinoza et al. 2002).

1.1.1.1 Life Cycle

In smuts sexual reproduction and pathogenicity are tightly linked. The life-cycle starts with the germination of resting spores, the teliospores (diploid cells that can survive extended

periods of time under harsh environmental conditions), which create haploid basidiospores (the spores of organisms of the division *Basidiomycota*) after germination via meiosis. Proliferation occurs by budding, a form of vegetative multiplication (Saville et al. 2012; Lanver et al. 2017). If two compatible mating types of basidiospores encounter, they form conjugation tubes and fuse, resulting in a pathogenic dikaryotic cell. In this plasmogamy stage, two haploid nuclei in one cell, it proliferates into a dikaryotic filament, senses plant signals and shapes a penetration structure, also known as appressoria (Castanheira and Pérez-Martín 2015). After infection the branches of the fungi can grow biotrophic within or between the host's cells, building a huge network of hyphae, a long, branching filamentous structure of a fungus and the main mode of vegetative growth (Saville et al. 2012). This leads to the characteristic disease symptoms, the tumours, also described as galls, on aerial parts of the plant (Kämper et al. 2006). In the meantime, the fungus-induced molecular alteration of the plant already begins. Moreover, *U. maydis* initiates sporogenesis in the tumours, which involves hyphal fragmentation and karyogamy, the fusion of two nuclei of one cell. Simultaneously, new diploid teliospores arise. Those dormant pigmented spores get dispersed by air, closing the life cycle (Perez-Nadales et al. 2014; Saville et al. 2012).

1.1.1.2 Effectors

After overcoming physical barriers, pathogenic fungi must suppress or evade the plant defence response and additionally manipulate the plant's physiology in order to propagate biotrophically. In the course of evolution, a pressure emerged to develop a set of secreted pathogenic proteins, the so-called effectors, to promote colonization of hosts (Chisholm et al. 2006). Effectors are small molecules that bind their target specifically and regulate its biological activity. For example, they can increase or decrease enzyme activity, gene expression, or cell signalling (Lanver et al. 2017; Toruño et al. 2016). Those host processes are usually termed effector-targeted pathways (ETP) and the result of the deployment of effectors that favours pathogenic virulence is called effector triggered susceptibility (ETS). Overall the research on effectors has helped remarkably to ascertain plant processes like plant development, plant receptors, signal transduction pathways, plant hormones and epigenetics. (Win et al. 2012).

New analysis identified 426 secreted proteins of which 70% could not be assigned a function, which is typical for effector candidates and almost 50% are unique for *U. maydis*

without homology to other genes (Kämper 2006). Moreover, most of the effectors are expressed exclusively during the biotrophic stage (Djamei et al. 2011). Unlike necrotrophic fungi, *U. maydis* possesses only a very small repertoire of plant cell wall degrading enzymes (Kämper 2006). Besides this, other sets were characterized to degrade and utilize cell components. Also, several genes were detected to encode putative secreted metabolic enzymes. These classifications are based on the presence of functional domains, general domain structure and cysteine pattern (Mueller et al. 2008).

Two distinct effector secretion systems have been identified classifying the effectors into apoplastic (AE) and cytoplasmic (CE). Apoplastic effectors get secreted in the apoplast, the non-protoplasmic component of a plant, including the cell walls and intercellular material, and the cytoplasmic effectors are delivered to the host's cytoplasm (Giraldo et al. 2013). At their target site they can unfold their true purpose (Lanver et al. 2017). AE can get recognised by plant cell surface receptors, which are usually referred to as pattern recognition receptors (PRR) and CE are targeted by intracellular immunoreceptors of the nucleotide-binding leucine-rich repeat (NB-LRR) class (Win et al. 2012).

1.2 Plant Model System

1.2.1 Zea mays

Zea mays belongs to the family *Poaceae* of the clade Monocots, which includes such plants as wheat, barley, rice, and sugarcane. First studies on *Zea mays* already reach back to Gregor Mendel in 1869 (Strable and Scanlon 2009). Since then it got more and more established as a model organism due to some basic characteristics, which lead to significant contributions to science. Its genome, which arose from an ancient tetraploidy event (Strable and Scanlon 2009) is the size of 2,3-gigabases, containing around 32,000 predicted genes and is saturated with molecular markers. The discovery of transposons, the so-called jumping genes, is owed to the high proportion (85%) of transposable elements in its genome (McClintock 1950). Maize is diploid and possesses 10 (n) large chromosomes (Schnable et al. 2009; Nannas and Dawe 2015). This makes it easy to study meiotic stages and uncover mutants and hence ideal for plant cytogenetic research. The application of forward and reverse genetic strategies helped generate a vast collection of genetic mutants. Moreover, thanks to the extraordinary level of genotypic diversity, specific traits could be linked to

certain candidate genes identifying the correlation between phenotypic and genetic diversity (Strable and Scanlon 2009). A lot of this valuable information on maize is provided by the Maize Genetic and Genomics Database (MaizeGDB) (http://www.maizegdb.org) (Lawrence et al. 2008). Mostly the standard inbred line B73 is utilized for basic research in laboratories (Strable and Scanlon 2009).

Z. mays is a naturally outcrossing species, which makes it genetically similar to humans. The ability to self-cross and quickly produce homozygotes or F2 populations makes it an advantageous genetic system (Strable and Scanlon 2009; Nannas and Dawe 2015). The pollination is controlled and performed easily, because the reproductive organs are readily accessible and separable, leading to several hundred seeds, which arise from a single pollinated ear (Strable and Scanlon 2009). Additionally, the time window for crossing is rather large (Nannas and Dawe 2015). Maize can be cultured on any scale; it can grow successfully in a broad range of climates and year-round in greenhouses and growth chambers with proper lighting. However, because it requires a lot of space due to its size and height, it cannot be cultured in small chambers. Another drawback is its relatively long-life cycle. One generation takes 13-weeks, which is significantly longer than *Arabidopsis thaliana* (6–8 weeks), the prominent plant model system (Nannas and Dawe 2015). Another flaw of the model organism is the genetic transformation, which is technically challenging and still relatively slow (Strable and Scanlon 2009; Frame et al. 2002).

1.2.2 Nicotiana benthamiana

In the 19th century surgeon Benjamin Bynoe, who travelled on board of the HMS Beagle with Darwin, was first recorded to discover and collect the relative of tobacco *Nicotiana benthamiana* (*N. benthamiana*, *N. b.*) (Goodin et al. 2008). *N. b.* possesses 19 pairs of chromosomes and its large haploid genome, emerged from allopolyploidy, is the size of around 3,100 Mbp and therefore 20-fold larger than the *Arabidopsis thaliana* genome. This feature restricts its use as a genetic system (Bennett and Leitch 2005; Bennett 2003). Another downside is that no floral-dip transformation system exists for *N. b.* (Goodin et al. 2008). In general, it is broadly utilized as a host for plant virology as well as for a wide variety of other plant pathogens. Nonetheless, the model organism gained popularity as a transgene powerhouse. *N. b.* is amenable to three major technical advances that facilitate the manipulation of protein and gene expression in plant cells. This gave *N. b.* the attractivity for

plant cell biology. Firstly, foreign genes from plant virus vectors can be expressed in *N. b.,* revealing new insights into fundamental aspects of plant biology, like subcellular addresses and unique interactions with cell components (Chapman et al. 1992; Goodin et al. 2008; Escobar et al. 2003). Secondly, the susceptibility of *N. b.* for this new technique, virus-induced gene silencing (VIGS), transformed it into a powerful reverse-genetics system by taking advantage of the plant RNAi-mediated antiviral defence mechanism. VIGS can theoretically target any gene-of-interest in plants and lead to its downregulation (Velásquez et al. 2009; Goodin et al. 2008). Another benefit of VIGS is that if the selected target is homologous to more members of a gene family it can overcome by silencing all problems of genetic redundancy. Thirdly, *N. b.* earned its title as leading role among plant model organisms, because agroinfiltration, a method, which only works poorly in other organisms, can be successfully performed on its leaves. In principle agroinfiltration facilitates the transient synthesis of proteins of interest in infected plants, which can further be sampled for microscopy and biochemical analysis (Goodin et al. 2002). However, agroinfiltration may result in artefacts due to overexpression (Goodin et al. 2008). Additionally, the above listed techniques can be applied in combination in order to investigate signal transduction (Gabriels, Suzan H E J et al. 2006) and protein trafficking (Kanneganti et al. 2007). In summary the model system *N. b.* is ideal for protein-protein interaction and protein localization studies thus for studies of host–pathogen interactions (Goodin et al. 2008).

1.3 Pathogen-Plant Interaction

1.3.1 Plant Pathology – the study of plant diseases

Plant pathology is the scientific study of diseases in plants caused by pathogens, which are infectious organisms, and environmental conditions, meaning all kinds of physiological factors. Pathogenicity is the ability of a parasite to cause diseased conditions by invading and becoming established in the host. Bacteria, viruses and fungi are groups that can parasitize plants. In order to infect, the pathogen and the plant must get in direct contact and thus interact. Additionally, environmental conditions must be within a favourable range to successfully develop a disease. This combination of the three components is known as disease triangle(Agrios 2008).

1.3.2 Overview of a disease cycle

The development of a disease cycle occurs in multiple stages. At first, the inoculation event, the initial contact, arises. Up next follows the penetration either directly through the plant's epidermis, through natural openings or wounds. In the infection stage the pathogen procures nutrients from the host for growth, reproduction and further invasion of the plant. The appearance of symptoms (detectable changes) classify the disease and is a trademark for successful infection. At the end of the disease cycle comes the dissemination of the pathogens responsible for plant disease outbreaks. If necessary, pathogens can overwinter and/or oversummer in plants before spreading (Agrios 2008).

1.3.3 Effects on physiological plant functions during infection

Pathogens target various physiological processes in order to successfully colonize the host plant. An effect of pathogens can be on photosynthesis which generates energy utilized for all cell activities. Pathogenic microbes can affect the translocation of water and nutrients in the host essential for surviving. Another way to manipulate the host is by targeting the respiration process which releases energy for several cellular functions. Disturbing the permeability of cell membranes eventuate in uncontrollable loss or undesired influx of substrates. Pathogenic organisms can disturb transcription and translation causing unfavourable changes in function and structure of the affected cell. Plants' reproduction mechanisms can also be targeted by infectious life forms. Moreover, pathogenic microorganisms prefer targeting the plant growth regulation by unbalancing the hormonal system resulting in abnormal growth responses. So, the interference with different physiological functions causes various symptoms to develop during infection (Agrios 2008).

1.3.4 Structural and chemical weapons applied by pathogens for infection

Pathogens live off substances manufactured by the host plant and in order to get to them, they have developed several methods to attack their prey. Some pathogens use mechanical force to invade the plant. For example, fungi have evolved a structure called appressorium to penetrate and substances to weaken and dissolve plants' barriers at the penetration site. Additionally, pathogenic organisms apply chemical weapons (among which are the effectors) to further make their way through their target and neutralize its defence reaction. They enzymatically degrade cell wall substrates like cutin, cellulose and lignin and

other cellular components like starch, lipids and proteins. Another weapon is toxins (phytotoxins) designed for the disruption of physiological processes and hence seriously damaging or killing the plant (Agrios 2008).

1.3.5 Three types of resistance among plants

There are three different concepts on resistance against diseases among plants. The first type of resistance is the nonhost resistance, meaning that a plant can defend itself easily against a pathogenic agent to which it is not the host because of the different genetic makeup. Although due to co-evolution it is more likely that plants are taking some intermediate position between host and nonhost status (Niks and Marcel 2009). The second type is called nonspecific or horizontal resistance (also many-gene resistance), meaning it is polygenic. If a host possesses this resistance, it has enough defence mechanisms to survive an attack of different races of a specific pathogen. The specific or vertical resistance is the third type and is oligogenic. It is specific for one pathogen and is defined based on the gene-for-gene relationship (see later) phenomenon (Agrios 2008).

1.3.6 Defence strategies to counteract pathogenic weapons

On the contrary, the host evolutionary developed several defences to fight back. The genetic material ultimately controls directly or indirectly the forms of defence or resistance applied against a pathogen (or an abiotic agent). Basically, plants use a combination of two defence sets: physical barriers to inhibit entrance and spreading and biochemical substances to poison or inhibit pathogenic growth. Plants came up with different strategies to defend themselves by developing pre-existing structural and chemical defences as well as inducible ones. At the front line against pathogenic attack is a plant's surface, which should hinder the penetration. These pre-existing structural defences include for example wax, cuticle, epidermal cell walls. Often the failure of a pathogen attack does not depend on the structural barrier, but more on the chemical substances produced before and after infection. For example, plants release inhibitors against certain pathogens into the environment. In other plants inhibitory compounds are present before infection. Lacking specific recognition factors is another strategy to protect oneself against potential enemies. By not synthesizing the substance essential for a pathogen's survival plants found another opportunity to escape the parasite. As soon as the pathogen establishes physical contact the plant can detect signal

molecules and react to the pathogen's presence. These signals, like toxins (e.g. alkaloids, terpenes and phenolics), carbohydrates and enzymes, are termed as nonspecific pathogenic elicitors that are sensed by the host triggering the plant's immune system. This recognition launches a series of intracellular biochemical and structural changes as well as in adjacent cells to fend off the pathogen by blocking the spread of toxic substances and invading structures. Therefore, plants evolved cell wall and histological defence structures as well as cytoplasmic and necrotic (hypersensitive) defence reactions. These processes contain formation of tyloses, cork and abscission layers and deposit gums (Agrios 2008).

1.3.7 Molecular mechanism of resistance

After the preformed physical and chemical barriers were overcome by the pathogens the plant host must then fight back on the next defence level. Since plants lack mobile defender cells and a somatic adaptive immune system, they designed a two-tiered innate immune system. A plant's immune system operates in 3 steps which appear as followed the detection of the pathogen, then the signal transduction which ends in the appropriate immune response inducing a locally or systematic resistance (Agrios 2008).

The first immune answer to the penetration attempt is PAMP-triggered-immunity (PTI) which is triggered by DAMPs (damage-associated molecular patterns), which are endogenous molecules released by mechanical and cellular damage, and by so called elicitors (Choi and Klessig 2016). Elicitors are general extrinsic foreign molecules that can be (also synthetic) chemicals, secreted compounds or constituents of the attacker (Zhang et al. 2013; Eder and Cosio 1994). Pathogen-associated-molecular-patterns (PAMPs) are elicitors common to many microbes that get perceived sensitively by pattern-recognition-receptors, short PRRs, on the cell surface of a host. Some PRRs are leucine-rich repeat receptor-like kinases like FLS2 (which binds bacterial flagellin) (Gomez-Gomez and Boller 2000) that propagate signalling upon PAMP binding and further leading to signal transduction cascades often involving mitogen activated protein kinase (MAPK) or calcium ion signalling and hormone production (Zhang et al. 2013; Jones and Dangl 2006). The PAMP recognition induces physiological responses that actively inhibit pathogen reproduction or make further infection more difficult. These responses can manifest themselves for example in reinforcement of the cell wall by callose, lignin or suberin deposition, synthesis of antimicrobial metabolites like phytoalexins, expression of pathogenesis-related (PR) proteins, oxidative stress protection via reactive

oxygen species (ROS) as well as the induction of hormones like salicylic acid (SA), jasmonate (JA) and ethylene (ET) (Bigeard et al. 2015).

PRs are newly expressed proteins solely under pathological or related situations and show very diverse antimicrobial defence-related functions. The induction of PRs and ROS can also lead to hypersensitive cell death response (HR). HR is a mechanism to prevent the spread of a microbial pathogen at the infection site by initiating rapid cell death. The activation of HR follows the systemic acquired response (SAR), an immunization of the hole organism against further infection (Boccardo et al. 2019).

By secreting effectors, usually a small molecule that selectively binds to a protein and regulates its biological activity, the pathogenic microorganism can interfere with PTI. The successful overpowering of the immune response is termed effector-triggered susceptibility (ETS). Once the pathogen surpasses PTI the second front line of the plant's innate immune system awaits. The effector-triggered immunity (ETI), especially effective against biotrophs, largely acts inside the cell and is initiated by the detection of effectors and usually results in hypersensitive cell death response (HR). Both PTI and ETI share downstream signalling as transcriptional reprogramming, hormonal changes and programmed cell death (PCD). Plants' resistance (R) genes are specialized on identifying effectors and moreover, triggering ETI. They are classified through their amino acid motif organization and their membrane spanning domains. The largest group of R genes encode for proteins containing a nucleotide-binding (NB) and leucine-rich repeat (LRR) domain hence the name NB-LRR protein. NB-LRRs are generally located in the cytoplasm (Zhang et al. 2013; Jones and Dangl 2006; Gururani et al. 2012).

1.3.8 The gene-for-gene relationship model

The gene-for-gene relationship postulates that the correlation between resistance and the ability to cause disease are controlled by pairs of matching genes. This pair is formed by the host's resistance genes (R) and the invader's avirulence genes (Avr). A compatible interaction of the plant-pathogen results in a successful infection leading to disease. If an Avr/R gene pair is formed, the Avr gene is neutralized and the interaction is therefore incompatible (Zhang et al. 2013; Keen 1990). Two recent/modern hypotheses are trying to explain the molecular mechanism of the gene-for-gene system. Firstly, in the elicitor-

suppressor model, the general elicitors initiate defence response and only specific pathogenic suppressors for these elicitors can prevent pathogenic identification and therefore circumvent resistance. Compared with this, the elicitor is recognized by specific host receptors, which then trigger the immune response in the elicitor-receptor model (Gomez-Gomez and Boller 2000). Until now, not very few molecular evidences could verify the direct interaction of Avr/R pairs. This led to the design of new models postulating indirect interaction of the Avr/R pairs. The second recent hypothesis, the guard model, tries to offer an explanation on how R genes sense effectors and mediate the host's response. It postulates that R proteins indirectly recognize pathogen effectors by monitoring the integrity of host cellular targets. On the other side, the decoy model says that an E has multiple host targets of which some are recruited as decoy by the plant and hence dispensable (Zhang et al. 2013).

To sum up, the molecular response to plant-pathogen interaction occurs in four phases. First is the effective defence of the pathogen through PTI. Second the pathogen circumvents PTI leading to ETS. Third ETI is successfully launched chasing away the intruder. Fourth the natural selection drives molecular changes in effectors to regain its harmful effect, but eventually leading to the adaptation of R genes again and so on (Jones and Dangl 2006).

1.4 Plant hormones

As mentioned above, during plant-pathogen interaction, pathogenic microbes target the complex hormone network that governs plant immunity significantly. By deregulating biosynthesis of hormones or by interfering with hormonal signalling pathways, the parasite overcomes the plant defence mechanisms. Therefore, science is keen on improving crop resistance to pathogens by manipulating hormone homeostasis and signalling (Denancé et al. 2013). For example, salicylic acid (SA) is strongly connected to biotrophic defence, whereas jasmonic acid (JA) and ethylene (ET) play a major role in necrotrophic defence. Hormones are of critical importance to pathogenesis, since plants depend on the fine-tuning of specific hormonal responses to regulate the balance of growth and defence. As a consequence, pathogenic invaders developed several strategies to disturb homeostasis and facilitate infection. Besides defeating immunity, the reprogramming of hormone pathways by pathogens has also effects on modification of habitat structure, optimization of nutrient acquisition and enabling of pathogen dissemination. These listed benefits can be achieved through two mechanisms: One, they suppress defence responses regulated by the "stress"

hormones like salicylic acid (SA), jasmonic acid (JA) and ethylene (ET), which facilitates an effective colonization. Two, they hijack plant development and nutrient distribution regulated by “growth” hormones like auxin, cytokinin (CK), gibberellin (GA) and brassinosteroid (BR), which facilitates the maintenance of colonization and dissemination. The manipulation of growth hormonal pathways can occur independently of defence response but can also have an indirect effect on plant resistance (Ma and Ma 2016).

1.4.1 Auxin

The “growth” hormone auxin plays the role of a mobile growth regulator in plants and is essential for cell growth including cell division and cellular expansion and contributes to cell differentiation and specification of cell fate (Leyser 2010). Therefore, the concentration of auxin in each cell type gives crucial developmental information directing processes like phototropism, root and shoot morphologic architecture, flower and fruit development, vascular formation, tissue differentiation, and cell elongation (Fu and Wang 2011). The most common member of the auxin family is IAA (indole-3-acetic acid). In detail, IAA regulates apical dominance, root gravitropism, root hair, lateral root, leaf, and flower formation, and plant vasculature development (Denancé et al. 2013).

Auxin directly and indirectly affects the regulation of pathogen resistance responses (Denancé et al. 2013). The suppression of plant defence can be achieved by modulating the pathway of auxin. Auxin acts as a negative regulator of plant immunity; hence it is repressed during infection. This is facilitated by SA, which plays the antagonist of auxin, meaning if auxin signalling is activated, PTI gets suppressed (Ma and Ma 2016). It has been shown that the exogenous application of auxin enhances susceptibility to the bacterial pathogen. This indicates that decreasing plant auxin signalling can increase resistance to bacterial pathogens (Navarro et al. 2006).

1.5 Aim of this study

This thesis wants to elucidate the molecular and functional characterization of *U. maydis* effectors that target hormonal signalling, more precisely auxin signalling. In a screen performed by Janos Bindics several effectors were identified to target the auxin signalling pathway upon which two candidates UMAG_00628 and UMAG_02852 were picked for this master thesis. The aim is to further investigate their molecular mechanism. Therefore, more

information about their activity within a cell was gathered via transient heterologous expression (lacking the signal peptide) in *N. benthamiana* and subsequently performing a subcellular localization assay. Moreover, their role as an auxin inducer is monitored with a DR5-induction assay. Additionally, in order to identify potential interaction partners the probes are analysed via mass spectrometry (MS) after co-immunoprecipitation (Co-IP). To prove the hypothesis of an interaction, the MS results were then knocked down via the virus-induced gene silencing technique to observe if changes in auxin signalling can be detected in the DR5-induction assay.

2 Results

Different assays were performed in *Nicotiana bentamiana* plants to illuminate how *Ustilago maydis* effectors UMAG_00628 and UMAG_02852 activate auxin signalling after pathogenic invasion. The following part of my master thesis will include a subcellular localization assay performed in *N. b.* that will give crucial information about the effector's activity within the cell. Additionally, this assay's results will be supported by microscopic images of the effector's localization. Further, potential interaction partners will be identified via mass spectrometry after co-immunoprecipitation. These candidates will be silenced by applying the virus-induced gene silencing technique and subsequently, the DR5 induction assay will detect possible changes of the effector's effect on the auxin signalling pathway further clarifying its functions.

2.1 Characterization

In the DR5 induction assay done by Janos Bindics which utilizes the auxin responsive promoter DR5 reporter system to monitor auxin response (Chen et al. 2013), these two effectors UMAG_00628 and UMAG_02852 were found to be inducers of the auxin signalling pathway. According to the screen UMAG_00628, which is the size of 54 kDa, showed a 2,65-fold and UMAG_02852, which is 16 kDa big, a 1,48-fold DR5 induction compared to the used negative mCherry control. Both are predicted to be secreted and non-apoplastic by the programs EffectorP and ApoplastP (Sperschneider et al. 2016; Sperschneider et al. 2018). The LOCALIZER prediction test performed by Jason Bosch suggested the assumption that UMAG_00628 is potentially localized in the nucleus (Sperschneider et al. 2017).

Table 1 Characteristics of the effector UMAG_00628 and UMAG_02852

Effector	Protein length (aa)	Mass (Da)	Genetic locus	Predicted secreted	DR5 induction (tobacco)	Localizer – nucleus (Jason Bosch)	Apoplast prediction
UMAG_00628	473	54,134	Chr 1	Y	Y (2,65 fold)	Y (RKRSSTPLQLEKRRES)	N
UMAG_02852	145	16,27	Chr 7	Y	Y (1,48 fold)	-	N

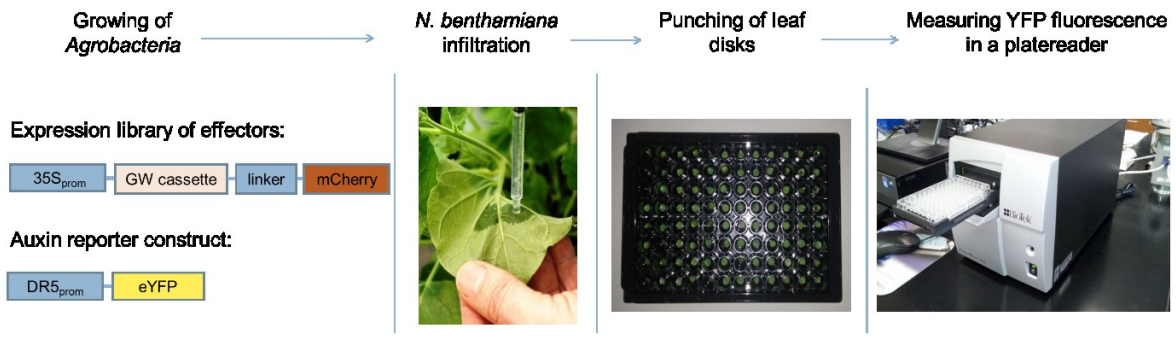

Figure 1 Schematic scheme of the screen-setup for auxin signalling induction (by Janos Bindics).
Abbr.: 35Sprom = 35S promotor; GW cassette = Gateway cassette; eYFP = enhanced yellow fluorescent protein, YFP = yellow fluorescent protein. Figure adapted from Janos Bindics.

2.2 Induction of auxin signalling in different cellular compartments and their microscopic detection

The effector's activity within the plant cell was tested by expressing the effector under the constitutive strong promoter 35S in *N. b.* and fusing different localization tags either at its C- or N-terminus of the gene sequence. These tags force the effectors to be active in only one cell compartment such as the plasma membrane (tagged with the myristylation tag - MYR), the nucleus (tagged with the nuclear localization signal - NLS) or the cytosol (tagged with the nuclear export signal - NES). A microscopic analysis followed confirming the correctness of the subcellular localization constructs. The negative control plant was infiltrated with mCherry and for the positive control TIP1 (TOPLESS Interacting Protein 1) was selected. The negative control for induction of auxin signalling for N-terminal tagged constructs is myc-mCherry-mCherry (myc-mCh-mCh). For the C-terminal tagged constructs mCherry-mCherry-myc (mCh-mCh-myc) was designed. All measurements of the N- and C-terminal tagged constructs were normalized and set in relation to the N- or C-terminus negative control, respectively. To measure the effects on or changes in auxin signalling, a reporter system was designed of the synthetic auxin responsive promotor DR5 fused to the detectable fluorescence protein YFP (yellow fluorescent protein) (Ulmasov et al. 1997). The fluorescence was measured with excitation wave length (λex) of 485 nm (nanometre) and the emission wave length (λemm) of 528 nm. The protein synthesis of the designed constructs within the agrobacteria-infiltrated plants was also measured at λex = 570 nm and λemm= 610 nm. Their full-length protein expression was further verified by western blot. Possible outliers, which are observations that stand far away from the most of other observations, were identified in R Studio and removed. By tipping in the command boxplot.stats()$out R calculates outliers via Tukey's method which

use interquartile (IQR) range approach. To test for significance of the measurement values GraphPad Prism 8.0.2 was used. With this software an unpaired t-test was performed. The DR5 induction assay was repeated three times independently and each time two biological replicates were performed per designed construct.

2.2.1 UMAG_00628 as inducer of auxin signalling

The subcellular localization assay verified that UMAG_00628 induces auxin signalling. According to the fold change values there is a tendency of the effector to prefer C-terminal to N-terminal tags. And its function takes full effect with smaller tags (see Um00628-myc). The microscopic images could detect an interesting localization preference of the effector: the nucleolus (Figure 13 CLSM images of subcellular localization variants of UMAG_00628.). According to the microscopic analysis the myristylation and the nuclear export signal tag could not force the effector completely out of the nucleus. The Myr-, both NLS- and the N-terminal myc-tag could not be detected via western blot (Figure 11 Proof of full-length expression of subcellular localization construct variants with the western blot technique.).

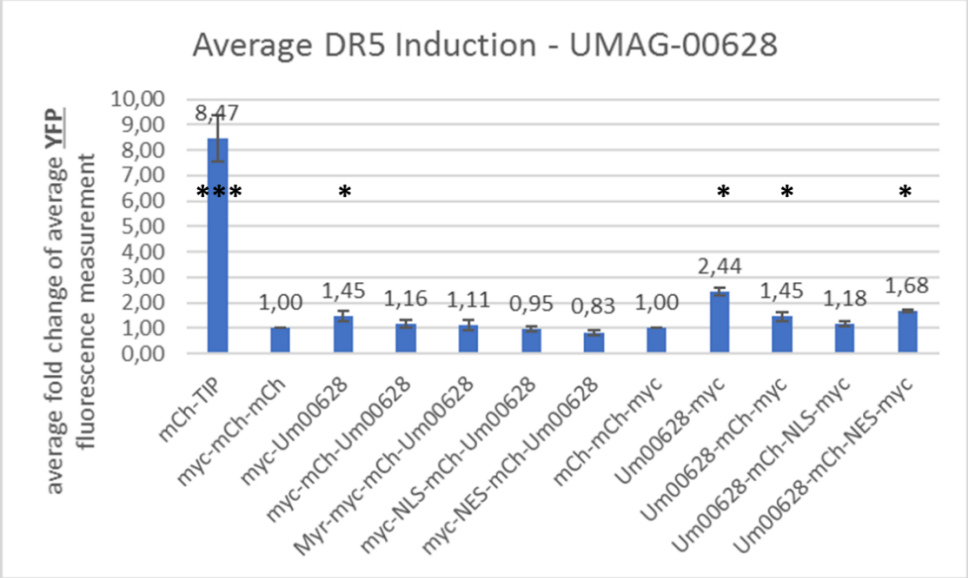

Figure 2 Relative induction of auxin signalling by UMAG_00628 in N. b.

The DR5:YFP reporter system was co-infiltrated to measure changes in induction caused by sending the effector UMAG_00628 to different subcellular localizations. The tags were fused either to the C- or N-terminus of the effector. Two plants per construct variation were infiltrated for one experimental setup. The relative induction of DR5:YFP, here referred to as fold change, was normalized to the basal reference level of the negative induction control myc-mCherry-mCherry (for all N-terminal tags) and mCherry-mCherry-myc (for all C-terminal tags), respectively. The experiment was repeated three times independently. Possible outliers were identified in R Studio and removed. Then the fold changes of each tag version in all three experiments were averaged in Excel. To determine if the results were significant an unpaired t-test was performed in GraphPad Prism 8.0.2. Abbr.: mCh = mCherry; TIP = TIP1; Um00628 = UMAG_00628; Um02852 = UMAG_02852, Myr = myristylation tag; NLS

= nuclear localization signal tag; NES = nuclear export signal tag; ns (not significant) = P value > 0.05, * = P ≤ 0.05, ** = P ≤ 0.01, *** = P ≤ 0.001, **** = P ≤ 0.0001.

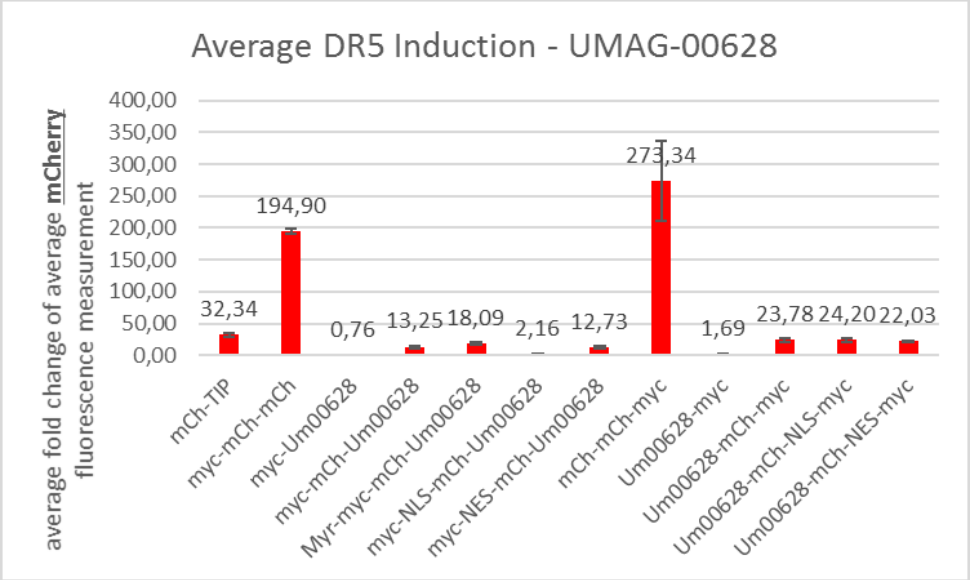

Figure 3 Protein synthesis of subcellular localization constructs of UMAG_00628 within the infiltrated leave area.

By measuring the mCherry fluorescence (at λex = 570 nm and λemm= 610 nm) all mCherry-tagged effector constructs can be detected meaning that those tag versions were synthesized and present in the inspected sample. The measurements were set in relation to the negative controls myc-mCherry-mCherry (for all N-terminal tags) and mCherry-mCherry-myc (for all C-terminal tags), respectively. The average fold change over all three experiments was calculated using Excel. Beforehand possible outliers were identified in R Studio and removed.Abbr.: λex = excitation wave length; λemm = emission wave length; mCh = mCherry; TIP = TIP1; Um00628 = UMAG_00628; Um02852 = UMAG_02852, Myr = myristylation tag; NLS = nuclear localization signal tag; NES = nuclear export signal tag.

2.2.2 UMAG_02852 as inducer of auxin signalling

The evaluation of the DR5 Induction measurements revealed an enhanced auxin signalling due to UMAG_02852. Tendentially the N- or C-terminal mCherry or NES tag do less interfere with the DR5 inducing activity compared to the other variations. The taken images of the confocal microscopy analysis visualize that UMAG_02852 is natively localized in the cytoplasm but also in the nucleus (Figure 14 CLSM images of subcellular localization variants of UMAG_02852.). No pictures could be taken of the Myr-tag. In the western blot only the myc-tagged versions of UMAG_02852 could not be visualized on the membrane (Figure 11 Proof of full-length expression of subcellular localization construct variants with the western blot technique.).

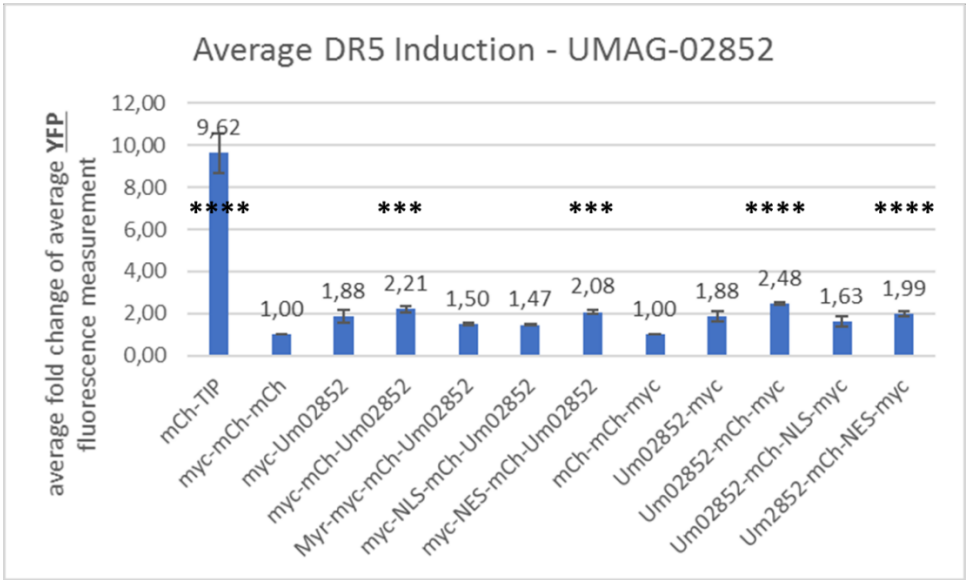

Figure 4 Relative induction of auxin signalling by UMAG_02852 in N. b.

The DR5:YFP reporter system was co-infiltrated to measure changes in induction caused by sending the effector UMAG_02852 to different subcellular localizations. The tags were fused either to the C- or N-terminus of the effector. Two plants per construct variation were infiltrated for one experimental setup. The relative induction of DR5:YFP, here referred to as fold change, was normalized to the basal reference level of the negative induction control myc-mCherry-mCherry (for all N-terminal tags) and mCherry-mCherry-myc (for all C-terminal tags), respectively. The experiment was repeated three times independently. Possible outliers were identified in R Studio and removed. Then the fold changes of each tag version in all three experiments were averaged in Excel. To determine if the results were significant an unpaired t-test was performed in GraphPad Prism 8.0.2. Abbr.: mCh = mCherry; TIP = TIP1; Um00628 = UMAG_00628; Um02852 = UMAG_02852, Myr = myristylation tag; NLS = nuclear localization signal tag; NES = nuclear export signal tag; ns (not significant) = P value > 0.05, * = P ≤ 0.05, ** = P ≤ 0.01, *** = P ≤ 0.001, **** = P ≤ 0.0001.

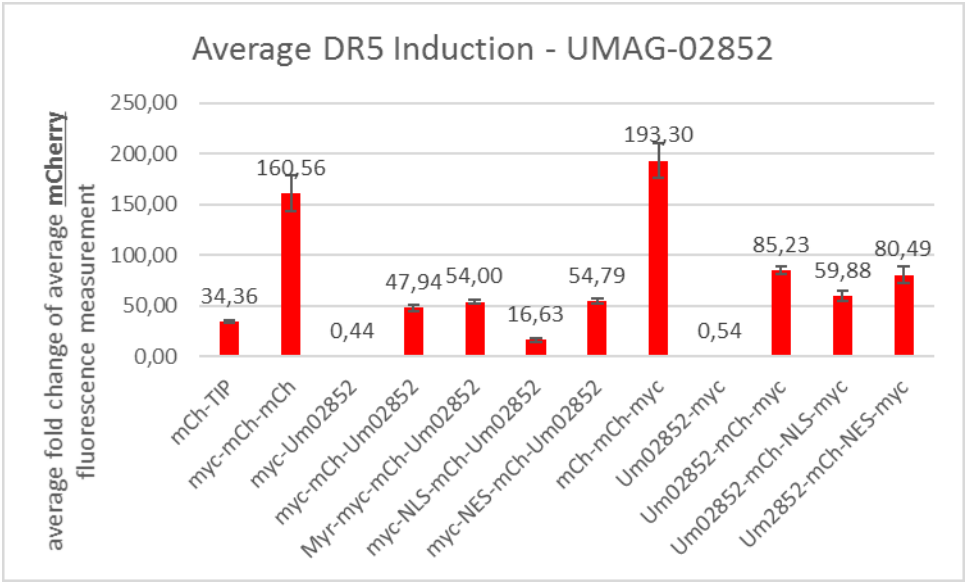

Figure 5 Protein synthesis of subcellular localization constructs of UMAG_02852 within the infiltrated leave area.

By measuring the mCherry fluorescence (at λex = 570 nm and λemm= 610 nm) all mCherry-tagged effector constructs can be detected meaning that those tag versions were synthesized and present in the inspected sample. The measurements were set in relation to the negative controls myc-mCherry-mCherry (for all N-terminal tags) and mCherry-mCherry-myc (for all C-terminal tags), respectively. The average fold change over all three experiments was calculated using Excel. Beforehand possible outliers which are observations that lie

outside 1.5 * IQR, where IQR, the 'Inter Quartile Range' is the difference between 75th and 25th quartiles, were identified in R Studio and removed. Abbr.: λex = excitation wave length; λemm = emission wave length; mCh = mCherry; TIP = TIP1; Um00628 = UMAG_00628; Um02852 = UMAG_02852, Myr = myristylation tag; NLS = nuclear localization signal tag; NES = nuclear export signal tag.

2.3 Mass Spectrometry Analysis of Possible Effector Interacting Proteins (PEIPs)

In order to further illuminate the functional role of the two effector candidates their expression level were verified via western blot and hence send for mass spectrometry (MS) to discover possible targets of their function. Both, the co-immunoprecipitation (Co-IP) and the MS analysis were performed by Pettkó-Szandtner Aladár and his laboratory in Hungary. For this analysis plants were infiltrated with either the UMAG_00628-mCherry-myc and the UMAG_02852-mCherry-myc construct and mCherry-mCherry-myc as control. Of each sample 0,5 g were weighted, frozen and shipped in dry ice. To reduce and avoid carry-over all samples were separated by two *Arabidopsis* RBR (retinoblastoma related protein) samples. All identified proteins that were further studied in this master thesis showed to be specifically co-immunoprecipitated with the investigated auxin signalling inducing effectors and were not found in the mCherry-mCherry-myc control sample. The candidates and general molecular information are listed in Table 2 Possible Effector Interacting Proteins (PEIPs) inclusive Mass Spectrometry analysis data and general information.

Table 2 Possible Effector Interacting Proteins (PEIPs) inclusive Mass Spectrometry analysis data and general information

Effector	Accession #	Gene Name	Protein Name	Protein Length (aa)	Molecular Weight (Da)	Unique Peptide Count	Coverage [%]	Molecular/ Biological Function
UMAG_00628	A0A1S3XHF8	LOC107765175	auxin transport protein BIG-like, E3 ligase	4,468	495,549	3	1,2	zinc ion binding (molecular), polar auxin transport (Gil et al. 2001; Luschnig 2001)
	A0A1J6K598	A4A49_29707	Uncharacterized protein	252	28,552	3	15,5	nucleic acid binding (molecular)
	A0A1S4AWJ2	LOC107802062	vesicle-associated membrane protein 714-like	220	24,977	2	16,4	vesicle-mediated transport (biological), Involved in the targeting and/or fusion of transport vesicles to their target membrane (Sanderfoot et al. 2000)
UMAG_02852	Q6JE37	CITRX2	Thioredoxin-like protein CITRX2, chloroplastic	181	20,560	1	9,9	protein disulfide oxidoreductase activity (molecular); cell death, cell redox homeostasis, defence response, glycerol ether metabolic process, negative regulation of plant-type hypersensitive response, regulation of defence response (biological)(Léveillard and Aït-Ali 2017; Rey et al. 1998; Rivas et al. 2004a)
	A0A1J6I3H4	A4A49_33514	Thioredoxin domain-containing protein 9-like protein	210	24,243	2	10,5	cell redox homeostasis (biological) (Gelhaye et al. 2005; Meyer et al. 2008)

2.4 Virus-induced gene silencing (VIGS) of PEIPs and subsequent detection of changes in DR5 induction

To study the possible role in auxin signalling of PEIPs virus-induced gene silencing (VIGS) can help to gather crucial information about the molecular mechanisms and bring more light on this subject. By silencing the target PEIP its native activity stops leading to detectable biological changes. In this paragraph the results of VIGS and their evaluation will be presented.

The following *N. b.* genes of PEIPs were silenced according to protocol: Niben101Scf06560g02002.1 (*Nb*BIG), Niben101Scf05306g02017.1 (*Nb*Unchar-Prot), Niben101Scf08515g00019.1 (*Nb*VAMP714-like), Niben101Scf15049g00002.1 (*Nb*CITRX2) and Niben101Scf00439g10054.1 (*Nb*TXNDC9). As a control for VIGS efficiency, *N. b.*'s phytoene desaturase (PDS) which causes photobleaching was silenced (TRV:*Nb*PDS). As a negative control for a protein interaction GFP (green fluorescence protein) was silenced (TRV:GFP). For the experiment 5 replicates were used and the experiment was repeated three times independently. The efficiency and specificity of gene silencing would still need to be confirmed by applying qPCR which quantifies transcription levels in the control and sample plants.

As a reporter system for the DR5 induction assay DR5:mCherry was infiltrated. Therefore, the fluorescence as change indicator of the auxin signalling induction level was measured at λex = 570 nm and λemm= 610 nm. As negative control for DR5 induction beta-glucuronidase (GUS) was selected and infiltrated as GUS-myc construct. The construct TIP1-myc was used as positive control for the induction of auxin signalling. UMAG_00628-myc or UMAG_02852-myc were co-infiltrated with the DR5:mCherry reporter system in their respective PEIP-silenced plant. All values were normalized and set in relation to the non-protein interaction control TRV:GFP infiltrated with the negative DR5 induction control GUS-myc. The relative fold change of the average mCherry fluorescence per construct was calculated. The fold changes of all three experiments were averaged and statistically evaluated for significance. To do so an unpaired t-test was performed with the software GraphPad Prism 8.0.2 (263). The setup for the experimental design was unpaired and the gaussian distribution parametric. Asterix indicate significant differences from the control GFP plant (unpaired t-test, ns (not significant) = P value > 0.05, * = P ≤ 0.05, ** = P ≤ 0.01, *** = P ≤ 0.001, **** = P ≤ 0.0001).

2.4.1 VIGS of UMAG_00628 Interacting Protein

By performing VIGS potential ways of UMAG_00628 being involved in auxin signalling induction during infection can be determined. Three potential interacting proteins previously identified by MS were taken into deeper analysis. *Auxin transport protein BIG-like* (BIG), *uncharacterized protein* (Unchar-Prot) and *vesicle-associated membrane protein 714-like* (VAMP714) were silenced in *N. b.* plants and their possible relationship to UMAG_00628 was further analysed in a subsequent DR5 induction assay.

2.4.1.1 *Nb*BIG silenced plants show abbreviated stem growth and significant changes in DR5 induction

According to literature BIG possesses zinc ion binding abilities and is involved in polar auxin transport (Gil et al. 2001; Luschnig 2001). Transient expression of TRV:*Nb*BIG compared to TRV:GFP controlled plants resulted in a changed phenotype of *N. b.* planta. The stem showed a conspicuously shortened length as well as stronger wrinkled young leaves compared to the control plant throughout all three independent experiments (Figure 15 Single-lens reflex camera pictures of VIGS phenotypes.). Compared to the base level of DR5 induction determined by TRV:GFP silenced plants infiltrated with the effector UMAG_00628, TRV:*Nb*BIG silenced plants infiltrated with UMAG_00628 showed a slight significant increase of DR5 induction (Figure 6 Relative induction of auxin signaling of VIGS planta.).

2.4.1.2 *Nb*Unchar-Prot silenced plants showed no remarkable alteration in natural phenotype and no significant changes in DR5 induction

The sequence of uncharacterized protein shows the characteristics of DNA binding domains (**uniport.org**). Silencing *N. b.* plants with the vector TRV:*Nb*Unchar-Prot resulted in no noticeable changes of the physical plant appearance contrasted to the TRV:GFP control (Figure 15 Single-lens reflex camera pictures of VIGS phenotypes.). Additionally, the DR5 induction assay performed on TRV:*Nb*Unchar-Prot silenced plants infiltrated with UMAG_00628 revealed no significant changes in contrast to the basal induction level of auxin signalling by TRV:GFP infiltrated with UMAG_00628 (Figure 6 Relative induction of auxin signaling of VIGS planta.).

2.4.1.3 *Nb*VAMP714 silenced plants showed no remarkable alteration in natural phenotype and no significant changes in DR5 induction

Previous research papers have demonstrated the involvement of VAMP714 proteins in the targeting and/or fusion of transport vesicles to their target membrane (Sanderfoot et al. 2000). No variation in the phenotype of TRV:*Nb*VAMP714 silenced plants arose compared to the TRV:GFP silenced control (Figure 15 Single-lens reflex camera pictures of VIGS phenotypes.). No significant differences between the average fold change of TRV:*Nb*VAMP714 silenced organisms and TRV:GFP silenced ones could be detected via unpaired t-test (Figure 6 Relative induction of auxin signaling of VIGS planta.).

2.4.2 VIGS of UMAG_02852 Interacting Protein

To clarify which functional role UMAG_02852 plays during plant-pathogen interaction VIGS is performed on two MS-identified interaction partners. *Thioredoxin-like protein CITRX2* (CITRX2) and *Thioredoxin domain-containing protein 9-like protein* (TXNDC9) were silenced and their potential interaction to UMAG_02852 was eventually evaluated by running a DR5 induction experiment.

2.4.2.1 *Nb*CITRX2 silenced plant's phenotype displays same symptoms as TRV:PDS one and results in a highly significant difference in DR5 induction

CITRX2's function is connected to plant defence and possesses protein disulfide oxidoreductase activity (Rivas et al. 2004a). The phenotype of TRV:*Nb*CITRX2 silenced plants displays photobleaching on many leaves and are in general of smaller size as the control TRV:GFP. In total their natural physique reminds more of the silencing control TRV:*Nb*PDS (Figure 15 Single-lens reflex camera pictures of VIGS phenotypes.). Furthermore, the average fold change of TRV:*Nb*CITRX2 is highly significant in contrast to the reference TRV:GFP infiltrated with UMAG_02852 (Figure 6 Relative induction of auxin signaling of VIGS planta.). Due to the high level of photobleaching the leaves were very thin and fragile which made punching leave discs more complicated that's why some leave discs were lost minimizing the pool of measurements.

2.4.2.2 *Nb*TXNDC9 silenced plants show a dwarf phenotype and a very significant DR5 induction level

TXNDC9 plays a part in the biological process cell redox homeostasis (Gelhaye et al. 2005; Meyer et al. 2008). Throughout all three experiments the silenced TRV:*Nb*TXNDC9 plants were dwarf-sized. The leaves were smaller and thicker and appeared darker green than the TRV:GFP control (Figure 15 Single-lens reflex camera pictures of VIGS phenotypes.). The evaluation of the DR5 induction measurement via unpaired t-test resulted in a very significant decrease of auxin signalling induction in comparison to TRV:GFP infiltrated with UMAG_02852 (Figure 6 Relative induction of auxin signaling of VIGS planta.).

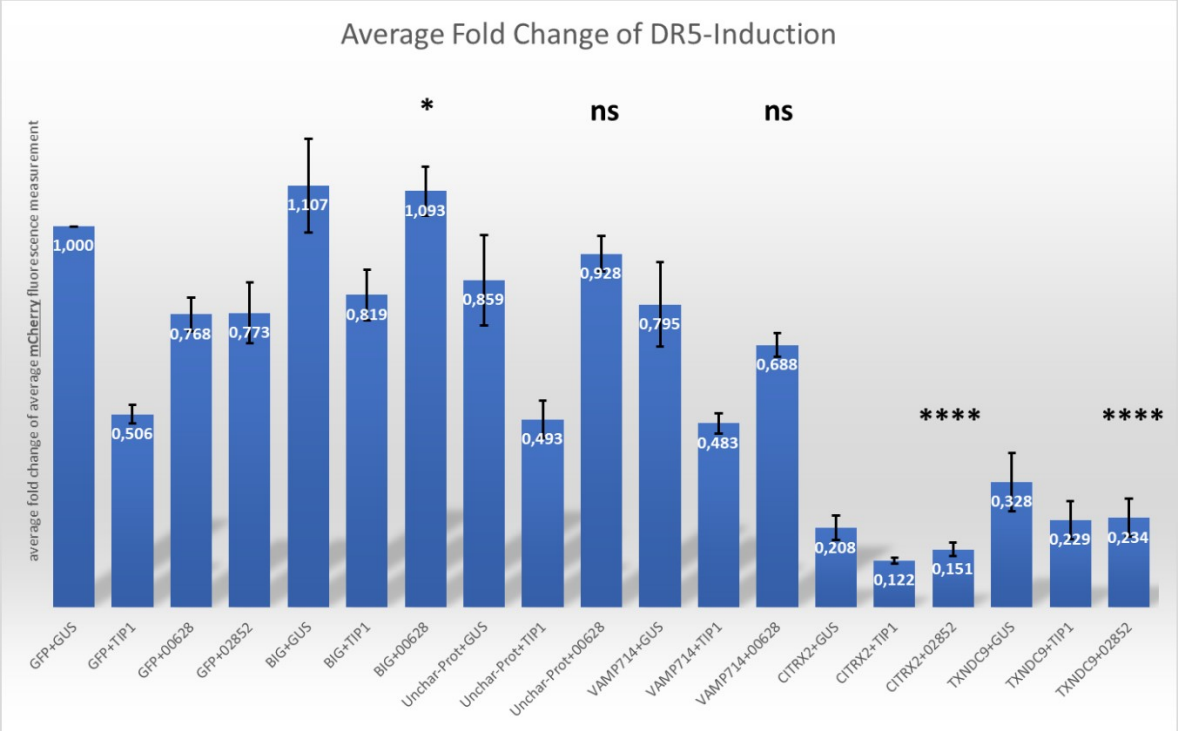

Figure 6 Relative induction of auxin signaling of VIGS planta.

The corresponding N. b. genes of the MS hits were silenced by applying VIGS. TRV:NbPDS is the control for the integrity of the VIGS technique. TRV:GFP serves as control for a silenced non-interacting partner of the effector. The PEIPs NbBIG, NbUnchar-Prot and NbVAMP714 were silenced to test for their interaction with UMAG_00628. The PEIPs NbCITRX2 and NbTXNDC9 were silenced to test for their interaction with UMAG_02852. Pictures of the silenced plant phenotype can be found in the supplementary.

Then the DR5 induction assay was performed by infiltrating the VIGS plants with the associated effector. The reporter system for DR5 induction is DR5:mCherry. As a negative DR5 induction control GUS was chosen. The positive control for auxin signalling is TIP1. Each VIGS candidate was infiltrated with GUS, TIP1 and the corresponding effecter, respectively. The fold change of the average mCherry fluorescence measurement per experiment was calculated in Excel. The fold change of each sample was normalized to the reference silencing model (TRV:GFP) infiltrated with the negative DR5 induction control (GUS), termed GFP+GUS. Then the average fold change of all three independent experiments was computed which is displayed in this figure. The performed unpaired t-test in GraphPad Prism 8.0.2 identified possible significant results.

Abbr.: MS = mass spectrometry; VIGS = virus-induced gene silencing; TRV = tobacco rattle virus; PEIP = possible effector interacting protein; PDS = phytoene desaturase; GFP = TRV:GFP; GUS = beta-glucuronidase; TIP1 = TOPLESS interacting protein 1; 00628 = UMAG_00628; 02852 = UMAG_02852; BIG = TRV:NbBIG; Unchar-Prot = TRV:NbUnchar-Prot; VAMP714 = TRV:NbVAMP714; CITRX2 = TRV:NbCITRX2; TXNDC9 = TRV:NbTXNDC9; ns (not significant) = P value > 0.05, * = P ≤ 0.05, ** = P ≤ 0.01, *** = P ≤ 0.001, **** = P ≤ 0.0001.

3 Discussion

3.1 Is UMAG_00628 involved in auxin signalling?

The DR5-reporter induction as an indicator for auxin signalling response in *N. benthamiana* confirmed the previous findings that UMAG_00628 is inducing this plant growth hormone signalling pathway. Furthermore, my results indicate that the effector has the tendency to tolerate C-terminal tags over the N-terminal ones as well as smaller tags better than the larger ones according to the statistical analysis with GraphPad Prism 8.0.2. (Figure 2). The mCherry fluorescence measurement represent the relative protein expression of the effector variants in the leaf discs and was used to normalize the DR5:YFP reporter fluorescence results. A correlation that C-terminal tags were more expressed due to their stabilizing effect on the protein could therefore be made. Furthermore, decreased DR5:YFP induction of some tags could be the result of mislocalization to compartments in which the effector could not interfere with the respective host components. The made observations are not a complete representation of the natural processes, and this experimental set-up can only give an one effector-view what might be going on with the effector in an infected cell. To confirm the fluorescence measurements as results of the different subcellular mislocalization tags, fluorescent microscopy has been performed.

The confocal microscopy images (Figure 13) strongly suggested that UMAG_00628 is localized in the nucleus, especially in the nucleolus, which contradicts the DR5 induction measurements, because particularly the NLS tags yielded no significant auxin response in contrast to the NES, mCherry or the small myc tag. Lightly overexposing the taken images of myc-mCh tagged constructs clearly showed that there was also a fair amount of UMAG_00628 located in the cytosol and membrane. However, the comparison between confocal microscopy detection and the DR5 induction must be regarded carefully, since they were two different and independent experiments. Therefore, it is possible that there were differences in the efficiency of infiltration between the experiments. On the other hand, three times independently the experiments repeatedly displayed the same outcomes and hence become valid observations.

These results could be interpreted as follows: that either this is the rest signal of the mCherry-tagged protein being translated in the cytosol or the transport machinery to the

respective subcellular compartment is due to overexpression of UMAG_00628 overloaded. Another explanation could be a dual localisation to the cytosol and the nucleus due to a dual function. Comparing the localisation to the DR5:YFP reporter assay results supports the idea that UMAG_00628 has a dual function, because the measurements for the NLS tags were not significant compared to the C-terminal mCh or NES tags. A cleavage of the protein from the NLS tag could be an explanation for this observation and is likely because the western blot could not detect the full-length protein twice. Nevertheless, because the nucleolus localization is such a prominent structure, it is highly likely that the observed localisation of UMAG_00628 has a connection with one of its function. The myristylation and nuclear export signal tags were repeatedly unable to localize the effector solely to the target localization. Always a rest signal of fluorescence could be detected in the nucleus and nucleolus which indicates some host binding factors for the respective effector candidate in the specific localisation. According to an informatic screen performed by Jason Bosch, UMAG_00628 was predicted to possess a nuclear localization signal, which could possibly interfere with the Myr or NES tag. By mutating the NLS sequence I would test if it comes again to the postulated interference with other localization tags in the microscopic detection. This interference could explain why the microscopic images showed that the nuclear and cytosolic localizations fluoresced.

The detection of the full-length protein expression via western blot of UMAG_00628 fused to different tags (Figure 11) can be compared with the observations of the DR5 induction assay and microscopic localization, although they were independent experiments because they consistently behaved the same yielding repeatedly very similar results. The N-terminal myc-tag, the Myr-tag and the NLS-tag could not be detected via western blot twice. Too low protein expression levels could be the reason for no detection via western blot - or the extraction of the tag variants differs in efficiency. In this case, the extraction protocol must be adapted for example by changing the buffer concentrations. However, there is no correlation between the tag types that were detected and the ones that were not, suggesting that this is more likely to be due to low protein levels in the sample.

According to mass spectrometry following Co-IP with UMAG_00628-mCherry-myc, we identified a regulator of auxin transport (auxin transport protein BIG-like), an uncharacterized protein (A4A49_29707) and a vesicle-associated membrane protein (714-like) to potentially

interact with the effector (Table 2). These hits were taken into closer consideration, because they were unique hits for this effector, showed sufficient high scores in “coverage” and in “unique peptide count”, respectively, as well as their promising functional or localisation-based connection to UMAG_00628.

3.1.1 BIG

BIG, despite being hypothesised to locate in the cytosol, which does not ideally go hand in hand with the observed localization of UMAG_00628, since it was apparently primarily localized in the nucleus, more precise in the nucleolus, caught our attention due to its link to the molecular role in growth hormone auxin signalling. According to modern literature, BIG is found to be a key player in polar auxin transport and maintains a normal auxin efflux (Gil et al. 2001). Moreover, it is required for auxin-mediated developmental responses (Guo et al. 2013), which can be observed once the integrity of BIG protein is deranged leading to diverse morphological symptoms (Ruegger et al. 1997). Further experimental findings also connect its molecular role to the ability to manipulate auxin signalling (Li et al. 2018). With 560 kDa BIG is of enormous size. The protein contains several conserved Zn finger domains. One of these is found in ubiquitin ligases, another one is common among eukaryotic transcription factors and a third appears in the ubiquitination pathway (Gil et al. 2001). These features would perfectly match the attributes necessary for auxin signalling, because in order to induce auxin signalling the active repressor (Tiwari et al. 2001) is modulated by ubiquitination through an E3 ligase (Kepinski and Leyser 2002). The region with transcription factor characteristics further affirms the theory that BIG might be involved in auxin signalling. However, because BIG is so tremendously large, it would need an active transport into the nucleus since passive diffusion only allows molecules of the size of 60 kDa. Here our effector would come into the picture: Due to the microscopic localization and the functional DR5 assay UMAG_00628 seems to be operating best in the cytosol and the nucleus. Therefore, one possible role of the effector could be to enhance the organism’s endogenous system to shuttle BIG into the nucleus to increase its presence there.

Silencing each candidate via VIGS resulted in some changes in the physical appearance of the model organism *N. benthamiana* (Figure 15). BIG silenced *N. benthamiana* plants displayed shortened stem growth and more strongly wrinkled young leaves. This finding is supported by previous literature, which states that the disruption of auxin transport affects

critical processes like stem elongation and petiole length (Gil et al. 2001; Morris et al. 2010; Lomax et al. 2013). Experiments in the future should focus on testing for the abbreviated apical growth, also the stem length of all plants from all three independent experiments should be measured, followed by a statistical analysis to prove that BIG silenced plants tend to be indeed of smaller size.

Evaluating the outcome of the DR5:YFP reporter induction performed on the PEIP silenced plants revealed a significant increase in the DR5 induction of BIG silenced plants (Figure 6). It appears that initially BIG gets manipulated by the effector which causes its inactivation so the auxin signalling pathway can be upregulated. On the other hand, BIG and UMAG_00628 are not connected because although BIG is missing it does not influence the effector's effect on auxin signalling because it is still inducing the reporter system. No further statement about the mechanism behind this observed behaviour can be made, because of the technical issue noticed with the performed DR5 induction assay. The reference module DR5::mCherry was contaminated yielding wrong fluorescence values and rendering all the measurements of this experimental set-up invalid (Figure 17).

3.1.2 Uncharacterized Protein A4A49_29707

Because we are dealing with an uncharacterized protein its amino acid sequence was blasted in NCBI to check for homologues, especially in the well characterized organism *Arabidopsis thaliana* (*A. th.*). The only annotated hit of this search yielded a ribosomal protein S24e family protein with about 40% identity. The similarity referred to the region containing a conserved domain at the middle and end part of the protein sequence (80-200 aa). This conserved domain was identified as a RNA recognition motif (RRM) which can be found in heterogeneous nuclear ribonucleoprotein H protein (hnRNP). RRMs are usually contained in RNA-binding proteins, which are responsible for RNA metabolism like post-transcriptional gene regulation of RNA (such as mRNA and rRNA processing, RNA export, translation, localization, stability, and turnover) (Lunde et al. 2007) and ribosome biogenesis (Andrade et al. 2018) (Maris et al. 2005) (ncbi). This research proposes that the uncharacterized protein (Unchar-Prot) might be a RNA-binding protein.

UMAG_00628 and Unchar-Prot could be interaction partners because in the microscopic localization analysis (Figure 13) the effector appeared primarily in the nucleolus

and nucleus (but also in the cytosol), which would overlap with the localization of RNA-binding proteins. The prominent nucleolus localization could indicate that UMAG_00628 might be also involved in the ribosome biogenesis since the nucleolus was identified to be the factory of ribosomes. Furthermore, the nucleus and the cytosol localization would match the synthesis pathway of a ribosome (Lam and Trinkle-Mulcahy 2015). Additionally, ribosome biogenesis factors which are RNA-binding proteins like the PEIP candidate are involved in this cellular process. This could be a potential link between UMAG_00628 and Unchar-Prot however not directly to the auxin signalling pathway.

Evaluating the outcome of the DR5:YFP fluorescence measurement resulted no significant DR5 induction (Figure 6). As UMAG_00628 could no longer generate the inducing effect on auxin signalling I postulate that the Unchar-Prot plays a positive part in the auxin signalling pathway. Because the protein is still uncharacterized I cannot make any more assumptions about how the molecular function of the PEIP is manipulated by the effector. Unfortunately, the result of the DR5 induction assay performed on VIGS plants was invalid because it became known that the reporter system was contaminated yielding wrong measurements (Figure 17).

The Unchar-Prot silenced plants exhibited no obvious alterations in the phenotype of the plant organism *N. benthamiana* (Figure 15). Indicating that either the silencing process was not successful, which can be tested via RT–qPCR using gene-specific primers to determine the mRNA levels or VIGS candidate does not play a role or its function is redundant and can be compensated in a plant's developmental process.

3.1.3 VAMP714

Recently published papers have provided evidence that besides the known active transport of auxin across the plasma membrane there likely exists a transport via vesicular carriers and signal-mediated vesicular trafficking as well. This unique polar cell-cell transport traversing the whole plant body is its most characteristic feature. A vesicular secretion of auxin would allow a more finely-tuned control of auxin influx and efflux, which would be a suitable match for a mobile multipurpose signalling and communicator molecule that is said to have hormone, morphogen and neurotransmitter-like properties depending on the developmental or environmental context (Baluška et al. 2003; Baluška et al. 2008).

Vesicle-associated membrane proteins (VAMPs) belong to the family of SNARE proteins, which are soluble NSF (N-ethylmaleimide-sensitive factor) attachment protein receptors that constitute the core membrane fusion machinery of intracellular transport and intercellular communication. Our PEIP VAMP714 was identified via blast search in NCBI to contain a longin (a long N-terminal domain of a subset of SNAREs) and a synaptobrevin domain, which is a small integral membrane protein of secretory vesicles and part of VAMPs (Daste et al. 2015). I postulate the connection of the auxin hormone pathway and the cellular vesicle transport. Since endosomes have been reported to associate with the nuclear envelope transporting molecules from the surface or shuttling the cargo from the membrane to the Golgi apparatus and further to the endoplasmic reticulum (Chaumet et al. 2015) this could be a mechanism to manoeuvre auxin to the nucleus in order to induce a directed signalling response.

The prevalently nucleolus and nuclear localized UMAG_00628 also displayed signal in the cytosol (Figure 13) and still showed DR5 induction activity (Figure 2) when translocated outside the nuclear localization. Therefore, I suppose that a dual function might be the cause for these observations, which could link its function as inducer of auxin signalling to the vesicle transport system. In the event of the VIGS-based forward genetics screen it was tested if the MS hit VAMP714 is involved with one of the suspected effector's functions. The evaluation of the DR5 induction assay performed on the VAMP714 silenced plants revealed no significant induction or reduction in the fluorescence measurement (Figure 6). By silencing VAMP714 UMAG_00628 appeared to have lost its function as an inducer of the auxin signalling pathway. However, these results cannot be interpreted further, because the reference module DR5::mCherry was contaminated yielding wrong fluorescence values (Figure 17) making the experimental outcome invalid.

The phenotype of VAMP714 silenced plants exhibited no noticeable alterations (Figure 15). This could mean that the silencing process was not efficient, which could be tested by performing RT-qPCR or that the silenced protein does not affect the development of the plant seriously.

3.2 UMAG_02852 interfering with auxin response?

UMAG_02852 induces auxin signalling. This observation is based on the effector library wide screen previously performed and could be confirmed by independent experiments performed in the framework of this thesis. The experimental outcome is backed by statistical analysis for significance via GraphPad Prism 8.0.2. discovering that all UMAG_02852 tag variations resulted in a significant induction of the DR5:YFP reporter (Figure 4). The highest significant results from the DR5 induction assay revealed that UMAG_02852 worked better when fused to big tags, especially the mCh alone as well as the NES tag, and slightly better with C-terminal than to the N-terminal tags. The allegedly preference to larger tags as well as the position of the tag might be a direct result of enhanced stability. The samples with a higher induction also showed the higher mCherry fluorescence measurement, meaning more proteins were present to induce more DR5:YFP reporter expression.

Regarding the confocal microscopy localization UMAG_02852 was initially located in the cytoplasm and the nucleus (Figure 14). All images of the various tags displayed signals in the target regions. No localization picture of the effector combined with the myristylation tag could be taken repeatedly although the DR5 induction assay demonstrated that it was inducing. This observation can be explained because both experiments were not performed on the same plant - therefore the protein expression after infiltration could have been more efficient than in the other. Another explanation could be that the fusion protein was cleaved but the detection of the full-length expression proved that this was not the case. Overexposing the microscopic images of the NLS tag constructs clearly showed no fluorescence outside the nucleus. The NES tag variants displayed fluorescence in the nucleus, but taking a closer look indicates that the signal is surrounding the nuclear envelope. Combining the observations of the DR5 induction and the microscopy the results indicate that for its proper function the effector needed a big stabilizing tag, but without a mis-localization signal and showed highest DR5:YFP reporter induction when localized to the nucleus and the cytoplasm.

By performing western blot, the full-length expression of subcellular localization construct variants was proven (Figure 11). All tag combinations, except for the small myc tags, were detected on the membrane. Although the effector tagged with myc showed induction in the DR5 induction assay these tags could not be detected via western blot. The most obvious explanation for this observation is that the expression level for this small fusion protein in this

independent experiment was too low to show any signal on the membrane. Alternatively, the myc-tag effector fusion protein could get processed so the tag is no longer detectable because the fragment is too small. However, against this theory speaks the finding that larger tags seem to stabilize the protein and do not inhibit its activity.

According to mass spectrometry UMAG_02852 showed to be co-immunoprecipitated with a chloroplastic protein (Thioredoxin-like protein CITRX2) and a protein involved in the cellular redox homeostasis (Thioredoxin domain-containing protein 9-like protein). These hits were taken into closer consideration, because they were unique hits for this effector, showed good scores in “coverage” and “unique peptide count”, respectively, as well as their hypothetical link to auxin signalling according to scientific papers (Table 2).

3.2.1 CITRX2

A protein blast search in NCBI revealed that CITRX2 possesses a putative conserved domain, which is found among members of the thioredoxin-like superfamily. Most of these proteins contain a classic thioredoxin (TRX) domain with a redox active CXXC motif, which gives them the ability to alter the redox state of target proteins via the reversible oxidation of their active site dithiol. So, they function as protein disulfide oxidoreductases (PDOs). In eukaryotes, these members reside in the cytoplasm and the mitochondria, but are also found in chloroplasts of higher plants (like *A. th.*). Generally, thioredoxins are key player in the maintenance of cellular redox homeostasis and essential for plant development, cell division and responses to environmental stress. They assist regulating various cellular processes like gene expression, signal transduction, proliferation and apoptosis and are also important for defence against oxidative stress (Lee et al. 2013).

The group of Bashandy et al. were the first to highlight a direct connection of the cellular redox system and the auxin signalling by generating a triple mutant in thioredoxin and glutaredoxin signalling. These redox regulated target proteins seemed to be involved in auxin activity, because those mutants showed a deficiency in auxin metabolism, transport and signalling caused most properly by the decreased auxin (IAA) concentrations (Bashandy et al. 2010; Bashandy et al. 2011; Eckardt 2010).

A recent paper on CITRX provided insight in its crucial role as regulator for diverse signalling pathways (MAPKs and CDPKs) that govern defence responses in tomato and tobacco

(Rivas et al. 2004b). Both MAPKs and CDPKs signalling pathways are suspected to be part of the auxin signal transduction (Tognetti et al. 2012). UniProt annotated CITRX2 to be located in the chloroplast and to play a role in its development. This is supported by the NCBI blast analysis that showed TRX family as a specific hit. There are more than 20 different TRX types in higher plants of which two are located in the chloroplasts regulating the activity of enzymes implicated in photosynthetic carbon assimilation (Meyer et al. 2008). Therefore, it was not too surprising to see that the morphology of the silenced CITRX2 plants was altered (Figure 15). The plants exhibited a smaller, dwarf-like phenotype with mostly bleached leaves. This strongly indicates that CITRX2 indeed is involved in chloroplast development and once silenced the chloroplast formation is hindered. A defect chloroplast leads to a malfunctional photosynthesis system which affects the plant's development drastically as can be seen by the tiny sized silenced plants in our experiment. Correspondingly, the DR5 induction assay performed on CITRX2 silenced *N. benthamiana* showed a significant decrease in fluorescence measurement, meaning that a weaker auxin signal transduction took place (Figure 6).

This result strongly supports what was mentioned in the theory part above, that a perturbation in the TRX signalling pathway has a far-reaching impact on different signalling pathways including auxin signalling. For those reasons, I propose that the effector UMAG_02852 targets a member of the TRX family to manipulate different signal transduction mechanism and operate downstream pathways. This postulation can however not be confirmed by the experiment's outcome, because the measurement turned out to be invalid due to contamination in the reporter system DR5::mCherry (Figure 17). It is also doubtful if performing the DR5 induction assay on a degrading plant makes sense, because with a degrading photosynthesis system the plant steadily shuts down, meaning the cellular activity in general would already be downscaled. A way to test this is to treat the plants with auxin to learn how the auxin capacity is changed in these plants.

3.2.2 TRXDC9

According to the protein blast search in NCBI TRXDC9 contains a putative conserved domain that belongs to the thioredoxin-like superfamily. The specific hit classified a region of the sequence as part of the phosducin (Phd)-like family, a thioredoxin (TRX) domain containing protein 9 subfamily. Those proteins comprise a TRX-like domain without the redox active CXXC motif. Members of the Phd-like family were shown to regulate G-protein signalling and

originally discovered in vertebrate's retina (NCBI). The research for homologs in *A. thaliana* via TAIR revealed TRX domain-containing protein 9 (TXND9) (a thioredoxin-like/ATP-binding protein) and a phosducin (Phd)-like protein 3 homolog (PLP3, functions in microtubule assembly) as two hits with the highest percentage of sequence identity (NCBI, Tair). Both TXND9 and PLP3 seem to be involved in cell redox homeostasis and are speculated to locate in the cytoplasm. PLP3 is also important for cell growth processes like cytokinesis via microtubule organization and is therefore also found in the nucleus (TAIR). Since both thioredoxin-like and phosducin-like proteins are connected to signal transduction pathways, I assume that UMAG_02852 might be aiming for upstream regulation mechanism, which then control auxin signalling.

The DR5 induction assay performed on TRXDC9 silenced plant organisms resulted in a very significant reduction of fluorescence measurement (Figure 6). Not only was UMAG_02852 unable to induce the DR5:YFP reporter system but the whole silenced plant in general showed a decreased activity of auxin signalling compared to the control plant. Reading the current scientific studies on thioredoxin-like superfamily lead to me hypothesizing that a breach in the signal cascade would engender a decline of auxin signalling induction. However, no further conclusion about the speculated connection between UMAG_02852 and TRXDC9 protein can be made based on the DR5 induction assay performed on VIGS plants because of the revealed technical issue of the experiment (Figure 17).

An interesting finding was the observed phenotype of the silenced plant model organism (Figure 15). The morphology severely changed to a dwarf-like size with thicker but more crippled young leaves. Also, the colour of the plant appeared overall darker green than the silencing control. By applying a software for colour quantification (like ImageJ) this subjective observation can be quantified. Which role TRXDC9 protein plays in the pigmentation of a *N. benthamiana*'s phenotype is unclear and needs to be elucidated.

4 Conclusion

It is safe to say that the results of Janos Bindics's effector-library wide screen for auxin signalling could be confirmed by this master thesis. Both effectors UMAG_00628 and UMAG_02852 were significantly inducing the fluorescent DR5 reporter system. The nature of this induction was further explored by performing a Co-IP, following a mass spectrometric analysis to evaluate if the effect of the effectors on the auxin signalling pathway was direct or indirect. The most promising interaction partners were silenced via VIGS tools and a DR5 induction assay was again performed to monitor any consequences to draw further conclusions about the effector's molecular mechanism and possible involvement of the silenced components in auxin signalling.

The subcellular localization study revealed that UMAG_00628 apparently preferred small C-terminal tags and, as shown by microscopic detection, mainly acted in the nucleolus (a nuclear localization signal was predicted by the prediction software LOCALIZER), however not solely. This was the derived conclusion by comparison of both experimental data sets. The subsequent VIGS analysis of three interaction partners - BIG, Unchar-Prot and VAMP714 - helped to assess the hypothetical dual function by enlightening the interaction mechanism of this effector. The silenced BIG protein plants, a major cytosolic component of polar auxin transport and recently linked to auxin signalling, was significantly stronger inducing DR5 than the internal control GUS. These results could indicate that BIG normally leads to degradation of the positive components of the auxin signalling pathway (at the membrane). The previously nucleus and nucleolus localized effector UMAG_00628 potentially possesses a dual function due to its cytosolic localization, which could be its molecular connection to BIG. Nevertheless, no clear statement about the molecular mechanism between the effector and the host protein can be made yet. BIG silenced plants displayed a phenotype similar to the ones described in other literature, which strongly indicates that the silencing method worked. UMAG

In Unchar-Prot silenced plants the heterologous expression of UMAG_00628 resulted in no significant DR5 induction. As UMAG_00628 was previously localized in the nucleus and nucleolus but also needed the ability to reside in the cytosol to maintain its effect on auxin signalling (and because its subcellular localization assay revealed that the effector could handle small tags) I postulate that UMAG_00628 would play the role of an assistant of the

innate active transport system and help to shuttle the folded Unchar-Prot into the nucleus and further into the nucleolus. Additionally, because the NCBI blast for homologues identified a conserved RRM domain in the Unchar-Prot I speculate that taking into consideration modern literature it may possess ribosomal character or be otherwise involved with RNA processing and modification. As a consequence, the effector would have an indirect effect on auxin signalling, because it would manipulate RNA metabolism like post-transcriptional regulation or ribosome biogenesis.

The measurement of the DR5 induction in the third VIGS candidate VAMP714 revealed no significant result. According to nowadays scientific findings VAMP714 is involved in vesicular trafficking, which was recently linked to the plant hormone auxin. However, I could not come up with an ideal model that could connect the prominent nucleolus localization of UMAG_00628 to the intracellular transport system and to the auxin signalling. Unchar-Prot and VAMP714 silenced plants showed no alteration in their physical appearance meaning either that the silencing process did not work or that the function of the silenced proteins is not important for the plant development or even redundant and hence no effects can be observed.

The effector UMAG_02852 significantly induced the expression of DR5 for all subcellular localization tags but performed best with the big mCh tag. According to the observed results it seemed like the larger tags had a stabilizing effect on the effector. The mCh-UMAG_02852 fusion protein was visualized via confocal microscope in the cytoplasm and the nucleus indicating that it may need both locations to fully unfold its potential. To analyse the molecular mechanism of the effector in more detail, two potential interaction partners CITRX2 and TRXDC9 were silenced via VIGS tools.

A significant reduction in the DR5 induction was observed in the activity assay of VIGS CITRX2 plants, a protein known to have thioredoxin character and to be involved in maintaining the redox homeostasis. It was already found in newly released papers that a plants' redox system interacts with auxin signalling. This experimental result could indicate that by silencing an important component of the redox system the signal transduction pathway was disrupted. Therefore, I assume that CITRX2 plays a role in the redox system to transduce signals to the auxin signalling pathway. Apparently CITRX2 is located in chloroplasts of higher plants, which was confirmed by the plant's phenotype because the leaves of the

silenced plants were bleached. However, no chloroplast localization of UMAG_02852 was seen in the microscopic images, which makes a direct interaction between ClTRX2 and the effector doubtful.

TRXDC9 a member of the thioredoxin-like family is regulating G-protein signalling which is in contact with the auxin signalling pathway. The DR5 induction on TRXDC9 silenced plants resulted in a significant decrease of auxin signalling. Therefore, I conclude that in plants missing TRXDC9 UMAG_02852 no longer has the ability to induce the auxin signalling pathway even more so the plant has a reduced auxin signalling activity. I suggest that UMAG_02852 boosts upstream signal transduction by manipulating TRXCD9, which finally ends in a response in auxin signalling activity. However, I suspect a dual function of UMAG_02852 because it was also localized in the nucleus where it could also interact directly with positive component of auxin signalling. A prominent alteration of the plant phenotype was observed, which strongly which implies an interference in pathways that are essential for development like auxin signalling.

Unfortunately, all results of the DR5 induction assays performed on silenced plants were invalid due to the contaminated reporter system.

5 Outlook

To expedite this project in the future, the subcellular localization assay, the confocal microscopy analysis and the detection of the full-length protein expression should be performed on the same plant to exclude differences of technical issues like infiltration efficiency and therefore lead to valid correlations between one another. Next, the mass spectrometric analysis should be performed on the tag fusion protein, which exhibits the most significant result in the DR5 induction assay. To check if the VIGS technique worked efficiently a qPCR should be performed on the silenced plants. This acts as a base for argumentations that following experimental results are really due to the changes caused by silencing. Then the DR5 induction assay on silenced plants needs to be repeated with an intact reporter system so the results can be assessed accordingly. Lastly, the most promising protein-protein interaction must be validated by another molecular technique like Y2H and BiFC analysis. Next, *Arabidopsis* estradiol inducible and *Arabidopsis* overexpressed stable lines carrying the effectors need to be grown to study their function further. Additionally, the respective A.

thaliana knock-out lines of the most promising interaction partners should be ordered from a gene-bank to investigate the molecular connection further. Finally, the virulence impact of effector knock-out strains has to be performed in the maize accession B73, to get a clearer view on their pathogenicity in maize.

6 Chemicals

For this master thesis the needed chemicals were purchased from the following companies: Analytik Jena, Carl-Roth, CenticBiotec, Merck, PanReacAppliChem, Qiagen, Roche, Sigma-Aldrich and Thermo Fisher Scientific.

6.1 Buffers and Solutions

The preparation of the standard buffers and solutions was done according to Ausubel et al. (Ausubel 1997) and Sambrook et al. (Sambrook et al. 1989). All the special buffers and solutions are described in the corresponding methods. If autoclavation of solutions and buffers was required, the conditions were set to 125°C for 15 minutes. In contrast, heat sensitive solutions were filter sterilized using a pore size of 0.2 µm.

6.2 Commercial kits

Kit	Purpose
Qiagen buffers and columns (Centic Biotec)	plasmid preparation
InnuPrep Doublepure Kit (Analytik Jena)	agarose gel elution of PCR products and DNA fragments
Gateway LR Clonasell Enzyme Mix (Thermo Fisher Scientific)	gateway cloning
Trans-Blot® Turbo™ Transfer System (Bio Rad, USA)	Western blotting
SuperSignal™ West PLUS Chemiluminescent Substrate (ThermoFisher Scientific, USA)	chemiluminescence detection
RevertAid First Strand cDNA Synthesis Kit (both Thermo Fisher Scientific, USA)	cDNA synthesis from RNA
Super lll First Strand Synthesis Super Mix Kit	cDNA synthesis from RNA
RNeasy (Qiagen)	RNA extraction

6.3 Enzymes and Antibodies

All restriction enzymes and Polymerases were bought from New England Biolabs and Thermo Fisher Scientific, lytic enzymes from Sigma-Aldrich. The α-MYC antibody (mouse) was ordered from Sigma-Aldrich and the and the HRP-coupled anti-mouse antibody (sheep) from GE Healthcare.

6.4 Plasmids, Vectors, Strains and Oligonucleotides

6.4.1 Plasmids

The following plasmids were used for further cloning:

Notation	Application	Resistance
pJet-Stuffer	advanced positive selection system for high-efficiency cloning of PCR products via blunt ends generated by EcoRV	AmpR
pEntry	NcoI NotI cleavable pEntry for Gateway Cloning in VIGS destination vectors	SpecR
TRV1	TRV1 destination vector for VIGS	KanR, ChlAR
TRV2	TRV2 virus vector for VIGS	KanR, ChlAR
pGG	Binary Green Gate destination vector (ccdB+) for Golden Gate Cloning via BsaI	SpecR, ChlAR

6.4.2 Vectors

The following vectors were used for further experiments:

Name	Resistance	Note
pGG DR5:YFP	SpecR, HygR	Reporter system for Auxin response
pGG_35S:H-mCherry-Tip1-d-dummy-UbqT-HygR	SpecR, HygR	Pos. control for an Auxin inducing effector

pGG-35s-OE-mCherry-mCherry-Myc-Ubq10-HygR	SpecR, HygR	Control for mislocalization studies
pGG-35s-Myc-mCherry-mCherry-dummy-Ubq10-HygR	SpecR, HygR	Control for mislocalization studies
pGG-35s-Myr-Myc-Mcherry-Umag_00628-Dummy-Ubq10-HygR	SpecR, HygR	Effector with myristoylation tag for mislocalization studies
pGG-35s-Myc-NLS-Mcherry-Umag_00628-Dummy-Ubq10-HygR	SpecR, HygR	Effector with nuclear localization signal tag for mislocalization studies
pGG-35s-Myc-NES-Mcherry-Umag_00628-Dummy-Ubq10-HygR	SpecR, HygR	Effector with nuclear export signal tag for mislocalization studies
pGG-35s-OE-Umag_00628-Mcherry-NLS-Myc-Ubq10-HygR	SpecR, HygR	Effector with nuclear localization signal tag for mislocalization studies
pGG-35s-OE-Umag_00628-Mcherry-NES-Myc-Ubq10-HygR	SpecR, HygR	Effector with nuclear export signal tag for mislocalization studies
pGG-35s-Myc-Mcherry-Umag_00628-Dummy-Ubq10-HygR	SpecR, HygR	For mislocalization studies

pGG-35s-OE-Umag_00628-Mcherry-Myc-Ubq10-HygR	SpecR, HygR	For mislocalization studies
pGG-35s-Myr-Myc-Mcherry-Umag_02852-Dummy-Ubq10-HygR	SpecR, HygR	Effector with myristoylation tag for mislocalization studies
pGG-35s-Myc-NLS-Mcherry-Umag_02852-Dummy-Ubq10-HygR	SpecR, HygR	Effector with nuclear localization signal tag for mislocalization studies
pGG-35s-Myc-NES-Mcherry-Umag_02852-Dummy-Ubq10-HygR	SpecR, HygR	Effector with nuclear export signal tag for mislocalization studies
pGG-35s-OE-Umag_02852-Mcherry-NLS-Myc-Ubq10-HygR	SpecR, HygR	Effector with nuclear localization signal tag for mislocalization studies
pGG-35s-OE-Umag_02852-Mcherry-NES-Myc-Ubq10-HygR	SpecR, HygR	Effector with nuclear export signal tag for mislocalization studies
pGG-35s-Myc-Mcherry-Umag_02852-Dummy-Ubq10-HygR	SpecR, HygR	For mislocalization studies
pGG-35s-OE-Umag_02852-Mcherry-Myc-Ubq10-HygR	SpecR, HygR	For mislocalization studies
pGG-35S-GFP-NLS-UbqT	SpecR, HygR	Nucleus staining
pEntry-auxin transport protein BIG	SpecR	pEntry construct for Gateway cloning

pEntry-uncharacterized protein	SpecR	pEntry construct for Gateway cloning
pEntry-vesicle-associated membrane protein	SpecR	pEntry construct for Gateway cloning
pEntry-Thioredoxin-like protein	SpecR	pEntry construct for Gateway cloning
pEntry-Thioredoxin domain-containing protein	SpecR	pEntry construct for Gateway cloning
TRV2-auxin transport protein BIG	KanR	TRV2 construct for VIGS
TRV2-uncharacterized protein	KanR	TRV2 construct for VIGS
TRV2-vesicle-associated membrane protein	KanR	TRV2 construct for VIGS
TRV2-Thioredoxin-like protein	KanR	TRV2 construct for VIGS
TRV2-Thioredoxin domain-containing protein	KanR	TRV2 construct for VIGS
TRV2-SU	KanR	TRV2 construct for VIGS
TRV2-GFP	KanR	TRV2 construct for VIGS
TRV1	KanR	TRV1 construct for VIGS
pGG-35s-OE-GUS-Myc-stop-UbqT-HygR	SpecR, HygR	Neg. control for Auxin induction
pGG-35s-OE-Luciferase-Myc-stop-UbqT-HygR	SpecR, HygR	Neg. control for Auxin induction
pGG-35s-OE-Tip1-Myc-stop-UbqT-HygR	SpecR, HygR	Pos. control for an Auxin inducing effector

pGG-35s-OE-Tip2-Myc-stop-UbqT-HygR	SpecR, HygR	Pos. control for an Auxin inducing effector
pGG-DR5:omega-mCherry-UbqT	SpecR, HygR	Reporter system for Auxin response

6.4.3 Escherichia coli (E. coli) strains

The following *E. coli* strains were used in this study:

Strain	Genotype	Application	Reference
One Shot® Mach1™-T1R Chemically Competent E. coli	F– Φ80lacZΔM15 ΔlacX74 hsdR (rK–, mK+) ΔrecA1398 endA1 tonA	Cloning	Invitrogen

6.4.4 Agrobacterium tumefaciens (A. tumefaciens) strains

The following A. tumefaciens strains were used in this study:

Strain	Genotype	Application	Reference
GV3101/pMP90 pSOUP	C58C1: pGv3101 RifR; pTiC58 ΔTDNA GentR; pSoup TetR	Plant Infection	Koncz & Schell, 1986; Hellens et al., 2000

The following *A. tumefaciens* strains were generated in this study:

Notation	Genotype	Application	Resistance
GV3101 pGG DR5:YFP	C58C1: pGv3101 RifR; pTiC58 ΔTDNA GentR; pSoup TetR; pGG DR5:YFP	Transient expression in *Nicotiana benthamiana*	RifR, GentR, TetR, SpecR
GV3101 pGG_35S:H-mCherry-Tip1-d-dummy-UbqT-HygR	C58C1: pGv3101 RifR; pTiC58 ΔTDNA GentR; pSoup TetR;	Transient expression in *Nicotiana benthamiana*	RifR, GentR, TetR, SpecR

	pGG_35S:H-mCherry-Tip1-d-dummy-UbqT-HygR		
GV3101 pGG-35s-OE-mCherry-mCherry-Myc-Ubq10-HygR	C58C1: pGv3101 RifR; pTiC58 ΔTDNA GentR; pSoup TetR; pGG-35s-OE-mCherry-mCherry-Myc-Ubq10-HygR	Transient expression in *Nicotiana benthamiana*	RifR, GentR, TetR, SpecR
GV3101 pGG-35s-Myc-mCherry-mCherry-dummy-Ubq10-HygR	C58C1: pGv3101 RifR; pTiC58 ΔTDNA GentR; pSoup TetR; pGG-35s-Myc-mCherry-mCherry-dummy-Ubq10-HygR	Transient expression in *Nicotiana benthamiana*	RifR, GentR, TetR, SpecR
GV3101 pGG-35s-Myr-Myc-Mcherry-Umag_00628-Dummy-Ubq10-HygR	C58C1: pGv3101 RifR; pTiC58 ΔTDNA GentR; pSoup TetR; pGG-35s-Myr-Myc-Mcherry-Umag_00628-Dummy-Ubq10-HygR	Transient expression in *Nicotiana benthamiana*	RifR, GentR, TetR, SpecR
GV3101 pGG-35s-Myc-NLS-Mcherry-Umag_00628-Dummy-Ubq10-HygR	C58C1: pGv3101 RifR; pTiC58 ΔTDNA GentR; pSoup TetR; pGG-35s-Myc-NLS-Mcherry-Umag_00628-Dummy-Ubq10-HygR	Transient expression in *Nicotiana benthamiana*	RifR, GentR, TetR, SpecR

GV3101 pGG-35s-Myc-NES-Mcherry-Umag_00628-Dummy-Ubq10-HygR	C58C1: pGv3101 RifR; pTiC58 ΔTDNA GentR; pSoup TetR; pGG-35s-Myc-NES-Mcherry-Umag_00628-Dummy-Ubq10-HygR	Transient expression in *Nicotiana benthamiana*	RifR, GentR, TetR, SpecR
GV3101 pGG-35s-OE-Umag_00628-Mcherry-NLS-Myc-Ubq10-HygR	C58C1: pGv3101 RifR; pTiC58 ΔTDNA GentR; pSoup TetR; pGG-35s-OE-Umag_00628-Mcherry-NLS-Myc-Ubq10-HygR	Transient expression in *Nicotiana benthamiana*	RifR, GentR, TetR, SpecR
GV3101 pGG-35s-OE-Umag_00628-Mcherry-NES-Myc-Ubq10-HygR	C58C1: pGv3101 RifR; pTiC58 ΔTDNA GentR; pSoup TetR; pGG-35s-OE-Umag_00628-Mcherry-NES-Myc-Ubq10-HygR	Transient expression in *Nicotiana benthamiana*	RifR, GentR, TetR, SpecR
GV3101 pGG-35s-Myc-Mcherry-Umag_00628-Dummy-Ubq10-HygR	C58C1: pGv3101 RifR; pTiC58 ΔTDNA GentR; pSoup TetR; pGG-35s-Myc-Mcherry-Umag_00628-Dummy-Ubq10-HygR	Transient expression in *Nicotiana benthamiana*	RifR, GentR, TetR, SpecR

GV3101 pGG-35s-OE-Umag_00628-Mcherry-Myc-Ubq10-HygR	C58C1: pGv3101 RifR; pTiC58 ΔTDNA GentR; pSoup TetR; pGG-35s-OE-Umag_00628-Mcherry-Myc-Ubq10-HygR	Transient expression in *Nicotiana benthamiana*	RifR, GentR, TetR, SpecR
GV3101 pGG-35s-Myr-Myc-Mcherry-Umag_02852-Dummy-Ubq10-HygR	C58C1: pGv3101 RifR; pTiC58 ΔTDNA GentR; pSoup TetR; pGG-35s-Myr-Myc-Mcherry-Umag_02852-Dummy-Ubq10-HygR	Transient expression in *Nicotiana benthamiana*	RifR, GentR, TetR, SpecR
GV3101 pGG-35s-Myc-NLS-Mcherry-Umag_02852-Dummy-Ubq10-HygR	C58C1: pGv3101 RifR; pTiC58 ΔTDNA GentR; pSoup TetR; pGG-35s-Myc-NLS-Mcherry-Umag_02852-Dummy-Ubq10-HygR	Transient expression in *Nicotiana benthamiana*	RifR, GentR, TetR, SpecR
GV3101 pGG-35s-Myc-NES-Mcherry-Umag_02852-Dummy-Ubq10-HygR	C58C1: pGv3101 RifR; pTiC58 ΔTDNA GentR; pSoup TetR; pGG-35s-Myc-NES-Mcherry-Umag_02852-Dummy-Ubq10-HygR	Transient expression in *Nicotiana benthamiana*	RifR, GentR, TetR, SpecR

GV3101 pGG-35s-OE-Umag_02852-Mcherry-NLS-Myc-Ubq10-HygR	C58C1: pGv3101 RifR; pTiC58 ΔTDNA GentR; pSoup TetR; pGG-35s-OE-Umag_02852-Mcherry-NLS-Myc-Ubq10-HygR	Transient expression in *Nicotiana benthamiana*	RifR, GentR, TetR, SpecR
GV3101 pGG-35s-OE-Umag_02852-Mcherry-NES-Myc-Ubq10-HygR	C58C1: pGv3101 RifR; pTiC58 ΔTDNA GentR; pSoup TetR; pGG-35s-OE-Umag_02852-Mcherry-NES-Myc-Ubq10-HygR	Transient expression in *Nicotiana benthamiana*	RifR, GentR, TetR, SpecR
GV3101 pGG-35s-Myc-Mcherry-Umag_02852-Dummy-Ubq10-HygR	C58C1: pGv3101 RifR; pTiC58 ΔTDNA GentR; pSoup TetR; pGG-35s-Myc-Mcherry-Umag_02852-Dummy-Ubq10-HygR	Transient expression in *Nicotiana benthamiana*	RifR, GentR, TetR, SpecR
GV3101 pGG-35s-OE-Umag_02852-Mcherry-Myc-Ubq10-HygR	C58C1: pGv3101 RifR; pTiC58 ΔTDNA GentR; pSoup TetR; pGG-35s-OE-Umag_02852-Mcherry-Myc-Ubq10-HygR	Transient expression in *Nicotiana benthamiana*	RifR, GentR, TetR, SpecR
GV3101 pGG-35S-GFP-NLS-UbqT	C58C1: pGv3101 RifR; pTiC58 ΔTDNA GentR; pSoup TetR;	Transient expression in *Nicotiana benthamiana*	RifR, GentR, TetR, SpecR

	pGG-35S-GFP-NLS-UbqT		
GV3101 TRV2-auxin transport protein BIG	C58C1: pGv3101 RifR; pTiC58 ΔTDNA GentR; pSoup TetR; TRV2-auxin transport protein BIG	Transient expression in *Nicotiana benthamiana*	RifR, GentR, TetR, KanR
GV3101 TRV2-uncharacterized protein	C58C1: pGv3101 RifR; pTiC58 ΔTDNA GentR; pSoup TetR; TRV2-uncharacterized protein	Transient expression in *Nicotiana benthamiana*	RifR, GentR, TetR, KanR
GV3101 TRV2-vesicle-associated membrane protein	C58C1: pGv3101 RifR; pTiC58 ΔTDNA GentR; pSoup TetR; TRV2-vesicle-associated membrane protein	Transient expression in *Nicotiana benthamiana*	RifR, GentR, TetR, KanR
GV3101 TRV2-Thioredoxin-like protein	C58C1: pGv3101 RifR; pTiC58 ΔTDNA GentR; pSoup TetR; TRV2-Thioredoxin-like protein	Transient expression in *Nicotiana benthamiana*	RifR, GentR, TetR, KanR
GV3101 TRV2-Thioredoxin domain-containing protein	C58C1: pGv3101 RifR; pTiC58 ΔTDNA GentR; pSoup TetR; TRV2-Thioredoxin domain-containing protein	Transient expression in *Nicotiana benthamiana*	RifR, GentR, TetR, KanR

GV3101 TRV2-SU	C58C1: pGv3101 RifR; pTiC58 ΔTDNA GentR; pSoup TetR; TRV2-SU	Transient expression in *Nicotiana benthamiana*	RifR, GentR, TetR, KanR
GV3101 TRV2-GFP	C58C1: pGv3101 RifR; pTiC58 ΔTDNA GentR; pSoup TetR; TRV2-GFP	Transient expression in *Nicotiana benthamiana*	RifR, GentR, TetR, KanR
GV3101 TRV1	C58C1: pGv3101 RifR; pTiC58 ΔTDNA GentR; pSoup TetR; TRV1	Transient expression in *Nicotiana benthamiana*	RifR, GentR, TetR, KanR
GV3101 pGG-35s-OE-GUS-Myc-stop-UbqT-HygR	C58C1: pGv3101 RifR; pTiC58 ΔTDNA GentR; pSoup TetR; pGG-35s-OE-GUS-Myc-stop-UbqT-HygR	Transient expression in *Nicotiana benthamiana*	RifR, GentR, TetR, SpecR
GV3101 pGG-35s-OE-Luciferase-Myc-stop-UbqT-HygR	C58C1: pGv3101 RifR; pTiC58 ΔTDNA GentR; pSoup TetR; pGG-35s-OE-Luciferase-Myc-stop-UbqT-HygR	Transient expression in *Nicotiana benthamiana*	RifR, GentR, TetR, SpecR
GV3101 pGG-35s-OE-Tip1-Myc-stop-UbqT-HygR	C58C1: pGv3101 RifR; pTiC58 ΔTDNA GentR; pSoup TetR; pGG-35s-OE-Tip1-Myc-stop-UbqT-HygR	Transient expression in *Nicotiana benthamiana*	RifR, GentR, TetR, SpecR

GV3101 pGG-35s-OE-Tip2-Myc-stop-UbqT-HygR	C58C1: pGv3101 RifR; pTiC58 ΔTDNA GentR; pSoup TetR; pGG-35s-OE-Tip2-Myc-stop-UbqT-HygR	Transient expression in *Nicotiana benthamiana*	RifR, GentR, TetR, SpecR
GV3101 pGG-DR5:omega-mCherry-UbqT	C58C1: pGv3101 RifR; pTiC58 ΔTDNA GentR; pSoup TetR; pGG-DR5:omega-mCherry-UbqT	Transient expression in *Nicotiana benthamiana*	RifR, GentR, TetR, SpecR

6.4.5 Oligonucleotides

The following oligonucleotides were ordered from Eurofins Genomics and generated using the Primer3 software (v.0.4.0) and CLC Main Workbench 7 software, respectively.
To generate DNA fragments for VIGS the following primers were used:

Name	Sequence (5'-3')	Application
9465_Silencing_Big_fw-2	ATATccatggATGCAACTCTGAGCAGGTCTC	Silencing of Auxin Protein BIG; Niben101Scf06560g02002.1 >best_target_region_(3914-4233)
9466_Silencing_Big_rv-2	ATATgcggccgcTTCCTGTGAAAGGATTCCAGA	
9467_Silencing_unchar_fw	ATATgcggccgcAGTTTCGATGATTCACCCTCA	Silencing of Uncharacterized Protein Niben101Scf05306g02017.1 >best_target_region_(301-600)
9468_Silencing_unchar_rv	ATATgcggccgcGAGAAGGGAACTGCACAAGG	

9469_Silencing_vesicle_fw	ATATccatggGCGATACTGTATGCGGTTGT	silencing of vesicle associated-membrane protein; Niben101Scf08515g00019.1 >best_target_region_(1-300)
9470_Silencing_vesicle_rv	ATATgcggccgcCCACCTTGCCGTAGTTCTTC	
9475_Silencing_Thioredoxin-F	ATATccatggTTCTCTTCTAAGCAACCTAATCAGC	silencing of Thioredoxin (NCBI Thioredoxin-like protein CITRX2, chloroplastic) (Niben101Scf15049g00002.1) >best_target_region_(60-379)
9476_Silencing_Thioredoxin-R	ATATgcggccgcTTGCTTTCATACTCTACAGCAAGC	
9477_Silencing_Thio_contain_F	ATATccatggCTGCCATTTCTACCGTGACA	silencing of Thioredoxin domain-containing protein 9 homolog IPR012336 (Niben101Scf00439g10054.1) >best_target_region_(331-650)
9478_Silencing_Thio_contain_R	ATATgcggccgcAGTTTCGATGATTCACCCTCA	

For sequencing purposes, the following primers were used:

Name	Sequence (5'-3')	Application
21_3´pEntry sequencing vector	CAGAGCTGCAGCTGGATGG	Sequencing of pENTRY vector constructs

23_pEntry 5´ sequencing	AGTTAGTTACTTAAGCTCG	Sequencing of pENTRY vector constructs
48_pJET-fwd	TGGAGCAGGTTCCATTCATTG	Sequnecing of pJet vector contructs
49_pJET-rev	GTTCCTGATGAGGTGGTTAG CATAG	Sequnecing of pJet vector contructs
83_GG35SPro_seqF	TCAAAGCAAGTGGATTGATG	Green Gate 35S promoter forward sequencing primer
86_Ubi_Term_SeqR	GAAAGAGATAACAGGAACG G	Green Gate Ubiquitin 10 terminator reverse sequencing primer
TRV2seq_F	TTCACTGGGAGATGATACGC	Sequencing of destination vector TRV2 constructs
TRV2seq_R	TACCGATCAATCAAGATCAG	Sequencing of destination vector TRV2 constructs

6.5 Media and culture conditions

6.5.1 Bacterial media

Agro LB liquid medium (in ddH_2O)

1 %	Tryptone (w/v)
0.5 %	Yeast extract
1 %	NaCl
10mM	MES-NaOH pH 5.6
0.15mM	Acetosyringone

dYT liquid medium (in ddH_2O)

1.6 %	Tryptone (w/v)
0.5 %	Yeast extract (w/v)
0.5 %	NaCl (w/v)

dYT agar (in ddH_2O)

1.6 %	Tryptone (w/v)
0.5 %	Yeast extract (w/v)
0.5 %	NaCl (w/v)
2.0 %	Bacto-Agar (w/v)

In case of selection the respective antibiotics were added to the media (but only when the liquid was cooler than 60°C). The following final concentration were used:

100 µg/ml	Ampicillin
100 µg/ml	Spectinomycin
20 µg/ml	Gentamycin
50 µg/ml	Rifampicin
100 µg/ml	Chloramphenicol

SOC medium

2 %	Bacto Tryptone (w/v)
0.5 %	Yeast extract (w/v)
0.05 %	NaCl (w/v)

added after autoclaving:

0.25 %	1M KCl (f.c. 2.5 mM)
1 %	1M MgCl2*6H2O (f.c. 10 mM)
0.72 %	50 % Glucose (v/v)

6.5.2 Bacterial growth conditions (*E. coli* and *A. tumefaciens*)

E. coli and A. tumefaciens cells were grown in the dark as liquid culture in dYT medium under continuous shaking at 180 rpm at 37°C and 28°C, respectively. Cells, that were streaked out on dYT plates, were cultivated under the same conditions but without shaking. For long-term storage, 800 µL over-night culture was mixed by pipetting with 800 µL of 80% glycerol and stored at -80°C.

7 Methods

7.1 Microbiological methods

7.1.1 Determination of cell density

To determine the cell density a spectrophotometer was used. The wavelength was set to λ=600. As a reference, the respective culture medium was used.

7.1.2 Transformation of chemo-competent *E. coli*

To facilitate efficient transformation, 50 µL of chemo-competent Mach1 E. coli cells were thawed on ice and mixed with ~100 ng plasmid DNA. After incubation on ice for 15 min, the cells were heat-shocked at 42°C for 1 min. Afterwards the cells were placed back on ice and resuspended in 200 µl SOC medium. After regeneration of the cells at 37°C (shaking at 700 rpm), the cells were plated onto selection plates and incubated at 37°C, ON. If Ampicillin was used for selection, regeneration was not necessary, and the cells were plated out directly after adding the SOC medium.

7.1.3 Transformation of electrocompetent *A. tumefaciens*

Electrocompetent bacterial cells were transformed by electroporation. Cells were thawed on ice and mixed with ~1 µg of DNA. The cells were then transferred into a pre-cooled electroporation cuvette and placed into the electroporation device (Gene Pulser Xcell from BioRad). A pulse of 1700 V was applied, and the cells immediately resuspended in 1ml SOC medium. The cells were recovered in SOC for 2h at 28°C, shaking. 200 µl of the recovered cells were plated onto LB plates containing suitable antibiotics and were incubated at 28°C for 2-3 days until colonies appeared.

7.2 Molecular biological methods

7.2.1 RNA extraction

Nicotiana benthamiana leaves were homogenized using Retsch MM400. 20 mg of powder was weighted into a 2 ml Eppendorf tube. A total volume of 450 µl GEX buffer was added and put for 30 mins on RT with shaking. Further processing of total RNA isolation was performed as given in the manufacturer's protocol (High performance RNA bead isolation, Molecular Biology Service).

7.2.2 DNase treatment of RNA and cDNA synthesis

mRNA was transcribed into cDNA employing the Super III First Strand Synthesis Super Mix Kit or RevertAid First Strand cDNA Synthesis Kit (Thermo Fisher Scientific). Reverse transcription was performed according to the manufacturers' protocols. Each reaction contained 1 µg DNase-treated total RNA. Reverse transcription was performed using oligo-d(T)-primers.

One reaction tube for cDNA synthesis contained:

1 µl	Oligo d(T) primers
1 µl	dNTPs
1 µl	of RNA
12 µl	Free RNase H2O

Incubation on 65°C, 5 min

Then the following substrates were added:

4 µl	RT buffer 5x
1 µl	Maxima H Minus Enzyme mix

Incubation on 50°C, 30 min and 85°C, 5 min

7.2.3 Plasmid DNA isolation from *E. coli*

First, the *E. coli* strain containing the plasmid of interest were grown in 3 mL dYT medium containing the corresponding antibiotics, ON. To harvest the cells the culture was centrifuged at 13000 rcf for 5 min. Then the supernatant was removed, and the cell pallet resuspended in 250 µL buffer P1. 250 µL of the second buffer P2 (Qiagen) was added to lyse the cells and the tubes were inverted several times. To neutralize the pH again, 350 µL neutralization buffer N3 (Qiagen) was added and the mixture was inverted to ensure homogenic pH distribution followed by a 10 min centrifugation step at 13000 rcf. The supernatant was loaded onto Miniprep columns (CenticBiotec). Next the columns were centrifuged at 13000 rcf for 1 min and the flow-through discarded. 500 µl PB solution were added to the columns and the centrifugation step repeated. The flow-through was discarded again and 700 µl PE solution were added to clean the membrane-bound DNA from salts and pollutants. Another centrifugation step helps to remove the residual ethanol from the columns. Then the dry columns are transferred into1.5 ml microcentrifugation tubes. Finally, 50 µl ddH2O are added to the columns, incubated for 1 min to ensure complete hydration and then centrifuged for another minute at 13000 rcf to elute the DNA from the columns. The DNA concentration purity were measured using ND-1000 spectrophotometer (Peqlab, Germany).

Buffer P1

50mM	Tris-HCl, pH 8.0
10mM	EDTA
100µg/ml	RNase A

PB solution

5M	Guanidine hydrochloride
30 %	Isopropanol

PE solution

10mM	Tris-HCl, pH 7.5
80 %	Ethanol

7.2.4 Isolation of genomic DNA

For genomic DNA isolation 1 cm^2 leaf material of *Nicotiana benthamiana* (*N. b.)*was sampled and immediately frozen in liquid nitrogen. Grinding was performed using the Retsch MM400 before adding GEX buffer. Afterwards, samples were centrifuged on maximal speed for 5 min on RT. Supernatant was transferred into columns with silica gel filters (CenticBiotec) and centrifuged for 1 min on maximal speed. Washing step was done using 500 µl of PE buffer (see PE buffer solution). Liquid was removed from the column and centrifugation was repeated for 2 min on maximal speed to dry the column. To elute the bound DNA, the columns were placed into a fresh 1.5 ml Eppendorf tube and 50 µl of water was added onto the filter. Samples were incubated for 2 min at room temperature before centrifuging 1 min at 13000 rpm. DNA concentrations were measured with ND-1000 spectrophotometer (Peqlab, Germany).

GEX buffer:

5.5 M	GuSCN
20 mM	Tris-HCl, pH 6.6

7.2.5 Polymerase chain reaction (PCR)

To amplify DNA fragments for cloning or analytical purpose polymerase chain reactions were performed. Different polymerases were used depending on the application. The PCR programs used for respective polymerases included the following thermocycling steps:

Step	
Initial denaturation	
Denaturation	
Primer annealing	X number of cycles
Elongation	
Final elongation	
Cooling	

The elongation time was chosen based on the expected fragment size and synthesis rate of the polymerase.

7.2.6 Direct PCR

For screening of positive clones of a transformation, *E. coli* cultures were directly used as a template.

5 µl	OneTaq© Quick-Load© 2x Master Mix (NEB)
4.8 µl	ddH2O
1 µl	PCR template
0.1 µl	each primer (20 pM)

Step	Temperature	Time
Initial denaturation	94 °C	30 sec
Denaturation	94 °C	20 sec
Primer annealing	primer specific	20 sec
Elongation	68 °C	60 sec/kb
Final elongation	68°C	5 min
Cooling	12 °C	∞

40x

7.2.7 Phusion PCR

Reaction volume of one reaction was 50 µl. For each reaction the following mix was prepared:

10 µl	5x Phusion HF buffer
36.5 µl	Mono Q H2O
1 µl	dNTP (10mM)
0.5 µl	forward primer (100µM)
0.5 µl	reverse primer (100µM)
0.5 µl	Phusion polymerase
1 µl	DNA template

Thermocycling conditions for Phusion:

Step	Temperature	Time	
Initial denaturation	98 °C	30 sec	
Denaturation	98 °C	10 sec	
Primer annealing	primer specific	20 sec	35x
Elongation	72 °C	15 sec/kb	
Final elongation	72°C	5 min	
Cooling	12 °C	∞	

7.2.8 Sequencing

Sequencing was performed at the Vienna BioCenter Core Facilities (VBCF). At least 150 ng plasmid DNA with 5 pg primer were prepared with ddH2O in a total volume of 7 µl. For direct sequencing of PCR products, 2 µl of a reaction were send directly with 5 pg primer in a total volume of 7 µl.

7.2.9 Agarose gel electrophoresis

Different percentages (0.8%, 1% or 2 %) of TAE-agarose gels were used to separate PCR amplified DNA fragments according to their size. For gel preparation, agarose was dissolved in 1xTAE buffer by boiling and 3 µl peqGreen dye per 100 ml agarose solution were added. Before loading, the DNA was mixed with loading dye (f.c. 1x). The runtime of a gel is 30min with a current of 120-130 Volt. The stained DNA-bands were excited by UV light and the fluorescence was detected. If purification of the DNA fragments was necessary, the

desired region of the gel was cut out under UV-light and the DNA from the gel section was eluted.

TAE Buffer:

40 mM	Tris
1 mM	EDTA, pH 8.0
20mM	acetic acid

6x DNA loading dye:

50 %	Saccharose (v/v)
0.1 %	Bromphenol blue (v/v)
	dissolved in TE buffer

7.2.10 DNA elution

After amplification via PCR and separation over an agarose gel, distinct DNA fragments were excised with a scalpel and the DNA purified using the Wizard® SV Gel and PCR Clean-Up System (Promega) according to the manufacturer´s protocol.

7.2.11 DNA restriction

To cleave the double-stranded DNA at the specific site that contains our desired sequence, type II restriction enzymes (New England Biolabs) were used. Reaction conditions were chosen according to manufacturer's recommendations. After digestion the fragment lengths were checked on an agarose gel.

For each reaction the following mix was prepared:

3 µL	vector DNA
2 µL	10x NEBuffer
15 µL	Mono Q H_2O
0.3 µL	restriction enzyme(s)

7.2.12 DNA ligation

For better storage and further cloning, gel-eluted DNA fragments were ligated into intermediate vectors (pJet-Stuffer or pEntry, respectively) using the T4 ligase (New England Biolabs). DNA fragments were employed in a vector-to-insert ratio of 1:5. The ligation reactions were incubated for 1 hour at RT before continuing with transformation into chemo-competent *E. coli* cells. For further use the plasmid was later isolated from the cells.

For each ligation the following mix was prepared in 10 µl ddH2O:

1 µl	vector
5 µl	insert
0.5 µl (150 U)	T4 DNA ligase
1 µl	10x T4 DNA ligase buffer

7.2.13 Golden Gate cloning

The Golden Gate cloning technique uses type IIs restriction enzymes, which cut outside of their recognition sequence, so the product cannot be re-digested by the same restriction enzyme, to assemble multiple DNA fragments into an entry vector (Engler et al., 2008). In this study the Golden Gate-based GreenGate vector system and the following six module types were used: plant promoter, N-terminal tag, coding sequence (i.e. the gene of interest), C-terminal tag, plant terminator and plant resistance cassette (Lampropoulos et al. 2013). Via Phusion PCR amplification the suitable overhangs containing the cleavage and recognition site were added to the DNA fragment and stored in the intermediate vector pJet-Stuffer.

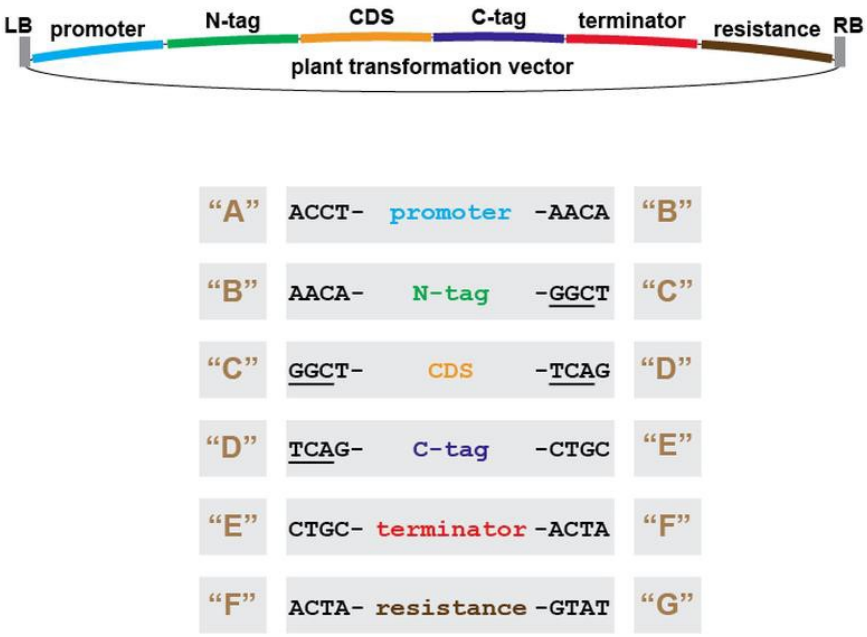

Figure 7 The six Golden Gate modules with specifically designed overhangs as developed by (Lampropoulos et al. 2013).

Golden Gate reaction:

x µl	Vector (~ 10 ng)
y µl	per Insert (~ 50 ng)
1 µl	T4 Ligase Buffer
0.5 µl	T4 Ligase
0.5 µl	BsaI (Type IIS restriction enzyme)
	add ddH2O to reach a final volume of 10 µl

Thermocycling conditions for Golden Gate:

Step	Temperature	Time	Note
1	37°C	10 min	1st digestion phase
2	37°C	5 min	Digestion phase
3	16°C	10 min	Ligation phase
4	37°C	10 min	Final digestion phase
5	50°C	5 min	Enzyme inactivation
6	12°C	∞	

10x

5 µl of the reaction were transformed into Mach 1 cells and plated according to the antibiotic resistance.

7.2.14 Gateway Cloning

The gateway cloning technique is an *in vitro* cloning strategy based on the site-specific recombination system to integrate and excise DNA fragments. Therefore, the entry vector containing the coding sequence which is flanked by attL sites and the destination vector encoding for the attR site flanked ccdB cassette are mixed and the reaction is catalysed by the LR-clonase®II-enzyme mix. In the end this reaction generates a destination vector with our desired sequence and a pEntry vector with a toxic by-product.

Gateway-reaction:

1 µl	destination vector (150 ng/µl)
0.5 µl	entry vector (50 – 100 ng)
0.5 µl	TE buffer, pH 7.5
0.5 µl	LR-Clonase ® II enzyme mix

The whole reaction was transformed into Mach 1 cells and plated according to the antibiotic resistance.

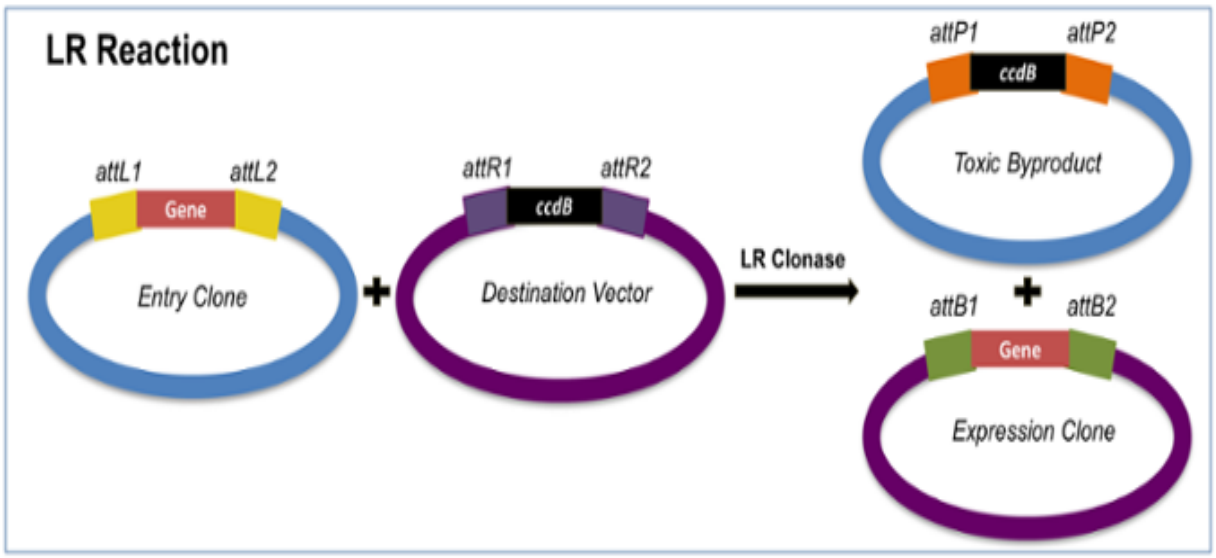

Figure 8 Principle of the Gateway Cloning technique via site-specific recombination system. Image adapted from (Maria Soriano 2017).

The LR-clonase®II-enzyme mix facilitates the transfer of the CDS from the entry vector to the expressing destination vector.

7.3 Biochemical methods

7.3.1 Mass Spectrometry

5 weeks old *N. benthamiana* plants were infiltrated to heterogeneously express the following U. maydis genes: pGG-35s-Omega element-Umag_00628-Mcherry-Myc-Ubq10-HygR and pGG-35s-Omega element-Umag_02852-Mcherry-Myc-Ubq10-HygR. After 3 days plant material was harvested and immediately frozen in liquid nitrogen. Then the samples were grinded, and 0.5 g of powder were put in 5 ml Eppendorf tubes and send out for Mass Spectrometry analysis.

7.3.2 Protein Extraction and sample preparation

Treated *N. benthamiana* leaves were collected in POLYVIALS® 20 ml Kunststoff-Szintillationflaschen (Zinsser Analytic) with two 8-mm and four 5-mm Retsch metal balls and instantly frozen in liquid nitrogen. With the Retsch® Schwingmühle MM 400 the samples were

grinded for 1:30 min at 25 Hz to avoid cracks in the plastic tubes. Then 50mg of powder were weighted and transferred into 2 ml Eppendorf tubes. 250 µl of extraction buffer (1/4 vol. 4xLDS buffer containing 25mM DTT and ¾ vol. H20) were added and the solution was properly vortexed before heating it at 75°C for 10 min in a heat block. This step disrupts the secondary and tertiary structures of the proteins. The heated solution was centrifuged for 5 min at max speed and the supernatant transferred in a new tube. The samples can be stored at -80°C.

4x LDS Sample buffer:

40%	Glycerol
1M	Tris-HCl pH 8.5
2mM	EDTA
8%	LDS
0.02%	Bromophenol blue

7.3.3 SDS-Polyacrylamide Gel Electrophoresis

Proteins in solution can be separated according to their molecular weight by an SDS polyacrylamide gel electrophoresis. The proteins are denatured prior to the run by cooking and coating with the anionic detergent SDS to disrupt endogenous charges in the now linearized polypeptide chain.

To separate the proteins, samples were loaded and fractionated on a 10% SDS-polyacrylamide gel consisting of a resolving gel and stacking gel. The higher, stacking gel is slightly acidic (pH6.8) and has large sized pores to concentrate all proteins into one band. The lower gel, the resolving gel, is basic (pH8.8) and allowed proteins then to separate according to their molecular weight.

To identify the size of the proteins, the pre-stained protein PageRuler (ThermoFisher Scientific, USA) was used as reference. Separation of the proteins was performed at different voltages. To concentrate the proteins on the same level the gel was run on 20mA, where the actual separation was at 25mA.

Resolving gel (1.5mm. 10%):

3 ml	MQ H_2O
1.88 ml	1.5M Bis-Tris-HCl pH 6.8
2.50 ml	30% Acrylamide
75 µl	10% SDS
3.75 µl	TEMED
37.5 µl	10% APS

Stacking gel (1.5mm. 4%):

2.25 ml	MQ H_2O
0.9 ml	1.5M Bis-Tris-HCl pH 6.8
0.5 ml	30% Acrylamide
37.5 µl	10% SDS
3.75 µl	TEMED
18.75 µl	10% APS

SDS Running buffer

1M	MES
1M	Tris
2%	SDS
20mM	EDTA

7.3.4 Western Blot analysis

The Western blot method was developed to specifically visualize proteins in a sample via antibody-binding. After gel electrophoresis, the separated proteins are transferred from the polyacrylamide gel onto a nitrocellulose membrane. The membranes are later incubated in antibody-solution and the labeled proteins visualized.

In this study after the gel electrophoresis, the Trans-Blot® TurboTM Transfer System (BioRad) was used for Western Blotting. After the electrophoresis run, the gel was placed on top of a nitrocellulose membrane and both were placed between several layers of soaking papers according to manufacturer's protocol.

After the blotting, the membrane was blocked with blocking buffer + 5% milk powder and incubated for 1 hour (overnight also possible) gently shaking at RT. Then the nitrocellulose membrane was rinsed two times with 1x washing buffer before incubating it in 7 ml primary antibody solution gently shaking for 1h at RT (ON also possible). For this experimental set-up, the suitable concentration for the α-MYC antibody (mouse) was a 1:2500 dilution. Before applying the secondary antibody (1:20000 diluted in 1x washing buffer, HRP-coupled anti-mouse antibody) for 1h at RT (also gently shaking), the membrane was rinsed briefly two times with 1x washing buffer followed by 4x 5 minutes washing. The washing step above was repeated after the second AB incubation. The binding of the antibodies was finally visualized using the SuperSignal™ West PLUS Chemiluminescent Substrate (ThermoFisher Scientific, USA) and imaged in the ChemiDoc™ imaging system (BioRad, USA) according to the manufacturers protocol.

Turbo blotting buffer:

200 ml	EtOH
200 ml	5x Trans-Blot® TurboTM Buffer
600 ml	MQ H_2O

Washing Buffer:

1x	10x TBS (media kitchen)
25%	Tween

Blocking Buffer:

100mM	1M Tris
200mM	5M NaCl
0.05%	25% Tween

7.3.5 Tobacco Rattle virus-based virus-induced gene silencing in *Nicotiana benthamiana* (TRV-VIGS)

The TRV-based VIGS system was used for gene silencing. First the amino acid sequence was copied from Uniprot via protein acc. #. The online source Sol Genomics Network blasted

the protein sequence (tblastn – match sequence) to get the CDS. With VIGS Tool the VIGS Analysis was run to select a ~320 nt fragment best suitable for silencing. Then primers were designed using CLC Main Workbench 7 and Primer3 tools was applied to select the size range. The primers were constructed as follows: Golden Gate adapter ATAT – restriction enzyme NcoI binding and cutting site – VIGS target region - restriction enzyme NotI binding and cutting site – TATA.To generate the silencing constructs, the ~300 bp fragment of the targeted gene was PCR amplified from *N. benthamiana* and the product was cloned into pJET and transformed into E. coli. The DNA fragment was then cut out using the restriction enzymes NotI and NcoI and subsequently ligated into the pENTRY vector (SpecR as selection marker). Finally, the Gateway LR-reaction between the pENTRY containing the VIGS target region and an empty pTRV2 vector (KanR) was carried out. To infiltrate planta the correct clones were transformed into *A. tumefaciens*.

7.3.6 Fluorescence-based reporter-gene assay (DR5-Induction Assay)

The DR5-Induction assay measures the biological activity of the DR5 promoter in this case coupled to a fluorescent protein (GFP) to study auxin response via a fluorescence spectroscopy method. Therefore, 4 leaf discs per leaf (in total 2 leaves per plant) of five weeks old *N. benthamiana* plants were collected using a Miltex biopsy punch with plunger (diameter=4mm) and floated in 100 µl water in a black 96-well plate. The abundance of GFP as a response to auxin can be measured fluorometrically at λex = 485 nm, λemm= 528 nm using the Synergy4 spectrophotometer (Biotek, USA). The transgenic protein expression was measured at λex = 570 nm, λemm= 610 nm for the mCherry fluorescence.

7.4 Plant methods

7.4.1 Cultivation of Nicotiana benthamiana (N. benthamiana)

N. benthamiana plants were grown in controlled short-day conditions (16h light/8h dark) at 22°C in 'Einheitserde SP ED63 T' (Einheitserdewerke Werkverband e.V.) with perlite. The plants were watered by flooding for 15 min every two days. Seedlings were transferred to single pots one week after sowing and used for experiments after a five-week growth period.

7.4.2 A. tumefaciens infection of N. benthamiana

Protein expression in planta was achieved by *A. tumefaciens* mediated transformation of *N. benthamiana*. Agrobacterium strains harbouring the expression plasmid were grown in liquid Agro LB medium with appropriate antibiotics by shaking at 28°C on 180 rpm overnight. The OD of the overnight cultures was measured at OD600 then set to the needed OD before harvesting the cells by centrifugation at 3000 g for 10 min. The cells were resuspended in the appropriate amount of ARM medium and incubated for at least 2 h. The bacteria solution was syringe infiltrated into *N. benthamina* plants usually at the 4-6 leaf stage if not noticed otherwise. Leaf discs were punched right around the infected area 48 h or 72 h post infiltration depending on the conducted experiment. For harvesting infiltrated leaves, the same timespan was used, and the leaves were immediately frozen in liquid nitrogen. Leaf samples were stored in -80°C until further use.

1) Subcellular mislocalization assay

For the subcellular localization assays, *N. benthamiana* plants were 5 weeks old before used for infiltration. For microscopy analysis two leaves per plant and one plant per construct was used. For DR5-Induction assay two leaves per plant and two plants per construct were infiltrated. 2-days post infection leave discs for microscopy were collected and 3-days post infection the DR5-Induction assay was performed.

2) VIGS

N. benthamiana plants that showed the first 2 true leaves emerging beside the cotyledons (usually around 2-3 weeks) were used for silencing. For each independent experiment, 5 plants per construct were used. The final OD was set to 0.4. The bacterial cultures containing the pTRV1(encodes the replication and movement of viral functions) were then mixed with each pTRV2 (harbours the coat protein and the target region used for VIGS) in a ratio 1:1 resulting in an OD of 0.2. To avoid cross-contamination, gloves were changed between infiltration of different constructs. After 25 days the silenced plants were again infiltrated with specific constructs (OD = 0.2) to continue with the DR5-Induction Assay. As a

control for VIGS efficiency, silencing of phytoene desaturase (PDS) was used which causes photobleaching.

LB (MES AS):

10 mM	MES NaOH, pH5.6
0.2 mM	Acetosyringone
	In LB media

ARM buffer:

10 mM	MES NaOH, pH5.6
10 mM	MgCl2
0.15 mM	Acetosyringone
	In LB media

7.5 Imaging methods

7.5.1 Microscopy

For the subcellular mislocalization assay, confocal laser scanning microscopy was performed using the LSM780 Axio Observer (inverted) microscope from Zeiss. Therefore, the leaf disc had to be filled with water by generating negative pressure. Images were processed using the software ZEN Black (2.3 SP1) or Blue edition.

7.5.2 Bioinformatics Tools

Database	Description	Reference/URL
UniProt	Protein sequences and general information of interacting proteins were acquired through this page	*https://www.uniprot.org*

Sol Genomics Network	Checking for coding region and best target for Virus Induced Gene Silencing.	*https://solgenomics.net* *http://vigs.solgenomics.net/*
NCBI	Homology searches and sequence analysis	*https://www.ncbi.nlm.nih.gov/*
CLC	Analysis of all DNA and protein sequences	*CLC main work bench 7 (Qiagen Bioinformatics)*
Primer3	Generating oligonucleotide sequences	*http://primer3.ut.ee*

7.6 Statistical Analysis

Two statistical packages were used to perform statistical analysis: Microsoft Office Excel 10, RStudio (Version 1.0.143-© 2009-2016 RStudio, Inc.). The Analysis of variance (ANOVA) test with Tuckey's comparison at a 95% confidence level ($p < 0.05$) was also used to perform statistics.

8 Publication bibliography

Agrios, George N. (2008): Plant pathology. 5th ed., [3rd print]. Amsterdam: Elsevier Academic Press. Available online at http://www.loc.gov/catdir/description/els051/2004011924.html.

Andrade, José M.; Dos Santos, Ricardo F.; Chelysheva, Irina; Ignatova, Zoya; Arraiano, Cecília M. (2018): The RNA-binding protein Hfq is important for ribosome biogenesis and affects translation fidelity. In *The EMBO journal* 37 (11). DOI: 10.15252/embj.201797631.

Ausubel, Fred M. (1997): Current protocols in molecular biology. New York: Wiley & Sons.

Baluška, František; Šamaj, Jozef; Menzel, Diedrik (2003): Polar transport of auxin: carrier-mediated flux across the plasma membrane or or neurotransmitter-like secretion? In *Trends in Cell Biology* 13 (6), pp. 282–285. DOI: 10.1016/S0962-8924(03)00084-9.

Baluška, František; Schlicht, Markus; Volkmann, Dieter; Mancuso, Stefano (2008): Vesicular secretion of auxin: Evidences and implications. In *Plant signaling & behavior* 3 (4), pp. 254–256.

Bashandy, Talaat; Guilleminot, Jocelyne; Vernoux, Teva; Caparros-Ruiz, David; Ljung, Karin; Meyer, Yves; Reichheld, Jean-Philippe (2010): Interplay between the NADP-linked thioredoxin and glutathione systems in Arabidopsis auxin signaling. In *The Plant cell* 22 (2), pp. 376–391. DOI: 10.1105/tpc.109.071225.

Bashandy, Talaat; Meyer, Yves; Reichheld, Jean-Philippe (2011): Redox regulation of auxin signaling and plant development in Arabidopsis. In *Plant signaling & behavior* 6 (1), pp. 117–119. DOI: 10.4161/psb.6.1.14203.

Bennett, M. D. (2003): Comparisons with Caenorhabditis (100 Mb) and Drosophila (175 Mb) Using Flow Cytometry Show Genome Size in Arabidopsis to be 157 Mb and thus 25 % Larger than the Arabidopsis Genome Initiative Estimate of 125 Mb. In *Annals of botany* 91 (5), pp. 547–557. DOI: 10.1093/aob/mcg057.

Bennett, M. D.; Leitch, I. J. (2005): Nuclear DNA amounts in angiosperms: progress, problems and prospects. In *Annals of botany* 95 (1), pp. 45–90. DOI: 10.1093/aob/mci003.

Bigeard, Jean; Colcombet, Jean; Hirt, Heribert (2015): Signaling mechanisms in pattern-triggered immunity (PTI). In *Molecular plant* 8 (4), pp. 521–539. DOI: 10.1016/j.molp.2014.12.022.

Boccardo, Noelia Ayelen; Segretin, María Eugenia; Hernandez, Ingrid; Mirkin, Federico Gabriel; Chacón, Osmani; Lopez, Yunior et al. (2019): Expression of pathogenesis-related proteins in transplastomic tobacco plants confers resistance to filamentous pathogens under field trials. In *Scientific Reports* 9 (1), p. 2791. DOI: 10.1038/s41598-019-39568-6.

Brefort, Thomas; Doehlemann, Gunther; Mendoza-Mendoza, Artemio; Reissmann, Stefanie; Djamei, Armin; Kahmann, Regine (2009): Ustilago maydis as a Pathogen. In *Annual review of phytopathology* 47, pp. 423–445. DOI: 10.1146/annurev-phyto-080508-081923.

Castanheira, Sónia; Pérez-Martín, José (2015): Appressorium formation in the corn smut fungus Ustilago maydis requires a G2 cell cycle arrest. In *Plant signaling & behavior* 10 (4), e1001227. DOI: 10.1080/15592324.2014.1001227.

Chapman, S.; Kavanagh, T.; Baulcombe, D. (1992): Potato virus X as a vector for gene expression in plants. In *The Plant journal : for cell and molecular biology* 2 (4), pp. 549–557.

Chaumet, Alexandre; Wright, Graham D.; Seet, Sze Hwee; Tham, Keit Min; Gounko, Natalia V.; Bard, Frederic (2015): Nuclear envelope-associated endosomes deliver surface proteins to the nucleus. In *Nature Communications* (6). DOI: 10.1038/ncomms9218.

Chen, Yiru; Yordanov, Yordan S.; Ma, Cathleen; Strauss, Steven; Busov, Victor B. (2013): DR5 as a reporter system to study auxin response in Populus. In *Plant cell reports* 32 (3), pp. 453–463. DOI: 10.1007/s00299-012-1378-x.

Chisholm, Stephen T.; Coaker, Gitta; Day, Brad; Staskawicz, Brian J. (2006): Host-microbe interactions: shaping the evolution of the plant immune response. In *Cell* 124 (4), pp. 803–814. DOI: 10.1016/j.cell.2006.02.008.

Choi, Hyong Woo; Klessig, Daniel F. (2016): DAMPs, MAMPs, and NAMPs in plant innate immunity. In *BMC Plant Biology* 16. DOI: 10.1186/s12870-016-0921-2.

Daste, Frédéric; Galli, Thierry; Tareste, David (2015): Structure and function of longin SNAREs. In *Journal of cell science* 128 (23), pp. 4263–4272. DOI: 10.1242/jcs.178574.

Denancé, Nicolas; Sánchez-Vallet, Andrea; Goffner, Deborah; Molina, Antonio (2013): Disease resistance or growth: the role of plant hormones in balancing immune responses and fitness costs. In *Frontiers in plant science* 4, p. 155. DOI: 10.3389/fpls.2013.00155.

Djamei, Armin; Schipper, Kerstin; Rabe, Franziska; Ghosh, Anupama; Vincon, Volker; Kahnt, Jörg et al. (2011): Metabolic priming by a secreted fungal effector. In *Nature* 478 (7369), p. 395. DOI: 10.1038/nature10454.

Doehlemann, Gunther; Ökmen, Bilal; Zhu, Wenjun; Sharon, Amir (2017): Plant Pathogenic Fungi. In *Microbiology spectrum* 5 (1). DOI: 10.1128/microbiolspec.FUNK-0023-2016.

Eckardt, Nancy A. (2010): Redox regulation of auxin signaling and plant development. In *The Plant cell* 22 (2), p. 295. DOI: 10.1105/tpc.110.220212.

Eder, Jürgen; Cosio, Eric G. (1994): Elicitors of Plant Defense Responses. In Kwang W. Jeon, Jonathan Jarvik (Eds.): International review of cytology. Survey of cell biology, vol. 148. San Diego, London: Academic Press (International Review of Cytology, v. 148), pp. 1–36.

Escobar, Nieves Medina; Haupt, Sophie; Thow, Graham; Boevink, Petra; Chapman, Sean; Oparka, Karl (2003): High-throughput viral expression of cDNA-green fluorescent protein fusions reveals novel subcellular addresses and identifies unique proteins that interact with plasmodesmata. In *The Plant cell* 15 (7), pp. 1507–1523.

FAO (2009): How to Feed the World in 2050. Available online at http://www.fao.org/home/en/.

Frame, Bronwyn R.; Shou, Huixia; Chikwamba, Rachel K.; Zhang, Zhanyuan; Xiang, Chengbin; Fonger, Tina M. et al. (2002): Agrobacterium tumefaciens-mediated transformation of maize embryos using a standard binary vector system. In *Plant physiology* 129 (1), pp. 13–22. DOI: 10.1104/pp.000653.

Freeman (2008): An Overview of Plant Defenses against Pathogens and Herbivores. In *PHI*. DOI: 10.1094/PHI-I-2008-0226-01.

Fu, Jing; Wang, Shiping (2011): Insights into Auxin Signaling in Plant–Pathogen Interactions. In *Frontiers in plant science* 2. DOI: 10.3389/fpls.2011.00074.

Gabriels, Suzan H E J; Takken, Frank L. W.; Vossen, Jack H.; Jong, Camiel F. de; Liu, Qing; Turk, Stefan C H J et al. (2006): CDNA-AFLP combined with functional analysis reveals novel genes involved in the hypersensitive response. In *Molecular plant-microbe interactions : MPMI* 19 (6), pp. 567–576. DOI: 10.1094/MPMI-19-0567.

Gelhaye, E.; Rouhier, N.; Navrot, N.; Jacquot, J. P. (2005): The plant thioredoxin system. In *Cellular and molecular life sciences : CMLS* 62 (1), pp. 24–35. DOI: 10.1007/s00018-004-4296-4.

Gil, P.; Dewey, E.; Friml, J.; Zhao, Y.; Snowden, K. C.; Putterill, J. et al. (2001): BIG: a calossin-like protein required for polar auxin transport in Arabidopsis. In *Genes & development* 15 (15), pp. 1985–1997. DOI: 10.1101/gad.905201.

Giraldo, Martha C.; Dagdas, Yasin F.; Gupta, Yogesh K.; Mentlak, Thomas A.; Yi, Mihwa; Martinez-Rocha, Ana Lilia et al. (2013): Two distinct secretion systems facilitate tissue invasion by the rice blast fungus *Magnaporthe oryzae*. In *Nature Communications* 4, p. 1996. DOI: 10.1038/ncomms2996.

Gomez-Gomez, L.; Boller, T. (2000): FLS2: an LRR receptor-like kinase involved in the perception of the bacterial elicitor flagellin in Arabidopsis. In *Molecular cell* 5 (6), pp. 1003–1011.

Goodin, Michael M.; Dietzgen, Ralf G.; Schichnes, Denise; Ruzin, Steven; Jackson, Andrew O. (2002): pGD vectors: versatile tools for the expression of green and red fluorescent protein fusions in agroinfiltrated plant leaves. In *The Plant journal : for cell and molecular biology* 31 (3), pp. 375–383.

Goodin, Michael M.; Zaitlin, David; Naidu, Rayapati A.; Lommel, Steven A. (2008): Nicotiana benthamiana: its history and future as a model for plant-pathogen interactions. In *Molecular plant-microbe interactions : MPMI* 21 (8), pp. 1015–1026. DOI: 10.1094/MPMI-21-8-1015.

Guo, Xiaola; Lu, Wenwen; Ma, Yurong; Qin, Qianqian; Hou, Suiwen (2013): The BIG gene is required for auxin-mediated organ growth in Arabidopsis. In *Planta* 237 (4), pp. 1135–1147. DOI: 10.1007/s00425-012-1834-4.

Gururani, Mayank Anand; Venkatesh, Jelli; Upadhyaya, Chandrama Prakash; Nookaraju, Akula; Pandey, Shashank Kumar; Park, Se Won (2012): Plant disease resistance genes: Current status and future directions. In *Physiological and Molecular Plant Pathology* 78, pp. 51–65. DOI: 10.1016/j.pmpp.2012.01.002.

Jones, Jonathan D. G.; Dangl, Jeffery L. (2006): The plant immune system. In *Nature* 444 (7117), pp. 323–329. DOI: 10.1038/nature05286.

Kämper, Jörg; Kahmann, Regine; Bölker, Michael; Ma, Li-Jun; Brefort, Thomas; Saville, Barry J. et al. (2006): Insights from the genome of the biotrophic fungal plant pathogen *Ustilago maydis*. In *Nature* 444 (7115), p. 97. DOI: 10.1038/nature05248.

Kanneganti, Thirumala-Devi; Bai, Xiaodong; Tsai, Chi-Wei; Win, Joe; Meulia, Tea; Goodin, Michael et al. (2007): A functional genetic assay for nuclear trafficking in plants. In *The Plant journal : for cell and molecular biology* 50 (1), pp. 149–158. DOI: 10.1111/j.1365-313X.2007.03029.x.

Keen, N. T. (1990): Gene-for-gene complementarity in plant-pathogen interactions. In *Annual review of genetics* 24, pp. 447–463. DOI: 10.1146/annurev.ge.24.120190.002311.

Kepinski, Stefan; Leyser, Ottoline (2002): Ubiquitination and Auxin Signaling: A Degrading Story. In *The Plant cell* 14 (suppl 1), S81-S95. DOI: 10.1105/tpc.010447.

Lam, Yun Wah; Trinkle-Mulcahy, Laura (2015): New insights into nucleolar structure and function. In *F1000prime reports* 7, p. 48. DOI: 10.12703/P7-48.

Lampropoulos, Athanasios; Sutikovic, Zoran; Wenzl, Christian; Maegele, Ira; Lohmann, Jan U.; Forner, Joachim (2013): GreenGate---a novel, versatile, and efficient cloning system for plant transgenesis. In *PloS one* 8 (12), e83043. DOI: 10.1371/journal.pone.0083043.

Lanver, Daniel; Tollot, Marie; Schweizer, Gabriel; Lo Presti, Libera; Reissmann, Stefanie; Ma, Lay-Sun et al. (2017): *Ustilago maydis* effectors and their impact on virulence. In *Nature Reviews Microbiology* 15 (7), p. 409. DOI: 10.1038/nrmicro.2017.33.

Lawrence, Carolyn J.; Harper, Lisa C.; Schaeffer, Mary L.; Sen, Taner Z.; Seigfried, Trent E.; Campbell, Darwin A. (2008): MaizeGDB: The maize model organism database for basic, translational, and applied research. In *International journal of plant genomics* 2008, p. 496957. DOI: 10.1155/2008/496957.

Lee, Samuel; Kim, Soo Min; Lee, Richard T. (2013): Thioredoxin and thioredoxin target proteins: from molecular mechanisms to functional significance. In *Antioxidants & redox signaling* 18 (10), pp. 1165–1207. DOI: 10.1089/ars.2011.4322.

Léveillard, Thierry; Aït-Ali, Najate (2017): Cell Signaling with Extracellular Thioredoxin and Thioredoxin-Like Proteins: Insight into Their Mechanisms of Action. In *Oxidative Medicine and Cellular Longevity* 2017. DOI: 10.1155/2017/8475125.

Leyser, Ottoline (2010): The power of auxin in plants. In *Plant physiology* 154 (2), pp. 501–505. DOI: 10.1104/pp.110.161323.

Li, Ningxiao; Wang, Wenzhao; Bitas, Vasileios; Subbarao, Krishna; Liu, Xingzhong; Kang, Seogchan (2018): Volatile Compounds Emitted by Diverse Verticillium Species Enhance Plant Growth by Manipulating Auxin Signaling. In *Molecular plant-microbe interactions : MPMI* 31 (10), pp. 1021–1031. DOI: 10.1094/MPMI-11-17-0263-R.

Lomax, Terri L.; Muday, Gloria K.; Rubery, Philip H. (2013): Auxin Transport. In Peter Davies (Ed.): Plant Hormones. Physiology, Biochemistry and Molecular Biology. 2nd ed. Dordrecht: Springer Netherlands, pp. 509–530. Available online at https://doi.org/10.1007/978-94-011-0473-9_24.

Lunde, Bradley M.; Moore, Claire; Varani, Gabriele (2007): RNA-binding proteins: modular design for efficient function. In *Nature reviews. Molecular cell biology* 8 (6), pp. 479–490. DOI: 10.1038/nrm2178.

Luschnig, C. (2001): Auxin transport: why plants like to think BIG. In *Current biology : CB* 11 (20), R831-3.

Ma, Ka-Wai; Ma, Wenbo (2016): Phytohormone pathways as targets of pathogens to facilitate infection. In *Plant molecular biology* 91 (6), pp. 713–725. DOI: 10.1007/s11103-016-0452-0.

Maria Soriano (2017): Plasmids 101: Gateway Cloning 2017, January 12, 10:30:00 AM. Available online at https://blog.addgene.org/plasmids-101-gateway-cloning.

Maris, Christophe; Dominguez, Cyril; Allain, Frédéric H-T (2005): The RNA recognition motif, a plastic RNA-binding platform to regulate post-transcriptional gene expression. In *The FEBS journal* 272 (9), pp. 2118–2131. DOI: 10.1111/j.1742-4658.2005.04653.x.

Martínez-Espinoza, Alfredo D.; García-Pedrajas, María D.; Gold, Scott E. (2002): The Ustilaginales as plant pests and model systems. In *Fungal genetics and biology : FG & B* 35 (1), pp. 1–20. DOI: 10.1006/fgbi.2001.1301.

McClintock, B. (1950): The origin and behavior of mutable loci in maize. In *Proceedings of the National Academy of Sciences* 36 (6), pp. 344–355. DOI: 10.1073/pnas.36.6.344.

Meyer, Yves; Siala, Wafi; Bashandy, Talaat; Riondet, Christophe; Vignols, Florence; Reichheld, Jean Philippe (2008): Glutaredoxins and thioredoxins in plants. In *Biochimica et biophysica acta* 1783 (4), pp. 589–600. DOI: 10.1016/j.bbamcr.2007.10.017.

Morris, David A.; Friml, Jiří; Zažímalová, Eva (2010): The Transport of Auxins. In Peter J. Davies (Ed.): Plant hormones. Biosynthesis, signal transduction, action! 3., rev. ed. Dordrecht: Springer Science+Business Media B.V, pp. 451–484. Available online at https://doi.org/10.1007/978-1-4020-2686-7_21.

Mueller, Olaf; Kahmann, Regine; Aguilar, Guillermo; Trejo-Aguilar, Blanca; Wu, Andy; Vries, Ronald P. de (2008): The secretome of the maize pathogen Ustilago maydis. In *Fungal genetics and biology : FG & B* 45 Suppl 1, S63-70. DOI: 10.1016/j.fgb.2008.03.012.

Nannas, Natalie J.; Dawe, R. Kelly (2015): Genetic and genomic toolbox of Zea mays. In *Genetics* 199 (3), pp. 655–669. DOI: 10.1534/genetics.114.165183.

Navarro, Lionel; Dunoyer, Patrice; Jay, Florence; Arnold, Benedict; Dharmasiri, Nihal; Estelle, Mark et al. (2006): A plant miRNA contributes to antibacterial resistance by repressing auxin signaling. In *Science (New York, N.Y.)* 312 (5772), pp. 436–439. DOI: 10.1126/science.1126088.

Niks, Rients E.; Marcel, Thierry C. (2009): Nonhost and basal resistance: how to explain specificity? In *The New phytologist* 182 (4), pp. 817–828. DOI: 10.1111/j.1469-8137.2009.02849.x.

OERKE, E.-C. (2006): Crop losses to pests. In *J. Agric. Sci.* 144 (01), p. 31. DOI: 10.1017/S0021859605005708.

Pechanova, Olga; Pechan, Tibor (2015): Maize-Pathogen Interactions: An Ongoing Combat from a Proteomics Perspective. In *International journal of molecular sciences* 16 (12), pp. 28429–28448. DOI: 10.3390/ijms161226106.

Perez-Nadales, Elena; Nogueira, Maria Filomena Almeida; Baldin, Clara; Castanheira, Sónia; El Ghalid, Mennat; Grund, Elisabeth et al. (2014): Fungal model systems and the elucidation of pathogenicity determinants. In *Fungal genetics and biology : FG & B* 70, pp. 42–67. DOI: 10.1016/j.fgb.2014.06.011.

Rey, P.; Pruvot, G.; Becuwe, N.; Eymery, F.; Rumeau, D.; Peltier, G. (1998): A novel thioredoxin-like protein located in the chloroplast is induced by water deficit in Solanum tuberosum L. plants. In *The Plant journal : for cell and molecular biology* 13 (1), pp. 97–107.

Rivas, Susana; Rougon-Cardoso, Alejandra; Smoker, Matthew; Schauser, Leif; Yoshioka, Hirofumi; Jones, Jonathan D. G. (2004a): CITRX thioredoxin interacts with the tomato Cf-9 resistance protein and negatively regulates defence. In *The EMBO journal* 23 (10), pp. 2156–2165. DOI: 10.1038/sj.emboj.7600224.

Rivas, Susana; Rougon-Cardoso, Alejandra; Smoker, Matthew; Schauser, Leif; Yoshioka, Hirofumi; Jones, Jonathan D. G. (2004b): CITRX thioredoxin interacts with the tomato Cf-9 resistance protein and negatively regulates defence. In *The EMBO journal* 23 (10), pp. 2156–2165. DOI: 10.1038/sj.emboj.7600224.

Ruegger, M.; Dewey, E.; Hobbie, L.; Brown, D.; Bernasconi, P.; Turner, J. et al. (1997): Reduced naphthylphthalamic acid binding in the tir3 mutant of Arabidopsis is associated with a reduction in polar auxin transport and diverse morphological defects. In *The Plant cell* 9 (5), pp. 745–757. DOI: 10.1105/tpc.9.5.745.

Sambrook, J.; Fritsch, E.; Maniatis, T. (1989): Molecular cloning. A laboratory manual : Vol. 2. 2. ed. S.l.: Cold Spring Harbor.

Sanderfoot, A. A.; Assaad, F. F.; Raikhel, N. V. (2000): The Arabidopsis genome. An abundance of soluble N-ethylmaleimide-sensitive factor adaptor protein receptors. In *Plant physiology* 124 (4), pp. 1558–1569.

Saville, B. J.; Donaldson, M. E.; Doyle, C. E. (2012): Investigating Host Induced Meiosis in a Fungal Plant Pathogen: IntechOpen, 2/29/2012. Available online at https://www.intechopen.com/citation-pdf-url/30385.

Schnable, Patrick S.; Ware, Doreen; Fulton, Robert S.; Stein, Joshua C.; Wei, Fusheng; Pasternak, Shiran et al. (2009): The B73 maize genome: complexity, diversity, and dynamics. In *Science (New York, N.Y.)* 326 (5956), pp. 1112–1115. DOI: 10.1126/science.1178534.

Sperschneider, Jana; Catanzariti, Ann-Maree; DeBoer, Kathleen; Petre, Benjamin; Gardiner, Donald M.; Singh, Karam B. et al. (2017): LOCALIZER: subcellular localization prediction of both plant and effector proteins in the plant cell. In *Scientific Reports* (7), p. 44598. DOI: 10.1038/srep44598.

Sperschneider, Jana; Dodds, Peter N.; Singh, Karam B.; Taylor, Jennifer M. (2018): ApoplastP: prediction of effectors and plant proteins in the apoplast using machine learning. In *The New phytologist* 217 (4), pp. 1764–1778. DOI: 10.1111/nph.14946.

Sperschneider, Jana; Gardiner, Donald M.; Dodds, Peter N.; Tini, Francesco; Covarelli, Lorenzo; Singh, Karam B. et al. (2016): EffectorP: predicting fungal effector proteins from secretomes using machine learning. In *The New phytologist* 210 (2), pp. 743–761. DOI: 10.1111/nph.13794.

States, National Research Council Committee on Examination of Plant Science Research Programs in the United (1992): Why Plant-Biology Research Today?: National Academies Press (US).

Strable, Josh; Scanlon, Michael J. (2009): Maize (Zea mays): a model organism for basic and applied research in plant biology. In *Cold Spring Harbor protocols* 2009 (10), pdb.emo132. DOI: 10.1101/pdb.emo132.

Tiwari, Shiv B.; Wang, Xiao-Jun; Hagen, Gretchen; Guilfoyle, Tom J. (2001): AUX/IAA Proteins Are Active Repressors, and Their Stability and Activity Are Modulated by Auxin. In *The Plant cell* 13 (12), pp. 2809–2822. DOI: 10.1105/tpc.010289.

Tognetti, Vanesa B.; Mühlenbock, P. E. R.; van Breusegem, Frank (2012): Stress homeostasis – the redox and auxin perspective. In *Plant, Cell & Environment* 35 (2), pp. 321–333. DOI: 10.1111/j.1365-3040.2011.02324.x.

Toruño, Tania Y.; Stergiopoulos, Ioannis; Coaker, Gitta (2016): Plant-Pathogen Effectors: Cellular Probes Interfering with Plant Defenses in Spatial and Temporal Manners. In *Annual review of phytopathology* 54, pp. 419–441. DOI: 10.1146/annurev-phyto-080615-100204.

Ulmasov, T.; Murfett, J.; Hagen, G.; Guilfoyle, T. J. (1997): Aux/IAA proteins repress expression of reporter genes containing natural and highly active synthetic auxin response elements. In *The Plant cell* 9 (11), pp. 1963–1971. DOI: 10.1105/tpc.9.11.1963.

Usman, Abubakar Bello; Abubakar, Salisu; Alaku, Chinweoma; Nnadi, Ogechi (2014): Plant: A Necessity of Life. In *ILNS* 20, pp. 151–159. DOI: 10.18052/www.scipress.com/ILNS.20.151.

Velásquez, André C.; Chakravarthy, Suma; Martin, Gregory B. (2009): Virus-induced gene silencing (VIGS) in Nicotiana benthamiana and tomato. In *Journal of visualized experiments : JoVE* (28). DOI: 10.3791/1292.

Win, J.; Chaparro-Garcia, A.; Belhaj, K.; Saunders, D. G. O.; Yoshida, K.; Dong, S. et al. (2012): Effector biology of plant-associated organisms: concepts and perspectives. In *Cold Spring Harbor symposia on quantitative biology* 77, pp. 235–247. DOI: 10.1101/sqb.2012.77.015933.

Zhang, Yan; Lubberstedt, Thomas; Xu, Mingliang (2013): The genetic and molecular basis of plant resistance to pathogens. In *Journal of genetics and genomics = Yi chuan xue bao* 40 (1), pp. 23–35. DOI: 10.1016/j.jgg.2012.11.003.

9 Supplementary

UMAG_00628 as inducer of auxin signalling

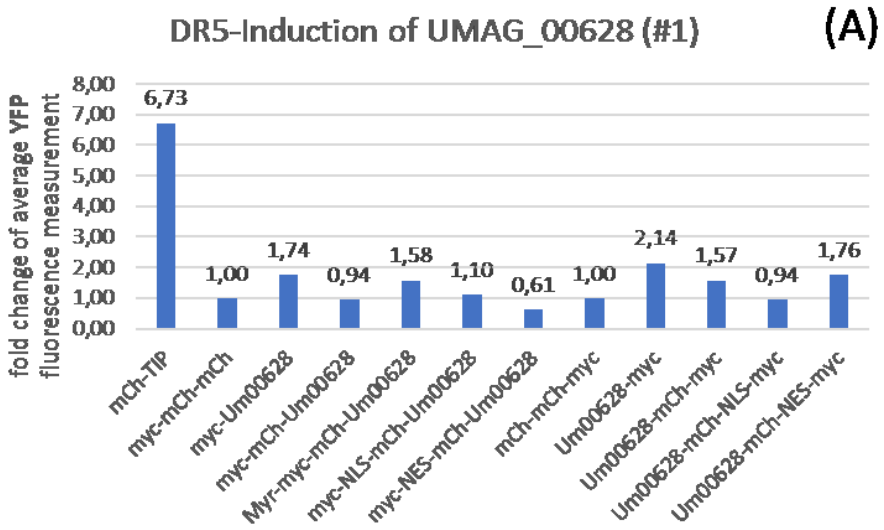

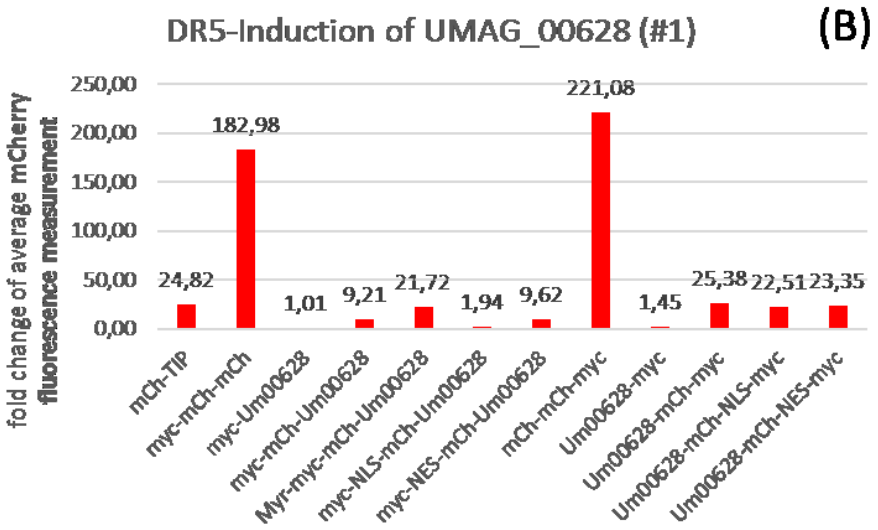

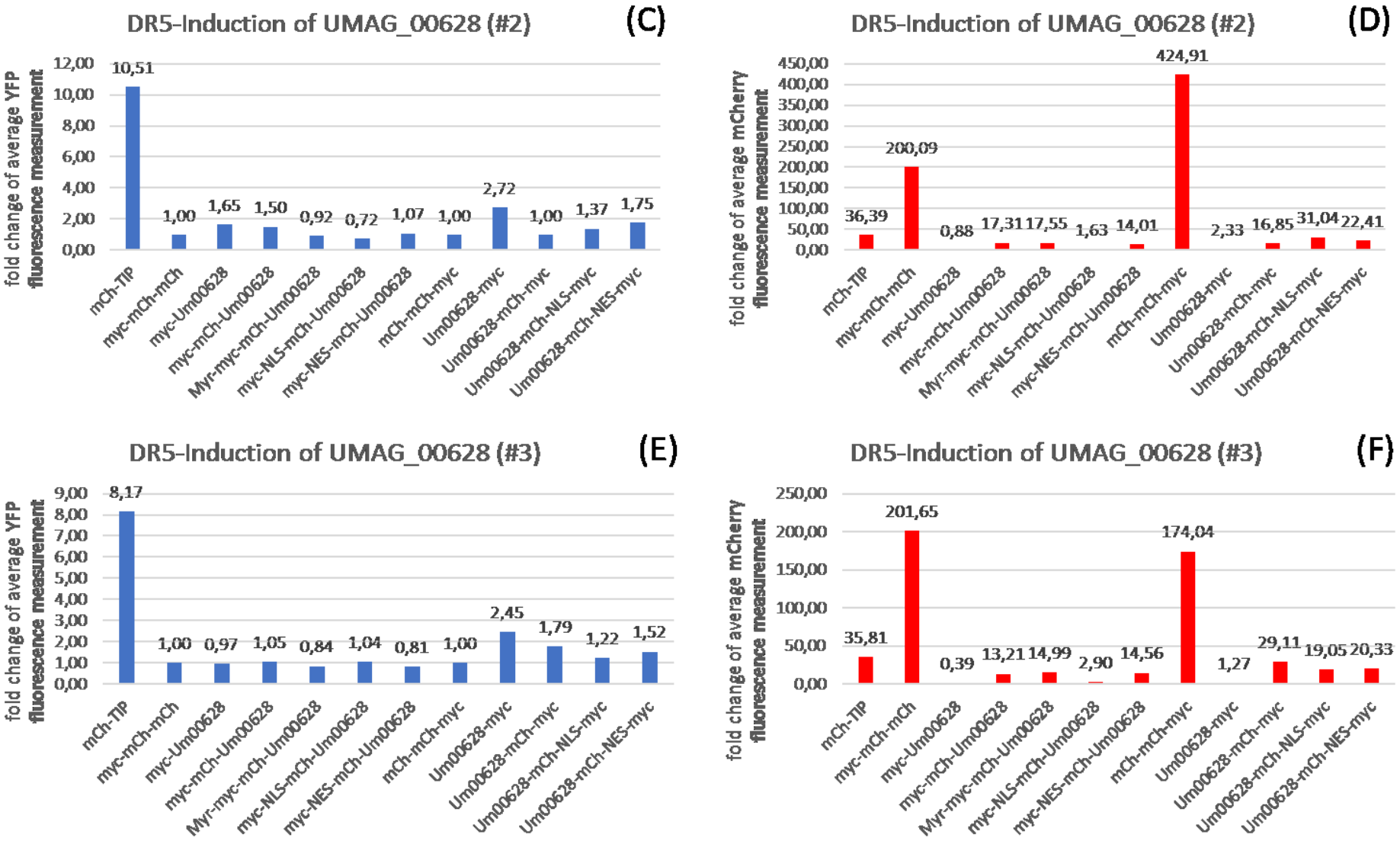

Figure 9 DR5 induction assay: YFP and mCherry measurements of subcellular localization versions of UMAG_00628

Figures (A), (C) and (E) represent each one experiment of the relative induction of auxin signalling caused by UMAG_00628. The DR5:YFP reporter system was co-infiltrated to measure changes in induction caused by sending the effector UMAG_00628 to different subcellular localizations. The tags were fused either to the C- or N-terminus of the effector. Two plants per construct variation were infiltrated for one experimental setup. The experiment was repeated three times independently. The fluorescence measurements were normalized accordingly to the negative induction control myc-mCherry-mCherry (for all N-terminal tags) and mCherry-mCherry-myc (for all C-terminal tags), respectively. The fold change was calculated using Excel. Possible outliers were identified in R Statistics and removed. Figures (B), (D) and (F) visualize the protein synthesis of subcellular localization constructs of UMAG_00628 within the infiltrated leave area. By measuring the mCherry fluorescence (at λex = 570 nm and λemm= 610 nm) all mCherry-tagged effector constructs can be detected meaning that those tag versions were synthesized and present in the inspected sample. The measurements were set in relation to the negative controls myc-mCherry-mCherry (for all N-terminal tags) and mCherry-mCherry-myc (for all C-terminal tags), respectively. The fold change was calculated using Excel. Beforehand possible outliers were identified in R Statistics and removed. Abbr.: λex = excitation wave length; λemm = emission wave length; mCh = mCherry; TIP = TIP1; Um00628 = UMAG_00628; Myr = myristylation tag; NLS = nuclear localization signal tag; NES = nuclear export signal tag.

UMAG_02852 as inducer of auxin signalling

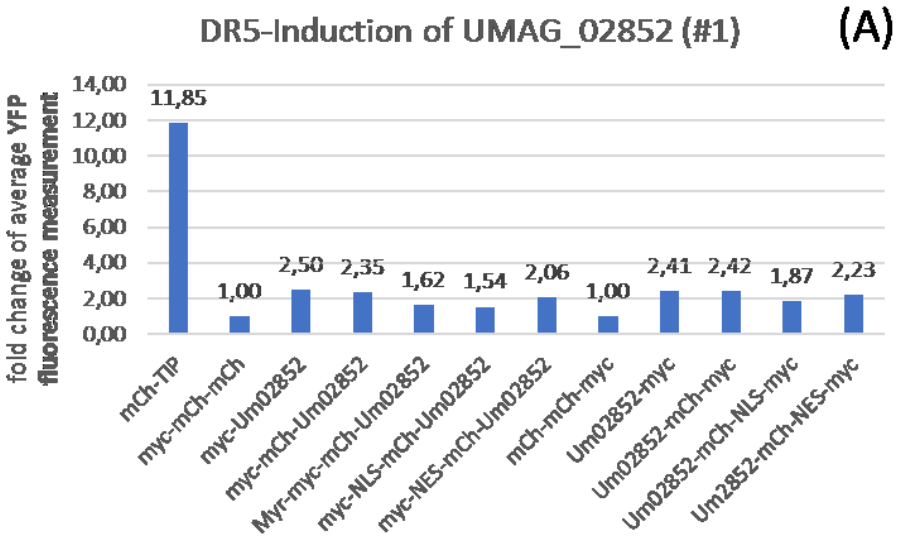

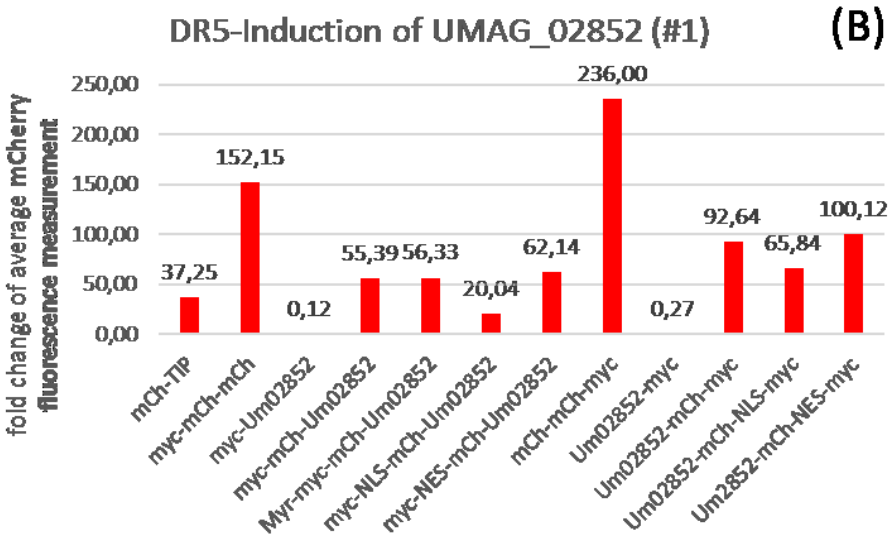

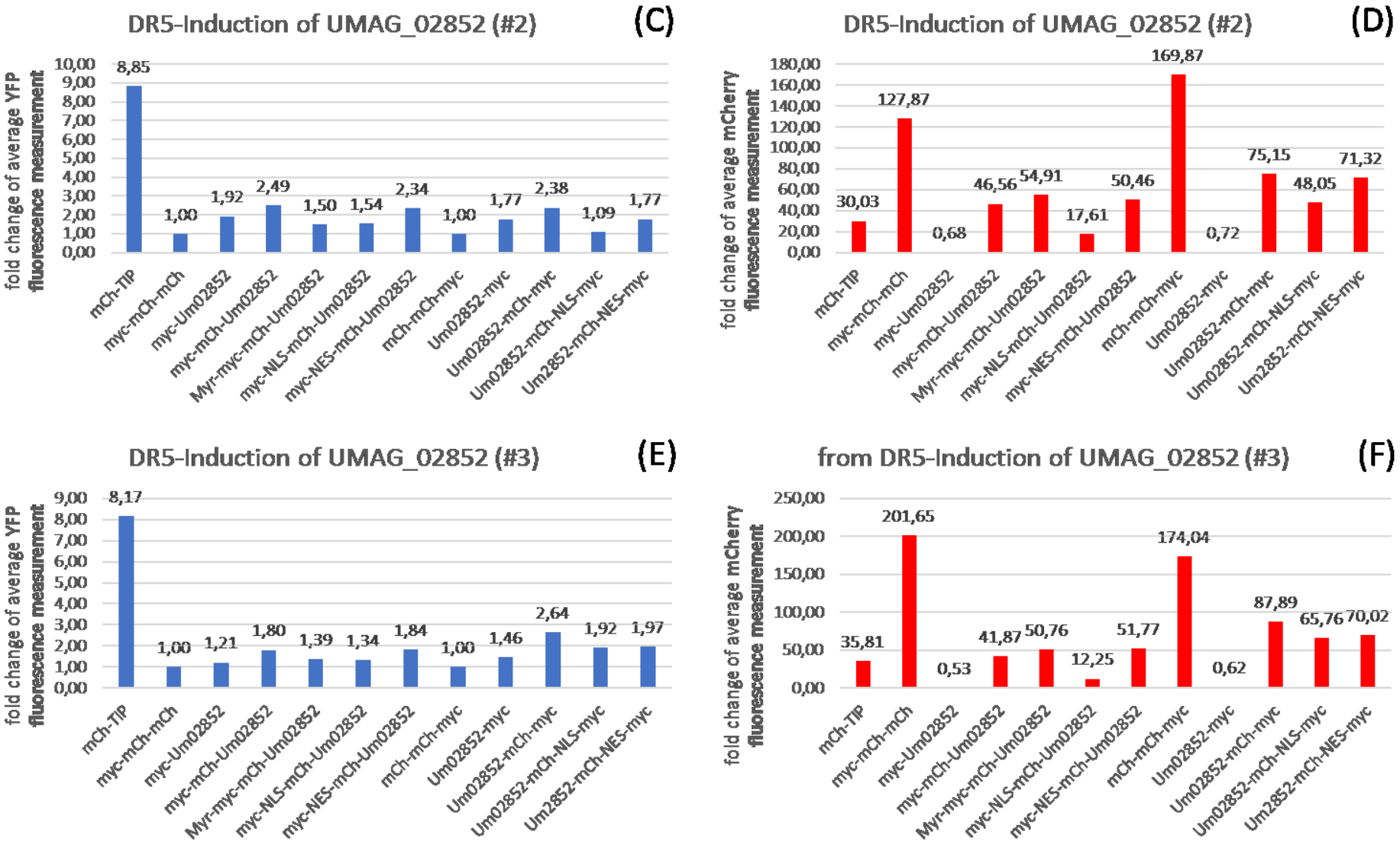

Figure 10 DR5 induction assay: YFP and mCherry measurements of subcellular localization versions of UMAG_02852

Figures (A), (C) and (E) represent each one experiment of the relative induction of auxin signalling caused by UMAG_02852. The DR5:YFP reporter system was co-infiltrated to measure changes in induction caused by sending the effector UMAG_00628 to different subcellular localizations. The tags were fused either to the C- or N-terminus of the effector. Two plants per construct variation were infiltrated for one experimental setup. The experiment was repeated three times independently. The fluorescence measurements were normalized accordingly to the negative induction control myc-mCherry-mCherry (for all N-terminal tags) and mCherry-mCherry-myc (for all C-terminal tags), respectively. The fold change was calculated using Excel. Possible outliers were identified in R Statistics and removed. Figures (B), (D) and (F) visualize the protein synthesis of subcellular localization constructs of UMAG_00628 within the infiltrated leave area. By measuring the mCherry fluorescence (at λex = 570 nm and λemm= 610 nm) all mCherry-tagged effector constructs can be detected meaning that those tag versions were synthesized and present in the inspected sample. The measurements were set in relation to the negative controls myc-mCherry-mCherry (for all N-terminal tags) and mCherry-mCherry-myc (for all C-terminal tags), respectively. The fold change was calculated using Excel. Beforehand possible outliers were identified in R Statistics and removed. Abbr.: λex = excitation wave length; λemm = emission wave length; mCh = mCherry; TIP = TIP1; Um02852 = UMAG_02852; Myr = myristylation tag; NLS = nuclear localization signal tag; NES = nuclear export signal tag.

Verification of full-length protein expression

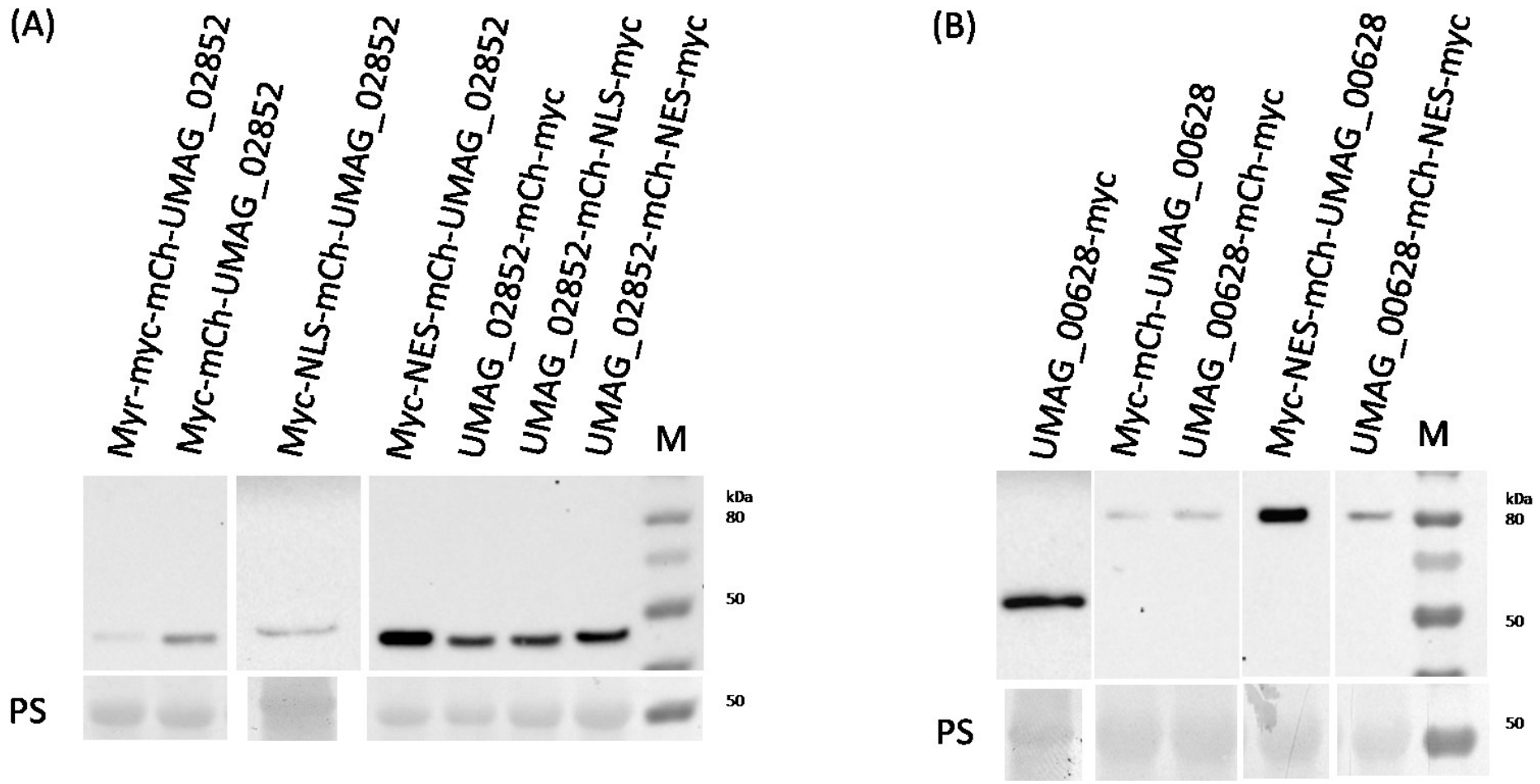

Figure 11 Proof of full-length expression of subcellular localization construct variants with the western blot technique.

Figure (A) represents the detection of UMAG_02852 N- and C-terminal localization tag variants via western blot which are supposed to appear around the size of 44 kDa. Only the N- and C-terminal myc-tagged versions of the effector could not be detected. Figure (B) displays the verification of the full-length protein expression of UMAG_00628 N- and C-terminal localization tag variants. The localization tag combinations have the size of approximately 80 kDa. The UMAG_00628-myc construct is 53 kDa large. The N- and C-

terminal myc-tagged versions as well as the N-terminal Myr- and NLS-tag could not be visualized. Abbr.: myc = myc tag; mCh = mCherry tag; Myr = myristylation tag; NLS = nuclear localization signal tag; NES = nuclear export signal tag; PS = Ponceau staining.

Microscopic analysis of subcellular localization assay

The expression and accumulation of the subcellular localization of the tagged effectors UMAG_00628 and UMAG_02852 were observed using confocal laser scanning microscopy. The microscopic analysis was performed with a confocal laser scanning microscope. Pictures were taken in the mCherry and the brightfield channel.

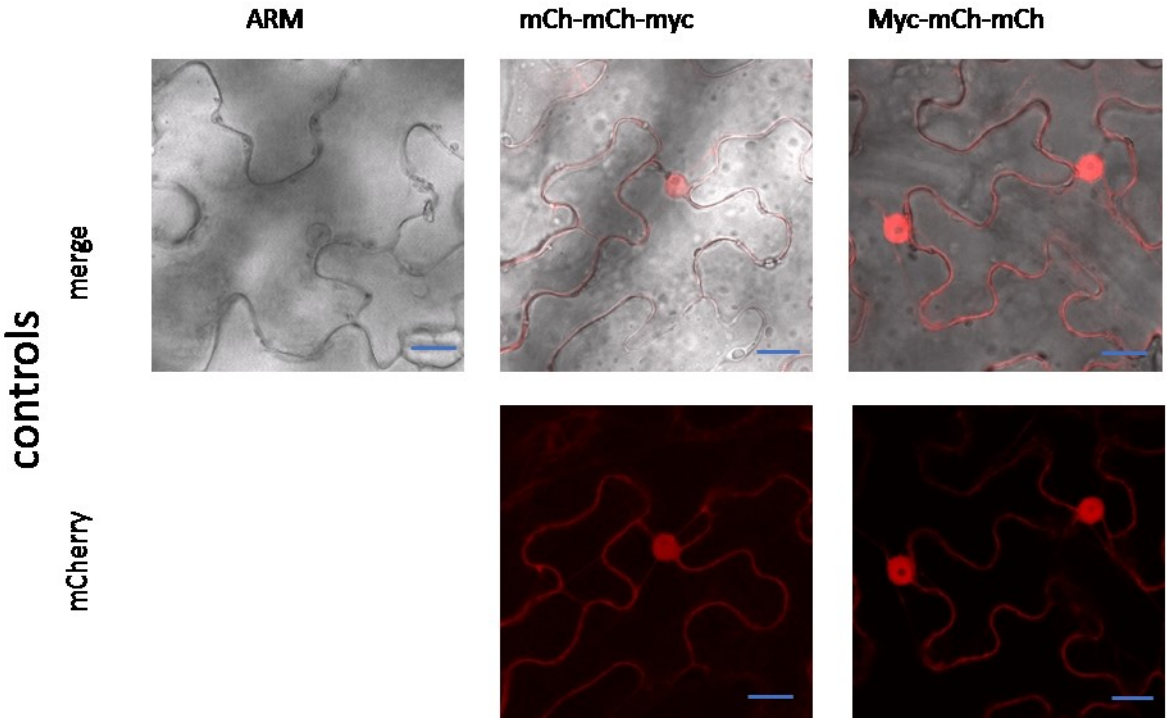

Figure 12 Confocal laser scanning microscopy images of subcellular localization controls.

The scale bar equals 20 µm. The merged picture is the fusion of the brightfield and mCherry channel of the CLSM. The ARM image should visualize possible auto-fluorescence. The mCh-mCh-myc version represents a C-terminal tag control and myc-mCherry-mCherry a N-terminal tag control. Abbr.: merge = brightfield combined with mCherry channel; mCherry = mCherry channel; ARM = ARM buffer; mCh-mCh-myc = mCherry-mCherry-myc; Myc-mCh-mCh = myc-mCherry-mCherry.

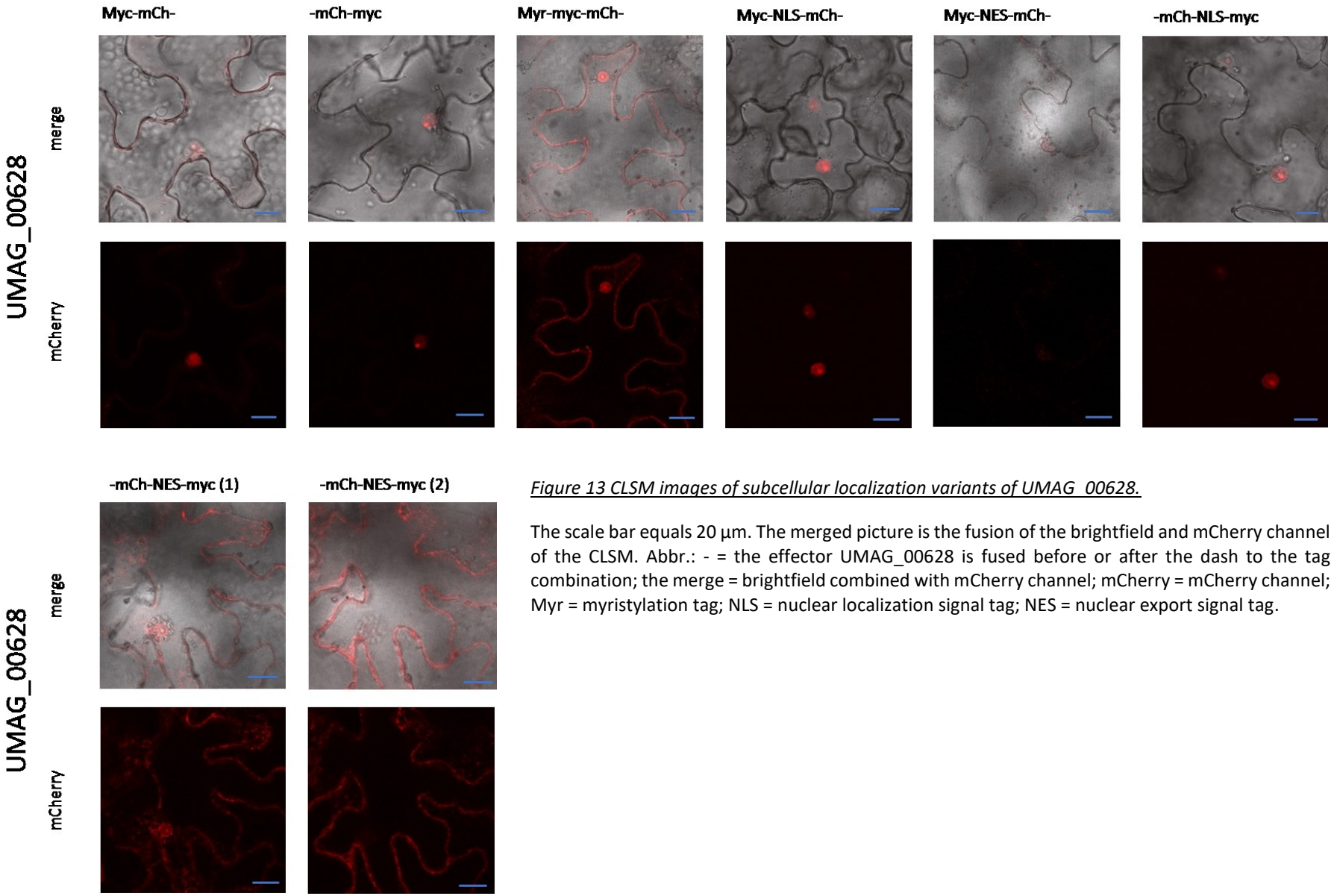

Figure 13 CLSM images of subcellular localization variants of UMAG_00628.

The scale bar equals 20 µm. The merged picture is the fusion of the brightfield and mCherry channel of the CLSM. Abbr.: - = the effector UMAG_00628 is fused before or after the dash to the tag combination; the merge = brightfield combined with mCherry channel; mCherry = mCherry channel; Myr = myristylation tag; NLS = nuclear localization signal tag; NES = nuclear export signal tag.

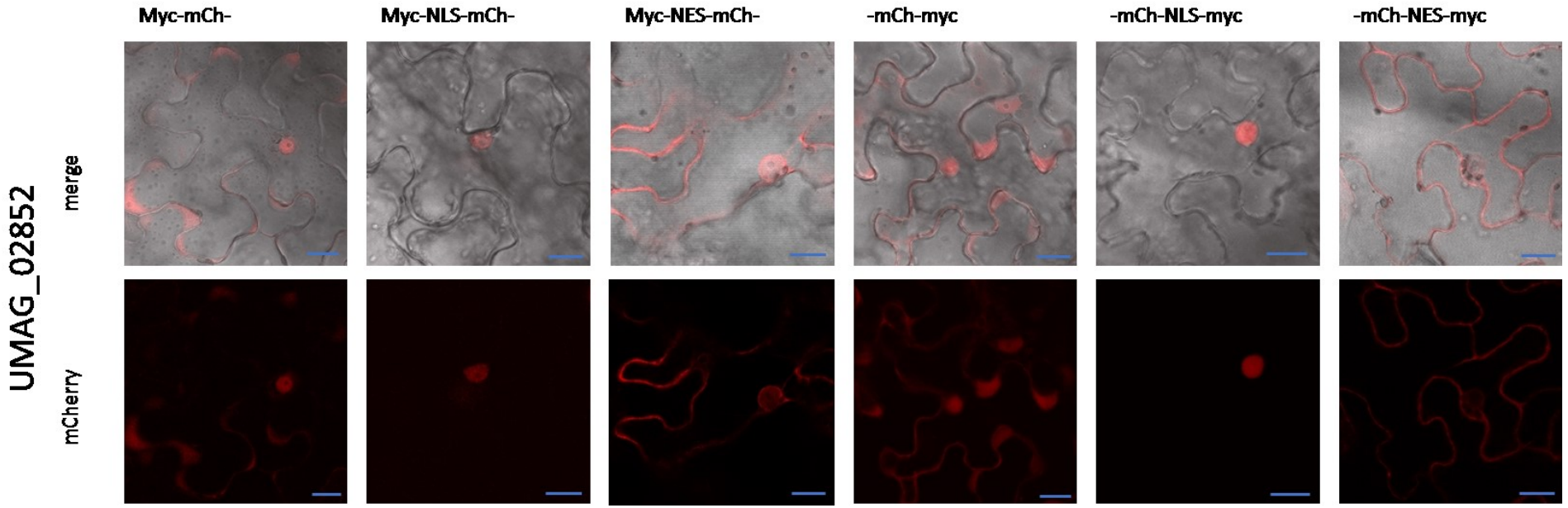

Figure 14 CLSM images of subcellular localization variants of UMAG_02852.

The scale bar equals 20 µm. The merged picture is the fusion of the brightfield and mCherry channel of the CLSM. An image of the Myr-myc-mCh- tagged construct could not be taken. Abbr.: - = the effector UMAG_02852 is fused before or after the dash to the tag combination; the merge = brightfield combined with mCherry channel; mCherry = mCherry channel; Myr = myristylation tag; NLS = nuclear localization signal tag; NES = nuclear export signal tag.

Phenotype of VIGS plants

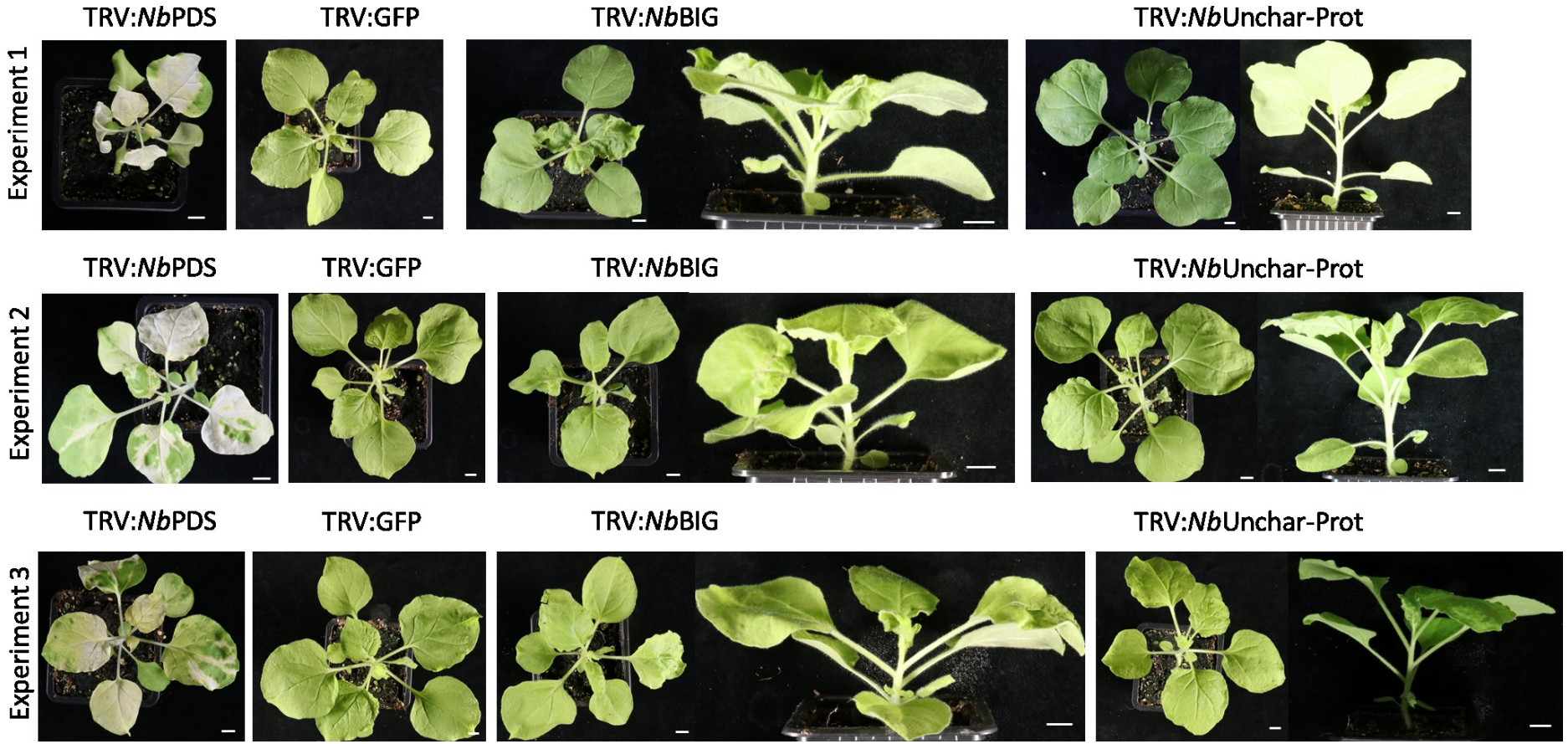

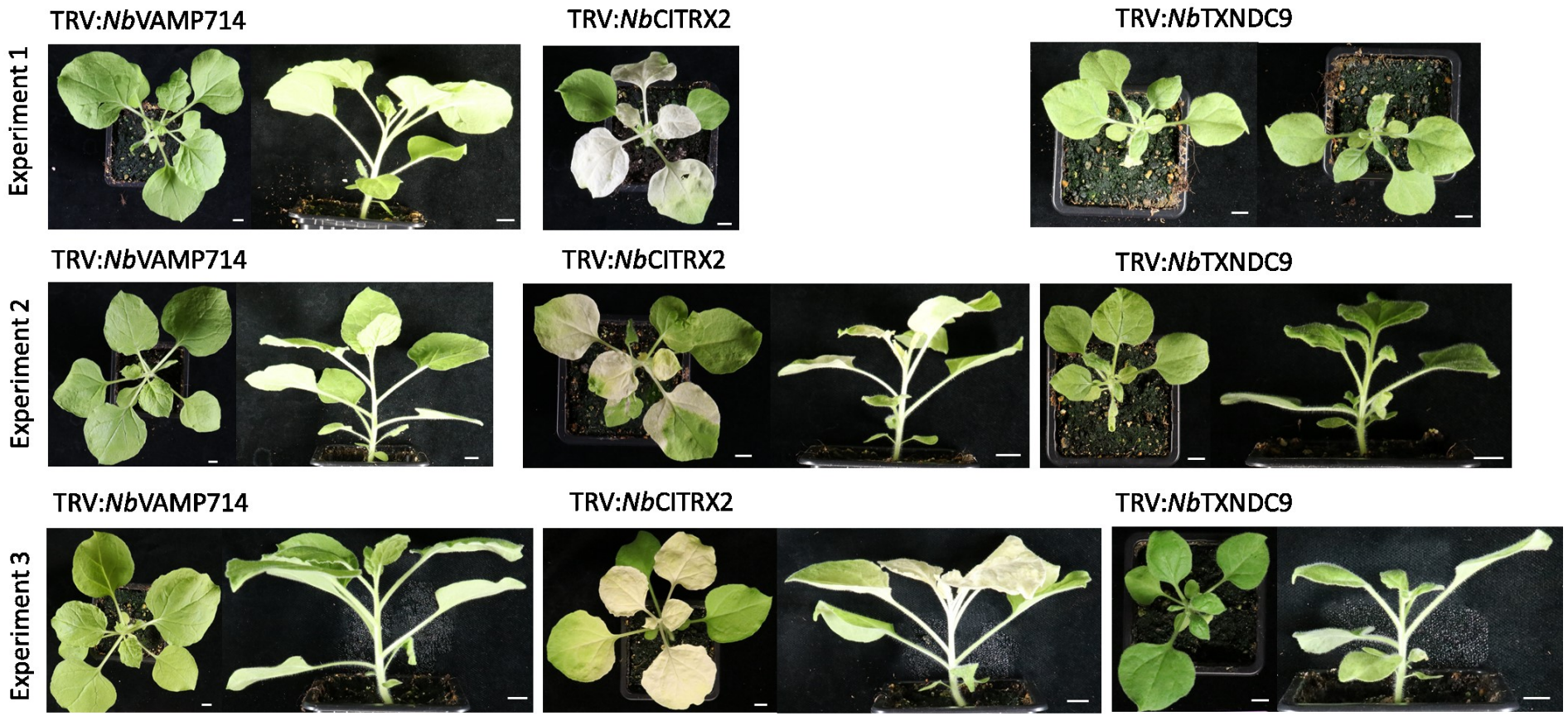

Figure 15 Single-lens reflex camera pictures of VIGS phenotypes.

The scale bars equal 1 cm. However, the camera settings were not the same between the three independent experiments. The phenotype of the VIGS variants of PEIP (TRV:NbPDS, TRV:GFP, TRV:NbBIG, TRV:NbUnchar-Prot, TRV:NbVAMP714, TRV:NbCITRX2 and TRV:NbTXNDC9) were monitored over all three experiments and are illustrated here. If possible, each time a picture was taken from above and side. TRV:NbPDS is the control for the integrity of the VIGS technique. TRV:GFP is the control for the silencing of a non-interacting partner of an effector. Abbr.: VIGS = virus-induced gene silencing; TRV = tobacco rattle virus; PEIP = possible effector interacting protein; PDS = phytoene desaturase; GFP = green fluorescence protein.

DR5 Induction of VIGS plants

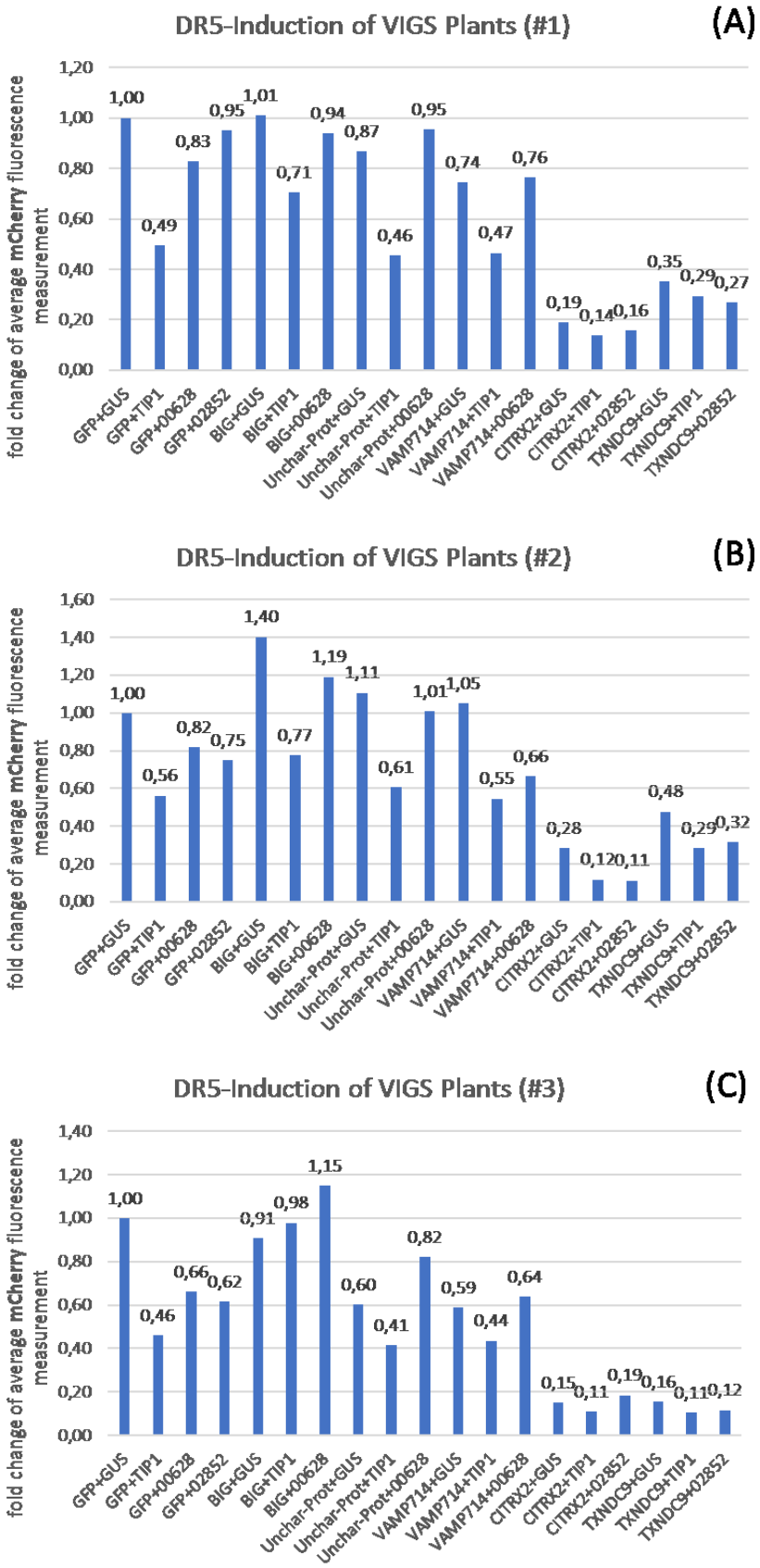

Figure 16 Relative induction of auxin signalling in VIGS planta.

The DR5 induciton assay was repeated three times independently. Each figure 8 (A), (B) and (C) represent the results of one experiment. The fold change was calculated by normalizing the fluorescence measurements to the reference probe TRV:GFP infiltrated with GUS-myc in Excel. Outlayers were removed via R statistics. TRV:GFP is the control for a silenced non-interacting partner of an effector. TRV:NbBIG, TRV:NbUnchar-Prot and TRV:NbVAMP714 are silenced PEIP in N. b. (VIGS variant) of the effetor UMAG_00628. TRV:NbCITRX2 and TRV:NbTXNDC9 are silenced PEIP in N. b. (VIGS variant) of the effetor UMAG_02852. Each VIGS variant was infiltrated with the negative DR5 induction control GUS, the positive control TIP1 and its associated effector. Abbr.: VIGS = virus-induced gene silencing; TRV = tobacco rattle virus; PEIP = possible effector interacting protein; GFP = TRV:GFP; BIG = TRV:NbBIG; Unchar-Prot = TRV:NbUnchar-Prot; VAMP714 = TRV:NbVAMP714; CITRX2 = TRV:NbCITRX2; TXNDC9 = TRV:NbTXNDC9; GUS = beta-glucuronidase fused to myc-tag; TIP1 = TOPLESS interacting protein 1 fused to myc-tag; 00628 = UMAG_00628-myc; 02852 = UMAG_02852-myc.

Validation of Reporter System (by Indira Saado)

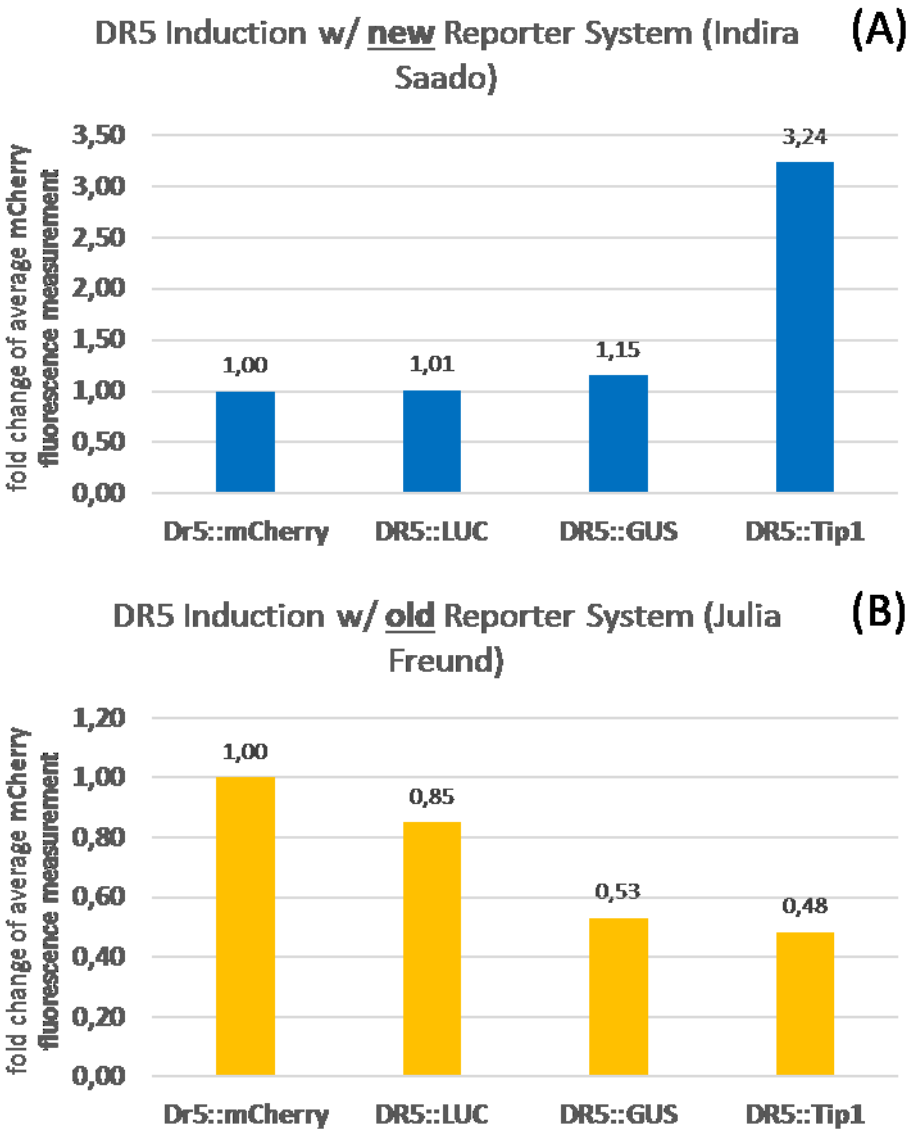

Figure 17 Validation and comparison of the DR5-mCherry reporter system

used for DR5 induction in VIGS planta and a newly cloned DR5-mCherry construct designed by Indira Saado. The following constructs were infiltrated in N. b. for the DR5 induction assay: $35S_{prom}$-GUS-HA (as negative induction control), $35S_{prom}$-TIP1-HA (as positive induction control), $35S_{prom}$-LUC-myc (as negative induction control) and the DR5-mCherry reporter (reference for the fluorescence measurement) alone. The fold change was calculated by normalizing the fluorescence measurements to the reference probe DR5-mCherry in Excel. In figure 9 (A) the

new DR5-mCherry construct was tested for DR5 induction. In figure (B) the DR5-mCherry reporter used in this thesis for the DR5 induction assay in VIGS planta was evaluated. Abbr.: w/ = with; LUC = Luciferase; GUS = beta-glucuronidase; Tip1 = TOPLESS interacting protein 1